UNIVERSITÀ DEGLI STUDI DI PADOVA
DIPARTIMENTO DI INGEGNERIA CIVILE, EDILE E AMBIENTALE
Department Of Civil, Environmental and Architectural Engineering

Corso di Laurea Magistrale in Ingegneria Civile

TESI DI LAUREA

INFLUENZA DEI NODI SUL MODULO DI ELASTICITÀ DI PALI DI FONDAZIONE IN LEGNO

INFLUENCE OF KNOTS ON THE MODULUS OF ELASTICITY OF WOODEN FOUNDATION PILES

Relatore:
Prof. Ing. ROBERTO SCOTTA
Correlatori:
Ing. GIORGIO PAGELLA
Delft University of Technology
Dott. Ing. GEERT J.P. RAVENSHORST
Delft University of Technology

Laureando:
GABRIELE DE MORI
1233954

ANNO ACCADEMICO 2021-2022

Acknowledgement

Desidero ringraziare le figure che hanno contribuito allo svolgimento e stesura di questo importante lavoro scientifico, come l'ing. Roberto Scotta, l'ing. Giorgio Pagella e l'ing. Geert Ravenshorst.

Vorrei poi ringraziare le numerose persone che mi hanno aiutato a raggiungere questo importante obbiettivo, iniziando dalla mia famiglia. Adriana e Michele che mi hanno sempre supportato nei miei percorsi di crescita professionale e come uomo. Un ringraziamento molto speciale va anche alla Marghe, che si prende sempre cura di me con amore e nei periodi più bui è riuscita sempre ad esserci per risollevarmi e che mi da ciò che ho sempre voluto: la libertà di essere me stesso in tutto e per tutto.

Intendo poi ringraziare mia sorella Giulia per le sedute personali da psicologa di supporto, mia nonna Rosanna per i consigli di vita e tutti i parenti che mi sono stati accanto in tutto il percorso fatto fino ad ora.

Ringrazio anche il mio capo e amico Ale, che mi ha insegnato e fatto divertire molto con le trasferte a Cortina. Insieme a lui bisogna ringraziare il club Nonsoloacqua di Belluno di cui faccio parte, per avermi dato modo di sfogare le mie gioie e frustrazioni universitarie.

Bisogna ringraziare molto anche i membri di Betahouse, meno uno. Fede e Rick che mi hanno supportato nei mesi del lockdown e con i quali ho condiviso un sacco di belle esperienze di vita che mi hanno segnato molto.

Non dimentico poi tutti i miei amici con i quali condivido parti importanti della mia vita come Matteo, Faghi, Tomin e tutto il team # ocioaltocio, di Non Casteo e di zona bianco... Ringrazio Marvin per i consigli sul diabete e per le ciacole al pub come anche la mitica Peach.

Un sentito grazie anche a Monica e Valter per avermi accolto al bivacco Libralon fornendomi un punto di appoggio fisico e morale nell'ultimo periodo di università.

Ringrazio Cristiana per avermi aiutato in tutta la ricerca di tesi e con la quale ho condiviso le esperienze, belle e brutte, dell'Olanda.

Abstract

Cities build on marshy undergrounds, such as Amsterdam and Venice, are based on timber foundation piles due to the low bearing capacity of the soil. Since wood is a natural material, the mechanical properties of timber piles are affected by structural defects like knots. With the aim to understand this aspect, this research studies the influence of knots on the modulus of elasticity in the longitudinal direction of wooden foundation piles.
The research analyzed 27 spruce and pine piles (from Germany and The Netherlands), that were divided in 110 segments. In particular, two main parameters that influence the stiffness of timber piles were considered: the knots size and layout. The study of segments was performed with large-scale mechanical testing that involved compression tests and frequency response measurement. The global analysis was validated by testing also wooden disks sawn from a section of the pile with and without knots, to further analyze the influence of knots on stiffness with local tests, besides the large-scale ones. A good correlation was observed between the MOE of pile segments and disks, and confirming that section with knots governs the stiffness when loading a pile in compression. An Overall Knots Ratio (OKR) was defined considering the layout of knots in each foundation pile and evaluating how the modulus of elasticity is influenced by dimension, number and layout of knots. The influence of knots was studied also performing a numerical model to predict the dynamic response of the segments. The model confirms again that knots are a relevant factor in the variation of the MOE of wooden foundation piles. Finally, a prediction model was performed. The model can predict the modulus of elasticity of a pile, by knowing density and knots layout.
The analysis of the obtained data showed that knots influence the deviation of longitudinal fibers and subsequently the modulus of elasticity. Therefore, the cross-section with knots in the axial direction of a pile, due to fiber deviation around a knot, resulted to have very low stiffness, that was neglected in the analysis. In addition, it was estimated that the zone around the knot, where the fibers in longitudinal direction deviate, has a slightly higher stiffness than the knot itself, but still very low. In conclusion, the equivalent size of influence was estimated approximately as 1.5 times the diameter of the knot itself.
These results were studied in detail with Digital Image Correlation (DIC) test. This technique was used to better investigate the behaviour of knots on the variation of the MOE. DIC was used to analyze the deformations on a small area around a knot, during a compression test of two pile segments. The results confirmed that the section with knots has a lower stiffness than the section without knots.

Sommario

Le città fondate su suoli di tipo paludoso, come Amsterdam e Venezia, sono caratterizzate da terreni con scarsa capacità portante, motivo per il quale vengono utilizzati pali di fondazione in legno. Essendo quest'ultimo un materiale naturale, le proprietà meccaniche dei pali vengono alterate dalla presenza di difetti strutturali, come possono essere i nodi. Al fine di comprendere questo aspetto, questa ricerca studia l'influenza dei nodi sul modulo di elasticità in direzione longitudinale dei pali di fondazione in legno.
Sono stati considerati 27 pali di abete rosso e pino (provenienti da Germania e Paesi Bassi), successivamente suddivisi in 110 segmenti ed analizzati. In particolare, sono stati considerati due principali parametri che più influiscono sulla rigidezza, quali la dimensione dei nodi e la disposizione di essi. Lo studio dei segmenti è stato condotto tramite test meccanici a grande scala che comprendono test a compressione e test di misurazione della risposta dinamica. L'analisi globale è stata validata testando dischi ottenuti da sezioni dei pali con e senza nodi, per analizzare ulteriormente, con test locali, l'influenza dei nodi sulla rigidezza longitudinale. Un Overall Knots Ratio (OKR) è stato definito analizzando la disposizione dei nodi di ogni palo di fondazione, e valutando come il modulo di elasticità è influenzato dalla dimensione, numero e disposizione di essi. L'influenza dei nodi è stata anche studiata creando un modello numerico per riprodurre la risposta dinamica dei segmenti di palo. Il modello conferma ancora che i nodi sono un fattore rilevante nella variazione di rigidezza dei pali di fondazione in legno. Infine, si è sviluppato un modello predittivo in grado di stimare il modulo di elasticità di un palo conoscendo la densità e la quantità di nodi nello stesso.
L'analisi dei dati ottenuti mostra che i nodi influiscono sulla deviazione delle fibre longitudinali e il modulo di elasticità. Quindi, le sezioni con nodi risultano avere una rigidezza molto bassa in direzione assiale di un palo che, per questo motivo, non è stata considerata nell'analisi. Inoltre, è stato stimato che la rigidezza dell'area attorno ad un nodo, dove le fibre sono deviate, sia leggermente più elevata del nodo stesso, ma ancora molto bassa. Infine, la larghezza di influenza equivalente è stata stimata approsimativamente come 1.5 volte la dimensione del nodo stesso.
Questi risultati sono stati studiati nel dettaglio con test di Digital Image Correlation (DIC). Questa tecnica è stata usata per meglio indagare il comportamento dei nodi nella variazione del MOE. Il test DIC è stato usato durante l'esecuzione di un test a compressione per analizzare le deformazioni di una piccola area attorno ad un nodo su due segmenti di palo. I risultati confermano che la sezione con nodi ha una rigidezza più bassa della sezione senza nodi.

Contents

List of Figures

List of Tables

Chapter 1

Introduction

Timber has a long history as a construction material for engineering structures. Its application can be found in many historic buildings, bridges and quay walls, all around Europe and north America. In particular, timber piles have been extensively used in areas with weak soils, due to their good performance and relative cost-efficient application.

Until the second world war timber pile foundations were the most common foundation method. It is estimated that 25 million timber piles are still in use nowadays around the world to support bridges and other types of construction on unstable ground [1]. In particular, the west part of the Netherlands is built in a river delta area that is a typical unstable soil. The ground in this area consists of sediment which has been deposited by the rivers over the years. This soft soil is not stable enough to support simple foundations for structures, so for centuries people used timber foundation piles to support structures on the stronger sand layers below the weak soil.

Nowadays, aging of the foundations can become a problem, since timber piles were driven into the soil up to 500 years ago. Therefore, the service life analysis of timber pile foundations is a crucial topic that involves the characterization and assessment of these structural elements, taking into account many aspects such as: material conditions, age of the structure, mechanical properties of wood, inspection techniques and biological degradation [1] , [2].

In order to study timber piles, it is important to gain insight into the mechanical and material properties of timber. In fact, timber used for engineering purposes is a non-homogeneous material, which is often characterized by the presence of defects such as: knots, grain deviations and irregular geometry. These defects can influence the mechanical properties making timber piles analysis difficult. In addition, several parameters could influence the strength of timber including wood species, origin, moisture content, and density.

Knots are the embedded basal portion of a branch in the trunk that causes deviations in the woody tissue. Therefore, the presence of knots causes deviations in the fiber direction affecting the anatomical structure of wood. The regions around knots present inclined fibers resulting in lower stiffness and strength when an axial force parallel to the fibers is applied. Thus, in the case of a timber pile, subjected to axial load during its service life, the presence of knots can be governing for the capacity of the pile. This is because only a very small amount of the load is taken up by the knots.

Figure 1.0.1: details of wood piles in Amsterdam (left) and wood knots in timber pile (right)

The effect of knots on mechanical properties of wooden piles can be influenced by factors such as: branch whorl that is the zone of the stem where several branches or knots occur at approximately the same cross-section (ISO 24294 2021), knot type (described in NEN-EN 1310), and knots layout on the surface of the pile [3].

In order to understand these processes and creating a sound basis for the assessment of wooden pile foundations, a large project has been initiated by the community of Amsterdam, with the goal of capturing many of the aspects that determine the current state of wooden foundations as well as their remaining service life estimation. This includes analysis of the geometry, stiffness and current short term strength of the piles [1].

The cultural heritage of foundations in the western part of the Netherlands is similar for each city due to the same soil composition, so spruce and pine piles represent almost all the wood species used for timber foundations in Amsterdam and Rotterdam area. It is estimated that spruce and pine piles include about 95% of all timber foundations in Rotterdam [2]. In this kind of piles, the presence of knots is mostly the failure initiating parameter [4]. This confirms the importance of knowledge about knots layout and their influence on the stiffness of the timber piles.

For timber piles, one strength class based on visual grading is defined in Dutch standard NEN 5491 (2010). The grade factors, defined with characteristic values in compression, were determined on the basis of experimental tests performed on heads of wooden piles with knots (van de Kuilen 1994). However, since this study investigated pile heads, values in compression for the full-length pile are not available.

Therefore, in accordance with the city of Amsterdam, the TU Delft started a research project to evaluate mechanical properties along the length of timber piles ([5] , [6] , [7]). On the basis of the data collected, in this thesis, the influence of knots as a stiffness-reducing factor of timber piles was studied over the length of the pile. Based on experimental tests, a model to predict the stiffness along the pile is presented.

Chapter 2

Literature Review

A little literature is available about the mechanical properties of wooden piles. For round wood, only strength classes based on visual grading are defined in Dutch standard 5491 (2010). This limits the optimal use of wooden foundation piles, and also hinders the research on the current state of existing foundation piles in Amsterdam.

In the standards, strength classes are assigned only to timber boards, which are visually or machine graded. Grading parameters can be knots (for visual grading) or modulus of elasticity and/or density (for machine grading). For these structural elements, studies were conducted regarding the influence of knots on the mechanical properties of timber beams subjected to bending [4] , [8] , or axial compressive strength of square cross-section [3].

In this chapter, a literature review is conducted on the most relevant studies about wood knots and modulus of elasticity (MOE), for a better understanding of the topic underlying this thesis.

2.1 Background and History

Timber piles have been used in construction for centuries. In the past, the main advantages of using wooden piles consisted of low initial costs and easy handling [9]. The use of driven piles was limited due to the difficulty in installation. With the invention of the steam engine, pile installation improved, as steam engines were utilized for pile driving to deeper levels. The oldest existing piled foundations in the city of Amsterdam date back to the 17th century. The usage of timber piles in this city became a traditional constructive process by the beginning of the 18th century [9].

The base level of timber piles in Amsterdam is typically of 25 centimeters of insertion into the first sand layer. Piles specifically used in Amsterdam have typical diameters ranging from 180 to 200 millimeters at the head and 120 to 140 millimeters at the tip. They are typically inserted 25 to 50 centimeters below the top of the first sand layer. A statistical analysis was carried out by Van Daatselaar, 2019, illustrating the variation of geometrical attributes of the piles (Fig.2.1.1) [10]. This analysis shows that the characteristics of wooden piles like density varies with the variation of the geometrical characteristics of the pile as length, diameter and tapering.

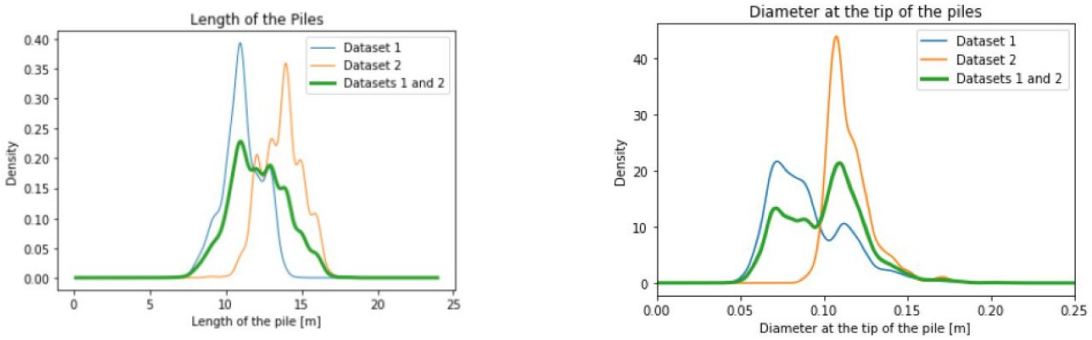

(a) Pile lengths

(b) Pile base diameters

Figure 2.1.1: geometrical attributes of piles in Amsterdam [10];

2.2 Natural Variability

Wood is a highly variable and heterogeneous material due to its biological origin. The natural high variability and heterogeneity of the material is the reason for complexity in the determination of the mechanical properties.

Wood can be described as an orthotropic material, meaning it has three mutual planes of elastic symmetry perpendicular to one another. The main is the longitudinal direction in which the fiber grows (parallel to the grain) [11]. Specific natural growth characteristics of trees have great influence on mechanical properties. These growth characteristics consist of aspects such as the existence of cross-grain, knots and branches [12]. The inclination of fibers due to the presence of knots, affecting mechanical properties locally.

The uncertainties and variability of mechanical properties, most significantly the modulus of elasticity, play a major role in the analysis of wooden piles [12]. Therefore, assuming an average constant modulus of elasticity along a timber pile does not take into account the variation in stiffness that is caused by knots and related fibers deviations.

2.2.1 Wood General Structure

Wood is a natural and organic material and it is composed of cellulose, hemicellulose, lignin and other elements. When a tree grows the wood developed in longitudinal direction of the cell walls leading to an anisotropic behaviour of the wood [13].

The most timber piles used in Amsterdam are made of coniferous trees [9]. In particular, the most common wood species used consist of pine and spruce. The structure of this type of wood is consistent of long strands connected together with small openings in the cell wall. These openings, called pits, allow for fluids to flow through cells. Therefore, timber consists of cells, composed of wood substance, that are cemented together by lignin. Fig. 2.2.1 illustrates the micro structure of a coniferous wood sample.

The trunk has the aim to support the crown and to grow longitudinally to get more energy from the sun (due to photosynthesis). For this reason, each part of a tree has different purposes and different compositions.

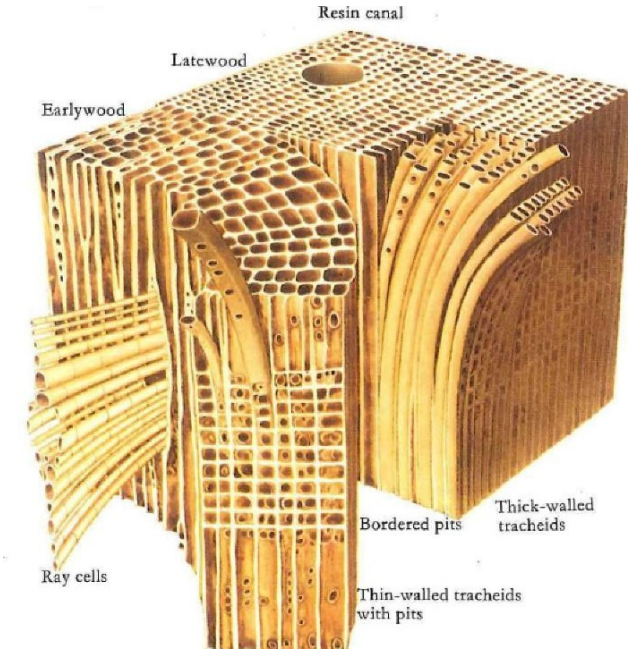

Figure 2.2.1: wood structure in softwood [14];

A cross-section can be subdivided in different areas and the density of each division can be different from the other (paragraph 2.2.1.1). The faster diameter growth in thinned stands can cause an increase in the size of the centre of juvenile wood [9]. In thinned stands, branches and hence knots are bigger and may be associated with more reaction wood [15].

The natural variability caused by the division in parts and tapering of a tree trunk creates a rather complex nature for wooden piles.

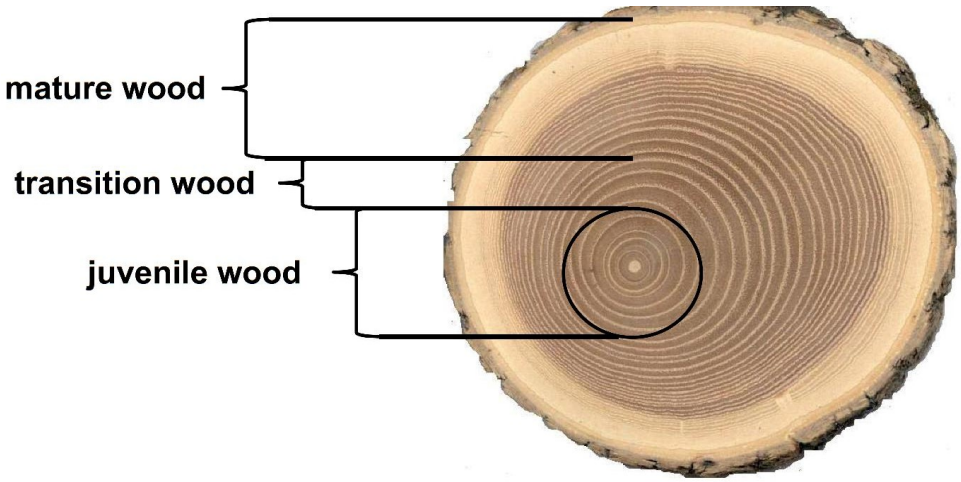

Figure 2.2.2: cross-section of tree [14];

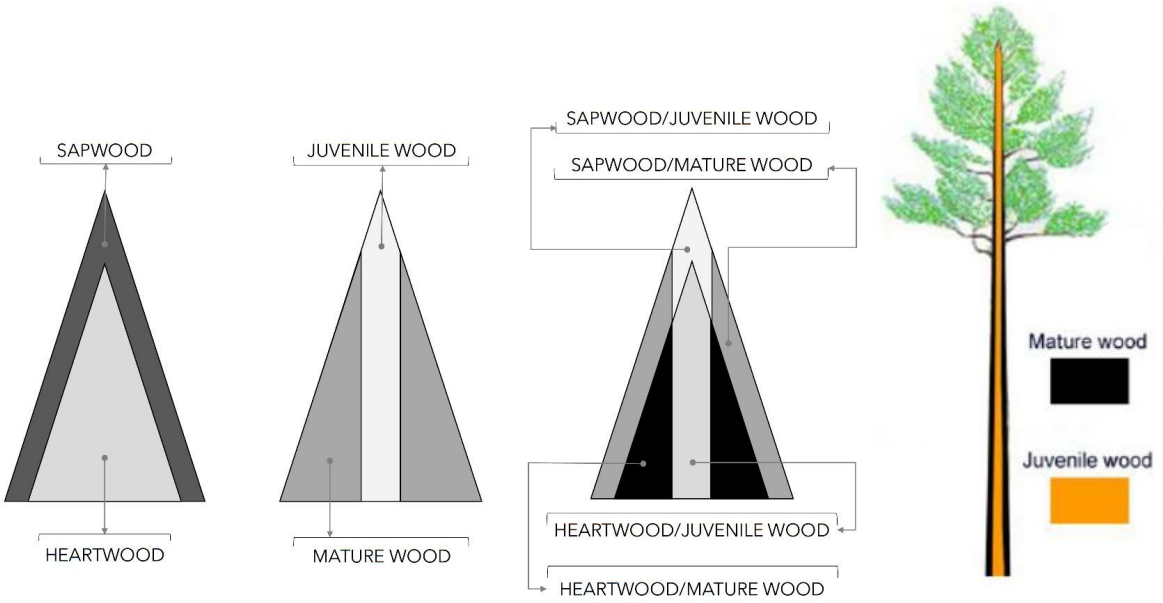

Figure 2.2.3: different type of wood along the length of a tree [9];

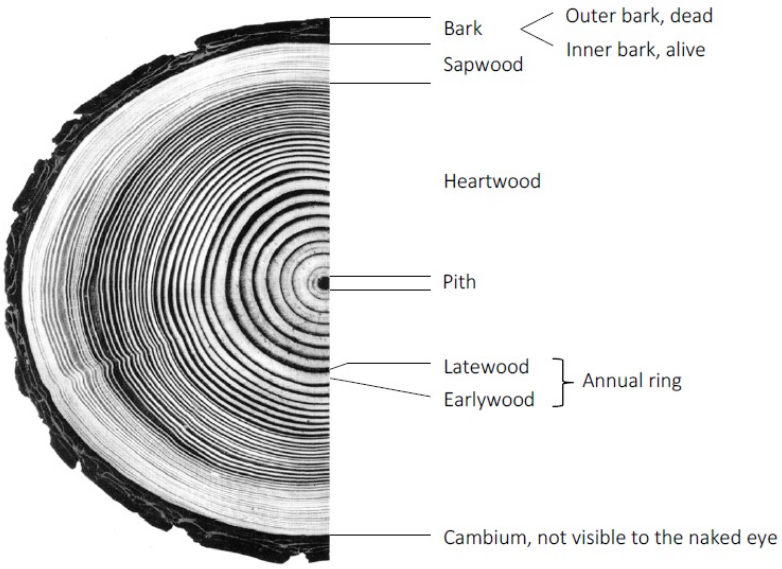

Figure 2.2.4: structure of the cross-section of a tree (Grosser,1977) [16];

2.2.1.1 Structure

Pith The pith is the center of a tree and its size is in the order of millimetres. The aim of the pith is to support the top-part transporting the water along the trunk.

Heartwood and Sapwood The external portion of the trunk is known as sapwood. Similar to the pith, sapwood contains water with functions as a storage recipient. Sapwood is made of living and physiologically active wood cells.
The inner portion, called heartwood, contains living cells and with the aim of stabilising and strengthening the tree [13] , [16] .

Cambium The cambium is a thin layer between the wood and the bark. This is the point in which the wood cells die, forming the bark.

Bark The outer bark comprises dead cells and functions to protect the trunk. The inner bark is made up of living cells and transports nutrients produced in the crown to the cambium and storage cells [13] , [16] .

Juvenile and Mature wood It is possible to distinguish the trunk into juvenile and mature wood. The part of the wood from the pith to the exterior is defined as juvenile wood; the part formed after the transition period is called mature wood [17]. This division is shown in Figure 2.2.2 with a combination of sapwood/heartwood and juvenile/mature wood (Figure 2.2.3) [9].

2.2.1.2 Taper

The geometry of each part is highly variable along the length of a pile. This is due to the tapering nature of a growing tree. A decline in diameter can be see in a tree starting from the base until the top part (Fig. 2.2.6) and it varies from 0.5 to 1 cm/m depending on types of tree [18] . The tapering leads to a reduction of the diameter of the trunk along a tree and a different kind of wood. Other study conducted in Amsterdam shows that the average tapering of piles in the city is assumed to amount to approximately 8 millimeters per meter length [9] , [10] . Figure 2.2.5 illustrates the variation in density correlated with tapering of piles extracted in Amsterdam. It was observed that the difference in tapering between piles is relatively small.

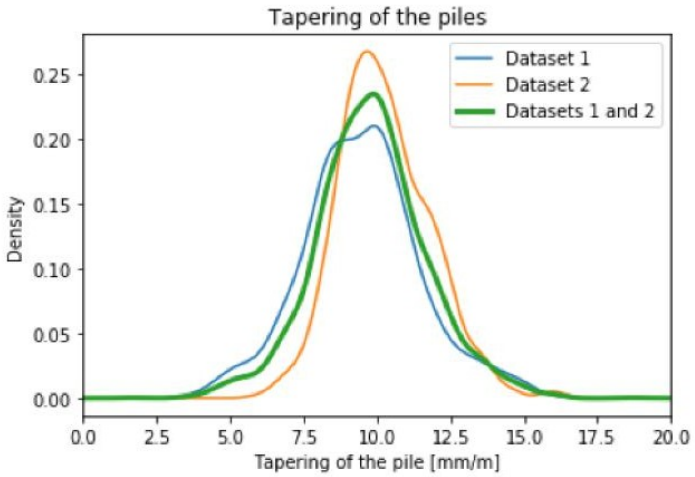

Figure 2.2.5: density and tapering of piles in Amsterdam [10];

2.2.1.3 Knots

Knots are the embedded basal portion of a branch in the trunk (fig. 2.2.7) that causes deviations in the woody tissue [3] . As a tree grows and increases the circumference of its trunk, the growing trunk begins to overtake the branches that grow out from it. Therefore, the presence of knots causes deviations in the fiber direction affecting the anatomical structure of wood [19] . Knots have a high influence on the wood structure. The fibers have to grow around the knot, therefore a knot cause a deviations from the straight grain. In general, this deviation can be higher on the top-part because the diameter of branches tends to increase on average from the bottom to the top of the tree [13].

Figure 2.2.6: tapering of a tree from *swedishwood* website;

Figure 2.2.7: branches on the cross-section of a tree [13];

2.2.2 Wood Physics and Properties

2.2.2.1 Moisture Content

The moisture content has a relevant influence on properties of wood; in particular on stiffness, strength, creep and biological attack.

When wood is dry, the cellulose chains are close together and this condition leads to strong intermolecular forces (the stiffness of wood increase). When the moisture increase due to the presence of water, the hydrogen bonds between the cell walls are weakened. Properties of wood are influenced by its moisture content that must be considered [20] . This phenomenon occurs until the point at which the excess water is accumulated in the cells cavities [13].

$$\omega = \frac{m_{wet} - m_{dry}}{m_{dry}} \cdot 100$$

where:
- ω *[%] : moisture content of the wood;*
- m_{ω} *[g] : mass in wet condition;*
- m_{dry} *[g] : mass in dry condition.*

When wood cells cannot absorb water more, the excess water becomes free water into the cavities. This value of ω is called fiber saturation point FSP (usually between 25 and 35%). When the moisture content is above FSP, the mechanical properties become constant for different values of ω. In the study of Nocetti M. (2014), the effect of moisture content on the modulus of elasticity is described with a specific equation reported in figure 2.2.8. The constant value of MOE above FSP is shown in figure 2.2.8.

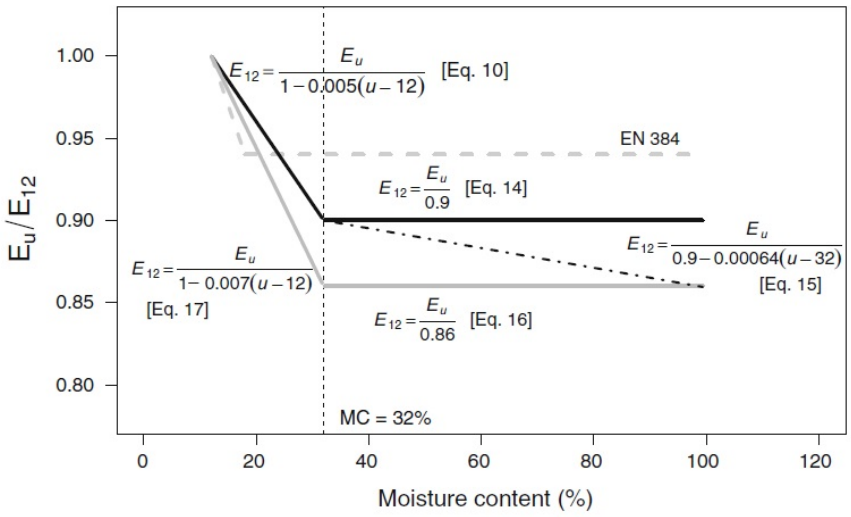

Figure 2.2.8: variation of the mechanical properties for different values of moisture content. Comparison between theoretical (gray lines) and observed (black lines) average adjustment equations [20].

2.2.2.2 Density

The density is defined as the ratio between the mass and the volume. The higher is the density of wood, the higher is the cell walls inside the wood at constant moisture content. At the same time the properties increase [13].

$$\rho_\omega = \frac{m_\omega}{V_\omega}$$

where:
- ρ_ω *[kg/m^3] : density of the wood at moisture content* ω*;*
- m_ω *[kg] : mass at moisture content* ω*;*
- V_ω *[m^3] : volume at moisture content* ω*.*

2.2.2.3 Stiffness

Wood shows different properties when load is applied in different directions due to its natural origin. Therefore, wood is an anisotropic material [13] . In tension parallel to the grain, wood has a brittle behaviour. However, in compression parallel to the grain wood has a plastic behaviour. The stiffness significantly decreases when the force is applied perpendicular to the grain (figure 2.2.9).

The typical values of the modulus of elasticity are [13] , [21] :

- parallel to the grain : $E_0 = 11000 \div 15000 Mpa$;
- perpendicular to the grain : $E_{90} = 400 \div 500 Mpa$.

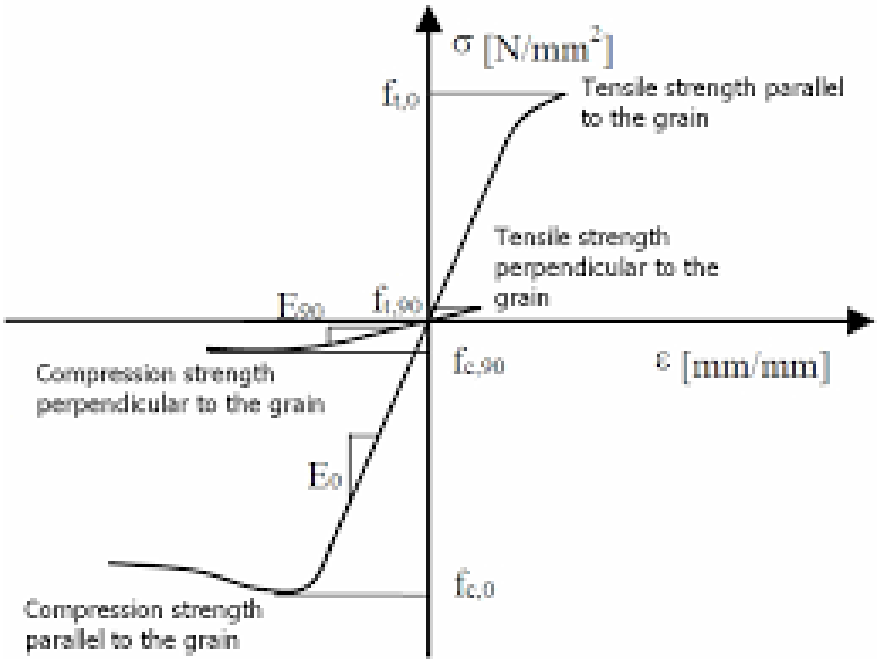

Figure 2.2.9: stiffness perpendicular to the grain E_{90} and parallel to the grain E_0;

2.3 Reference Standard

The presence of knots is one of the most influencing parameters that affect the mechanical properties of timber. Knots have been studied to evaluate the influence on mechanical properties and to define grade boundaries in wooden beams [4].

In the last decades, the improving knowledge on the topic has led to a standardization of the method to evaluate the presence of knots. In the Netherlands, the procedure to take into account the presence of knots in timber boards are reported in NEN-EN 1310 and NEN 5499 (Figure 2.3.1).

In these standards, the method for the classification of knots depends on the type of knot (round, oval, arris,...). The size shall be the width of the knot or knot cluster, measured at right angles to the longitudinal axis of the piece (NEN-EN 1310). However, this method does not take into account the influence of knots on the fibers orientation.

Knots with a diameter smaller than 7 mm are not considered in accordance with NEN 5499, since small knots do not significantly influence the mechanical properties of timber.

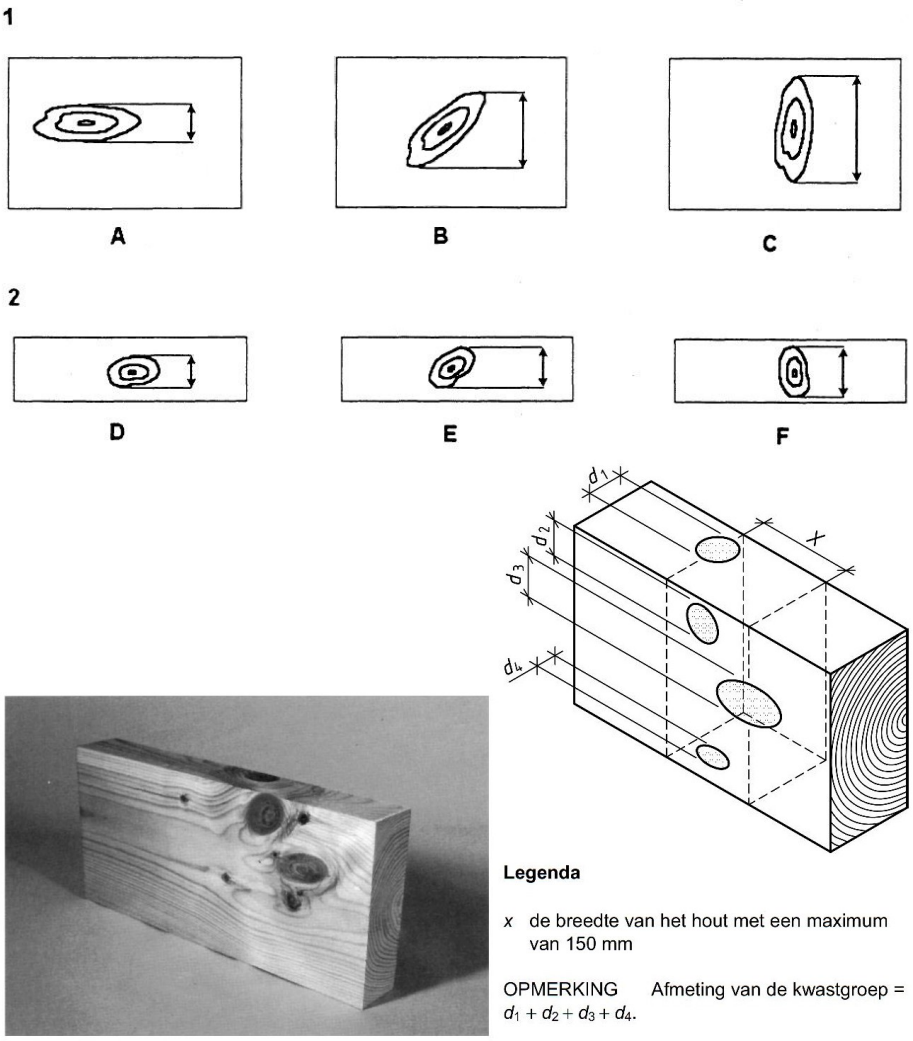

Figure 2.3.1: types of knot in NEN-EN 1310 above and width of knots in NEN 5499 below;

2.4 Knots

Since the MOE and the compressive strength are influenced by knots, it is important to find a correlation between size, position of knots and the MOE.

2.4.1 Knots layout

A method for the classification of knots in the cross section of timber beams and piles is being introduced by several studies carried out at TU Delft [5], [6], [7]. This is done through the determination of a knot ratio, based on an observation of the presence of knots on the pile surface.

For example, in a beam section, the presence of knots is often quantified as a knot ratio, which can be defined as the knot dimension divided by the beam side dimension but the dimension of the knot differs between national visual grading standards. The following equation gives an example of the knot ratio defined as the ratio between knot dimension d_1 perpendicular to the beam axis and the beam width h perpendicular to the beam axis (see Fig.2.4.1):

$$KR = \frac{d_1}{h}$$

where:
- d_1 *[mm] : knot dimension perpendicular to the beam axis* ;
- h *[mm] : beam width perpendicular to the beam axis* ;

The knots influence on the mechanical properties of timber beams is studied by Vieira et al. [3]. The classification of the knots was divided in 3 classes: class 1 for small knots up to 8.31 mm^2, class 2 for medium knots from 8.31 mm^2 to 33.43 mm^2 and class 3 for large knots from 33.44 mm^2 to 105.36 mm^2 [3] in specimens with nominal dimensions of 100 x 25 x 25 mm. Unfortunately, this is a basic classification and it cannot be directly used for wooden foundation piles.

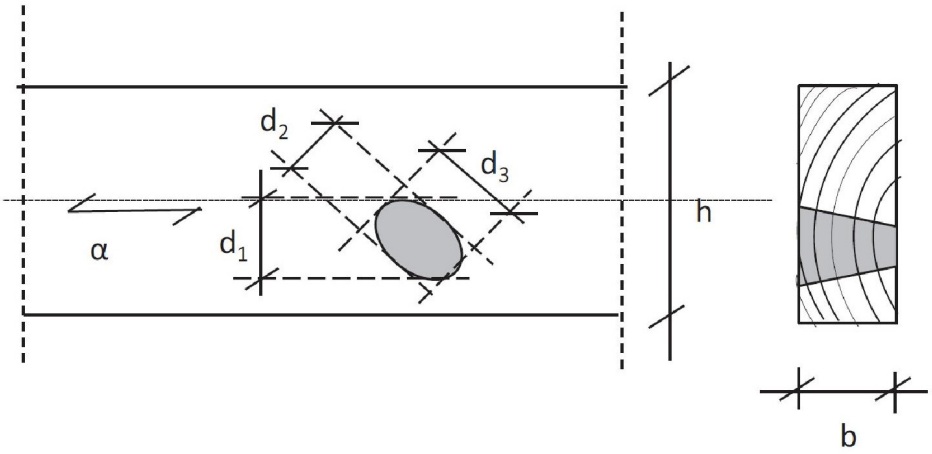

Figure 2.4.1: example of KR calculation for timber beams [4];

2.4.2 Knots shape

Knots in wooden piles have a three-dimensional development. In two studies carried out by TU Delft [22], [23], a CT scanning analysis, based on density variation, was performed on pile segments. Since knots have a higher density than the surrounding wood, it is clear to distinguish between the two. From these tests, the shape of knots is shown figure 2.4.2 on the left. A clear behaviour of the growth of branches inside the trunk is shown. Knots start from the pith and continue to the bark with a conical shape.

Another characteristic is shown by Kavelaars (2019) and Lukacevic (2014), knots have a higher density than the rest of the pile. In dry conditions, density of a knot (ρ_{knot}) can varies about 2 times the density of wood without knot [24], [25]. The knot has higher hardness as well as the tensile strength due to the higher compactness of cells present into the knot [19].

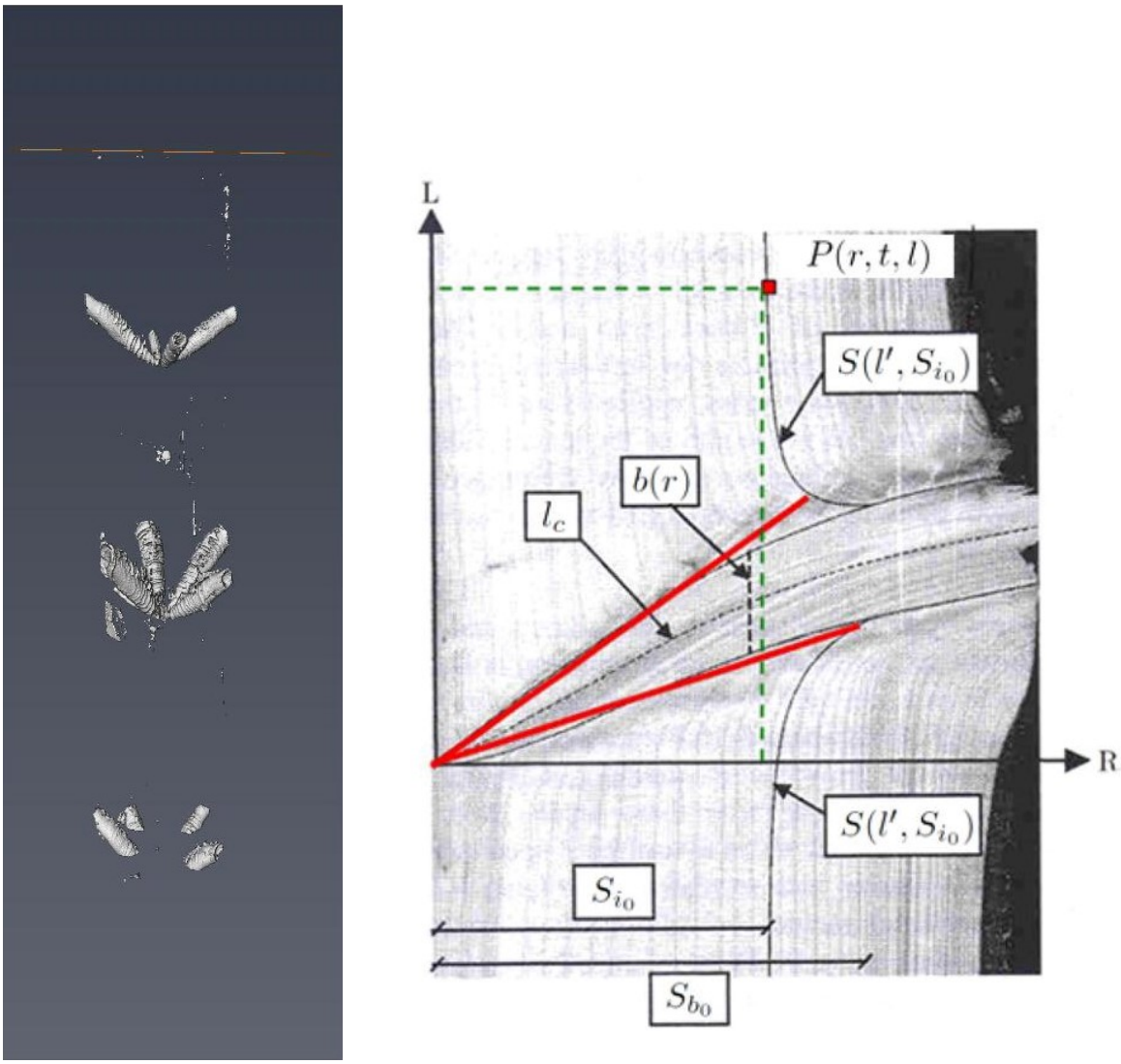

Figure 2.4.2: CT scan on a wooden pile on the left [23], the tapering of a knot [24];

2.5 Dynamic MOE

The measurement of the dynamic MOE of timber with stress wave measurements consists in a nondestructive evaluation method that can be used to assess the stiffness of wood. Stress-wave-based nondestructive testing techniques have been investigated extensively during the past few decades, showing good results for the investigation of the mechanical properties of wood. The research conducted in Wang et al. (2001) [26] shown a good correlation between longitudinal stress-wave-based modulus of elasticity (MOE) in logs and static MOE of segments cut from the log. Therefore, longitudinal stress wave methods can be used to evaluate the stiffness of wooden piles.

These measurements are carried out according to the following procedure. The specimens are placed on two sticks to avoid the influence of the floor and they are tested in the longitudinal direction. Longitudinal stress waves are generated on one end using a hand-held hammer with the accelerometer attached to the opposite end. Following a mechanical impact, a stress wave propagates back and forth along the length of the specimen. The stress wave signals are detected by the accelerometer, and the waveform is monitored and recorded by the software. Subsequently, the vibration signal acquired in the time domain is converted into the frequency domain using fast Fourier transformation (FFT). The first three eigenmodes are obtained from the resulting FFT spectra.
Subsequently, the specific longitudinal modulus of elasticity and shear modulus are evaluated using Timoshenko beam equations [27] with a dedicated software that determines the resonance frequency with high precision and calculates elastic properties. The following figure (Fig. 2.5.1) shows a typical signal obtained by monitoring the propagation of longitudinal stress waves in a pile section.

The stress wave speed (SWS) is determined by coupling measurements of the time Δt between pulses and the length L of the specimen by:

$$SWS = \frac{2L}{\Delta t}$$

where:
- *L [mm] : length of the specimen;*
- *Δt [s] : time request to the wave from the input of the hammer to the accelerometer;*

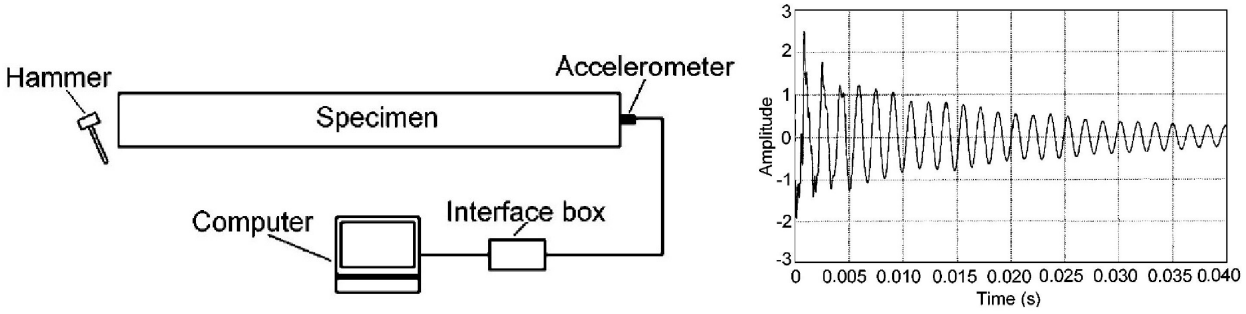

Figure 2.5.1: signal obtained by hammering a wooden pile and therefore converted in frequency with FFT (fast Fourier transformation) [26];

Based on stress wave measurements, the dynamic MOE (MOE_{dyn}) of piles is calculated using a one-dimensional wave equation:

$$MOE_{dyn} = (SWS)^2 \cdot \rho$$

where:
- ρ *[kg/mm^3] : density of the specimen;*

The stress wave is variable along the length of a pile. The head (biggest section of the pile) exhibits higher values of SWS than the next several sections in a wooden pile. This behaviour is related to the different service conditions that these two sections experienced in their service life [26] (as shown in fig.2.5.2).

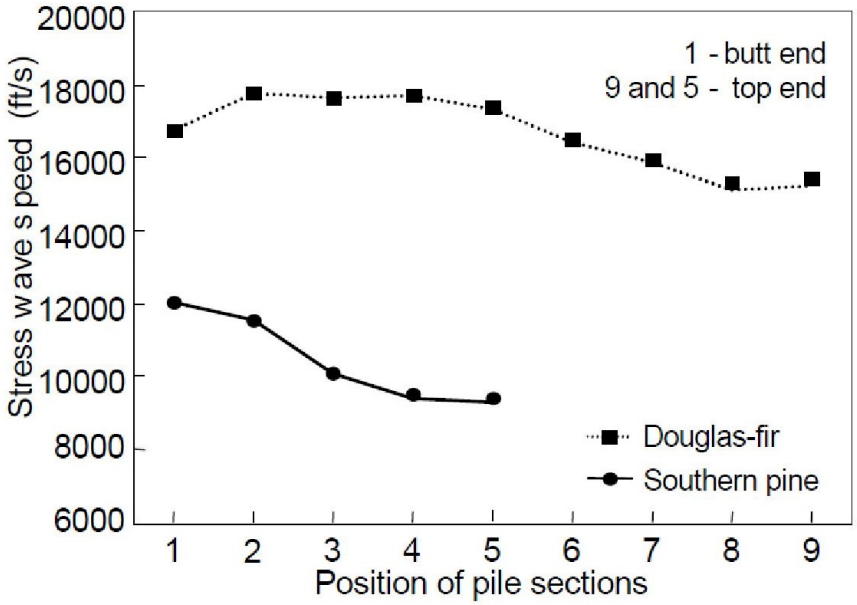

Figure 2.5.2: variation of SWS values along the pile [26];

2.6 Correlation Between Knots and MOE

A few articles studied the influence of knots in wooden beams. In Ravenshorst et al.[4] the knots influence in timber beams was taken into account calculating a KR as previously mentioned (par. 2.4.1). In this research, the MOE for timber beams tested in bending was calculated considering the reduction of the stiffness caused by knots:

$$MOE_{KR} = (\rho C_2 + \varepsilon_M) \cdot (1 - C_8 KR)$$

where:
- ρ *[kg/mm^3] : density of the beam;*
- C_2 *[-] : ratio between the clear wood stiffness and the density;*
- C_8*[-] : magnitude of the influence of the knot ratio on the reduction of the bending MOE;*
- ε_M *[-] : scatter around the mean regression lines for the MOE;*

$$\varepsilon_M = X_1 v_m \rho C_2$$

where:
- X_1 *is a stochastic variable following the standard normal distribution N(0,1);*
- v_m *is the coefficient of variation for the error for the bending strength.*

A correlation between the MOE and KR was determined. In general, a decrease of the MOE was observed between the analysed specimens. (Fig.2.6.1).

A reduction ratio was calculated:

$$red, ratio_{MOE} = \frac{E_{KR}}{E_A}$$

where:
- E_{KR} *is the modulus of elasticity reduced due to the presence of knots;*
- E_A *is the modulus of elasticity of wood without knots.*

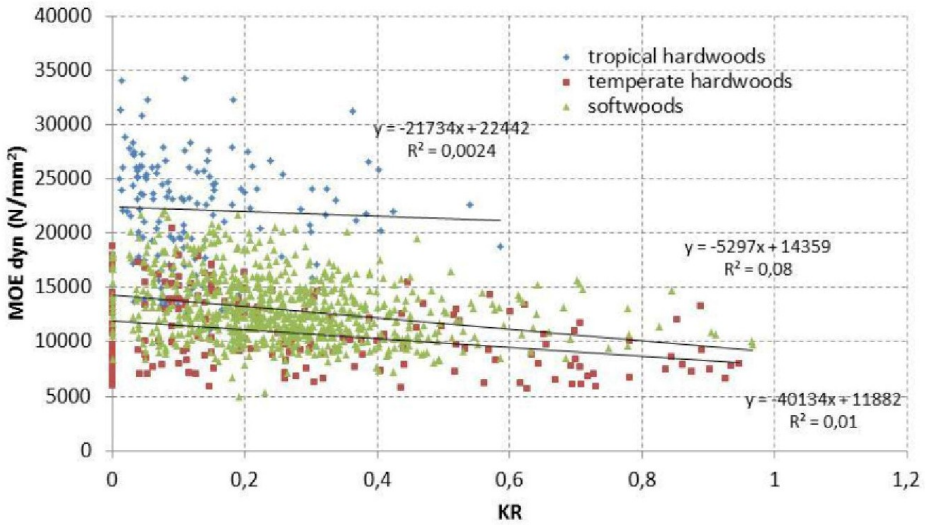

Figure 2.6.1: correlation between KR and bending MOE for different type of species [4];

This ratio describes how the MOE value is influenced for different KR, compared to the bending MOE value of wood without knots (Fig.2.6.2). The average values of samples with knots ratio equal to zero were studied [4] . The unreduced MOE (E_A) was calculated considering the analyzed samples.

In Vieira et al. [3], the variation of the longitudinal MOE obtained testing wooden beams in compression parallel to the grain was studied, considering wooden beams with the same mechanical properties but with different knots layout (par. 2.4.1). The difference in the MOE between beams with different classes of KR was estimated: 6.26% for Class 1, 15.22% for Class 2 and 23.20% for Class 3 as shown in Fig.2.6.3.

A correlation between the MOE of the beams without knots and the MOE of the beams with knots is shown, presenting coefficient of determination R^2 values of 0.309, 0.312 and 0.280 for Classes 1, 2 and 3 respectively. The mechanical strength during compression parallel to the grain presents a tendency for reduction in the precision of the models with the increase of the area of the knot [3].

In the end, the effect of knots on the mechanical properties of wood depends on the dimensions occupied by these defects in the wood. Therefore, the area occupied by knots presents an inverse correlation to the wood mechanical properties (figure 2.6.3).

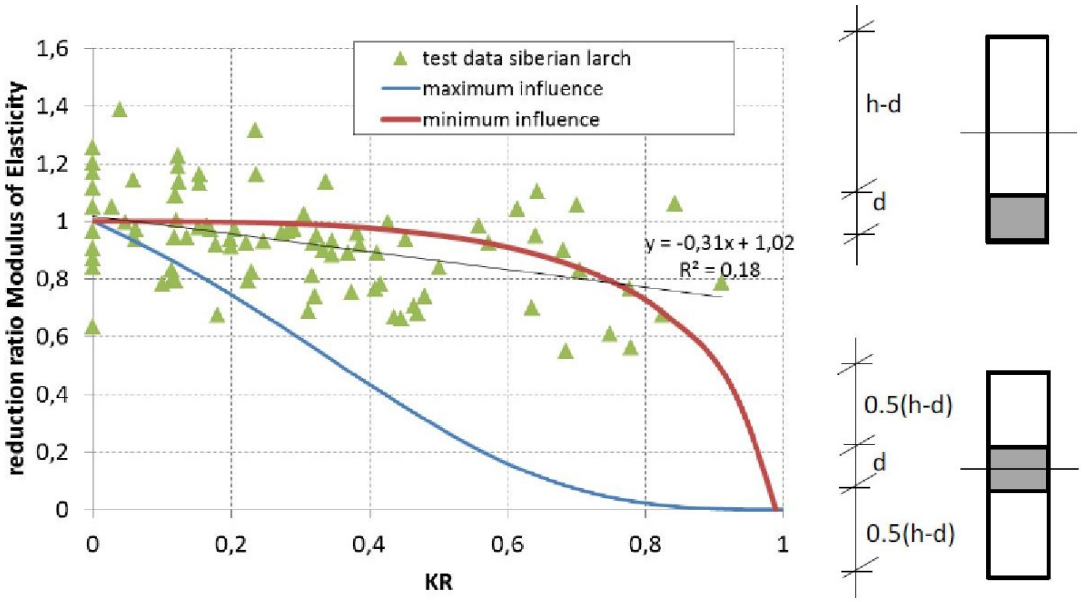

Figure 2.6.2: on the left the correlation between KR and bending reduction ratio MOE for different type of species, on the right two positions for a knot with the same size (top figure: maximum influence for the KR-value; bottom figure: minimum influence for the KR-value) [4];

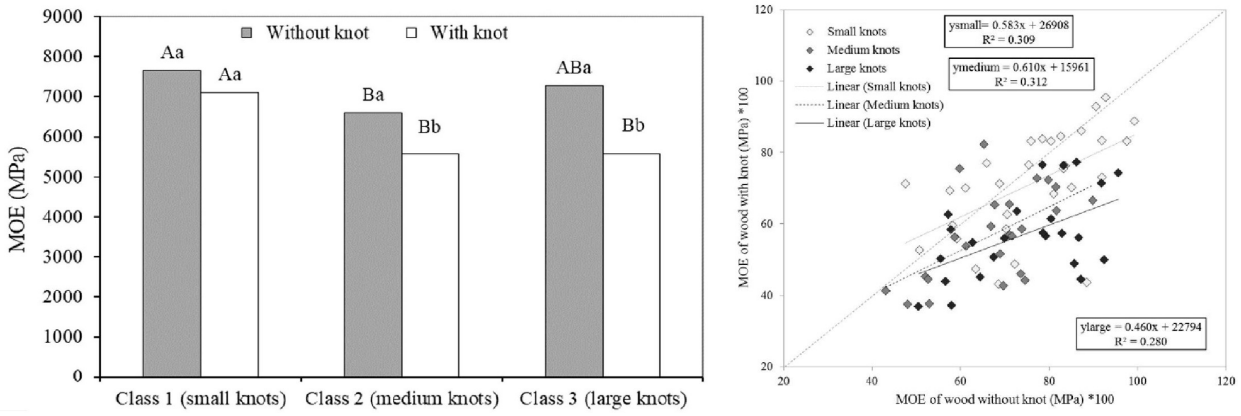

Figure 2.6.3: on the left a direct comparison for similar wooden beams (same diameter and same length) but with different influence of knots, on the right a linear regression analysis to analyse the variation of the MOE in samples with knots and samples without knots [3];

2.7 DIC Test

In the last decade, the utilization of non-contact deformation measurement systems based on digital image correlation (DIC) increased in the area of wood technology research [28] , [29] , [30] , [31] . Based on deformations measured by DIC systems, high resolution strain fields on the surfaces are calculated.

This technique is widespread due to its high precision. It is based on strain measurements from many images acquired during the application of the loads. For example, some advantages of this method are the precision of the strain measurements and the calculus of the modulus of elasticity without the need of conventional instrument such as linear potentiometers usually adopted for compression tests.

The equipment used in this test includes: parts of camera, lenses, calibration tables, lighting, commercial software for image acquisition and processing. It is assumed, according to the Euler–Bernoulli beam theory, that plane cross-sections perpendicular to the longitudinal axis of the beam remain plane and perpendicular to the longitudinal axis during the deformation. The latter means that no shear deformations are supposed to occur.

Research by Ali Abdulqader et al. [29] shows a 3D DIC test on a concrete sample. In that research, it was used StereoDIC, non-contacting technique capable of acquiring surface strain measurements as small as $50\mu\varepsilon$ (ε=10^{-6}) and displacements as small as 10 μm.

The tests procedure was divided into 3 steps:

1. Cylindrical surface was first sprayed with a flat, bright white paint. Subsequently, the speckled pattern was applied either with a black ink 0.5mm pen or sprayed on.

2. Before each test, the DIC camera system was calibrated by taking images of a calibration tablet in order to determine the geometric attributes of the camera system. The calibration tablet was placed near the specimen and a pair of images were acquired at each orientation [29]. The typical definition of images are 30x30 or 40x40 pixels in order to take second order displacement gradients into account [32]. In this test, 50 images were taken before the application of the load and for each load step till the end of the entire compression test.

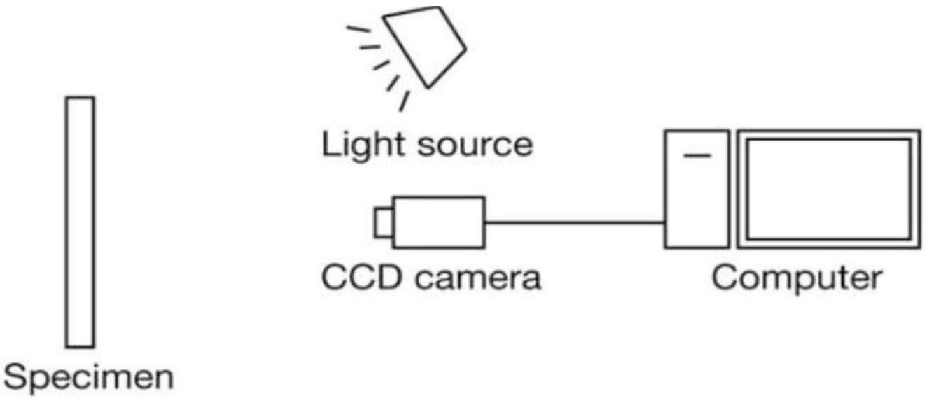

A. Abdulqader, D.C. Rizos

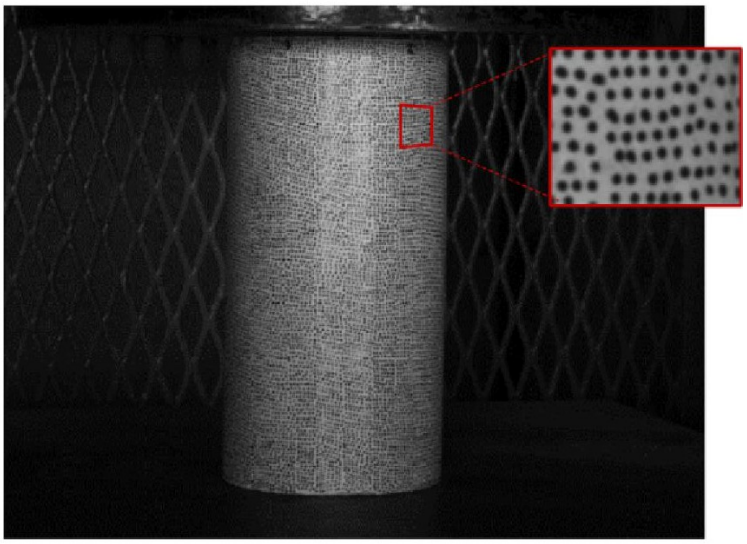

Figure 2.7.1: the test setting of a DIC test above [32]; an example of sprayed surface below [29];

3. The analysis of the images has the aim to search a matched point from one image to another. By comparing these images, the strain and the MOE were evaluated.

The precision of the test can be as high as the precision of conventional instrumentation. It can be extract a large amount of data compared to conventional methods, suitable for statistical analysis in estimating the desired properties.

Another study carried out by Hu Min et al. [28] performs a DIC test on a wooden beam. The procedure was the same as before, but in this case, the influence of a knot in the case of bending a beam was evaluated.

The following image (Fig.2.7.2) shows multiple knots in the examined board. If smaller knots are disregarded, the remaining larger knots are grouped into a number of clusters scattered along the x-direction and any sections between are more or less free from knots. When comparing the strain distribution to the board images, strain concentrations at knots emerge very clearly. Furthermore, some strain concentrations are also located where no knots are visible on the examined surface, but on other surfaces at the same position in the x-direction.

The E_b profile represented by the light blue line was thus calculated as:

$$E_b = \frac{E_{b,1} + E_{b,2} + \dots}{n}$$

while the E_b profile represented by the darker blue line was calculated as:

$$E_b = \frac{1}{(\frac{1}{E_{b,1}} + \frac{1}{E_{b,2}} + \dots)\backslash n}$$

At the end, the research concludes that MOE profiles established on the basis of different load levels were almost identical, and the result is thus regarded as stable and reliable. The MOE profiles illustrate weak sections along the board, due to the presence of knots and knot clusters, in the form of local drops in the curve [28].

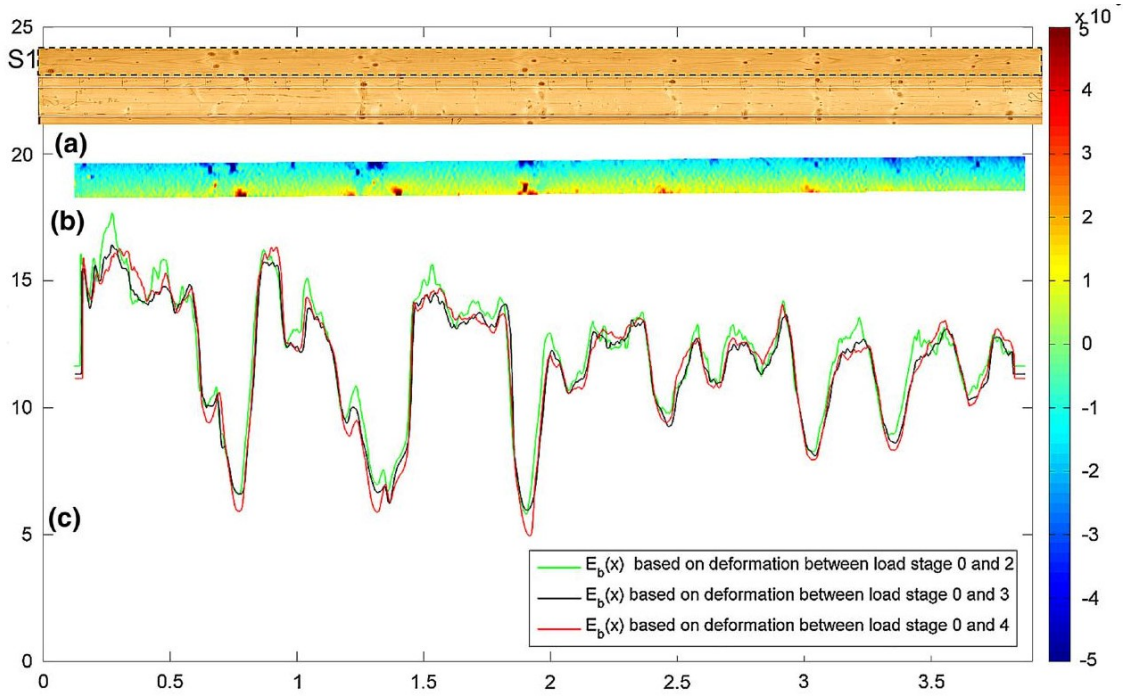

Figure 2.7.2: analysis of the MOE in longitudinal direction with DIC [28];

Chapter 3

Research Questions

The research investigates the influence that knots could have on the mechanical properties of timber piles. In particular, these defects modify the slope of the grain around the knot area, causing a local stress alteration.

Since wooden foundation piles are subjected to axial loads in the longitudinal direction during their service life, knots could have a significant effect on the fiber deviation with a consequent alteration of the stiffness. In order to investigate this problem, the following overarching question was formulated:

Which is the influence of knots on the Modulus of Elasticity (MOE) of wooden foundation piles?

In order to answer to the main research question, other sub-research questions were formulated:

1. *Is it possible to estimate the presence of knots on the surface of a wooden foundation pile with a knots ratio?*

2. *How can the MOE of a wooden foundation pile be evaluated ?*

3. *Is it possible to find a correlation between the knots ratio and the modulus of elasticity of a wooden foundation pile?*

4. *How can the MOE around a knot area be evaluated by testing a wooden pile in compression?*

5. *Is it possible to obtain an equation to predict the influence of knots on the modulus of elasticity?*

Chapter 4

Materials

The following materials were investigated in this research:

- 18 spruce (*picea abies*) piles from the Netherlands;
- 9 pine (*pinus sylvestris*) piles from Germany.

All piles were felled in 2019, they had an average length of 14 meters, average head diameter of 255 mm and average tip diameter of 145 mm. The piles were driven into the ground in a test field in Amsterdam with the main objective to determine geotechnical parameters (Fig.4.0.1).

In spring 2021, the 27 wooden piles were extracted from the location, cut in three parts and transported to the TU Delft Stevin 2 laboratory. At the arrival, all the piles were cut into 110 segments with a length of approximately six times the average diameter.

Figure 4.0.1: pre-load in situ of piles driven in Amsterdam, 2019 (left); timber piles extraction and storage in Amsterdam, 2021 (right);

When piles were cut, each one was divided in 3 main parts, respectively:

- K: kop (head-part);
- M: middenstuk (middle-part);
- V: voet (tip-part).

For most piles, three segments (sawn from the head, middle and tip part) were tested according to the procedure described in section 5.2. For six piles, eight segments over the length of the piles were tested to gain insight into a more precise distribution of knots and stiffness along the pile. Segments K x.x K (the first segment of a pile) were not taken into account for the evaluation of the mechanical properties due to the smallest length in a longitudinal direction compared with others segments. The coding scheme remains the same, so each main part (K, M and V) was subdivided in other sub-parts which are coded as follows:

- Head-part: K1.1K - K1.1M - K1.1V;
- Middle-part: M1.1K - M1.1M - M1.1V;
- Tip-part: V1.1K - V1.1V.

With the aim to obtain a more precise distribution of knots and stiffness along the pile, last segments (which are identified as Vx.xV) were subdivided in others 3 segments. All segments of a pile can be observed in figure 4.0.2.

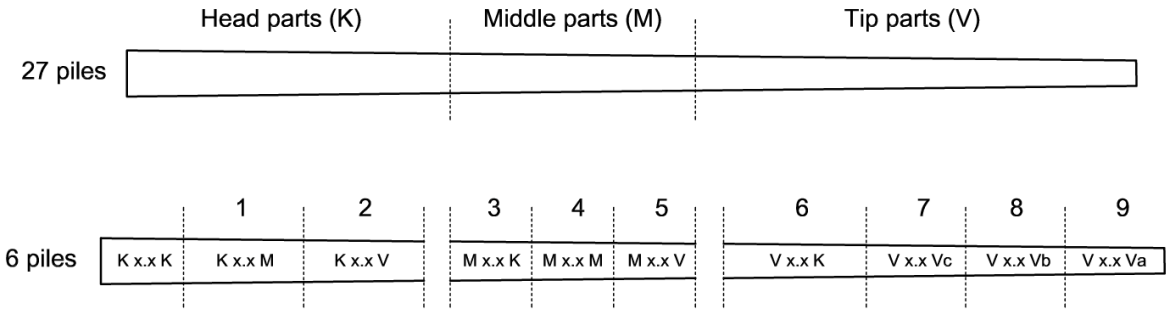

Figure 4.0.2: labelling of a pile before begin tested and stored;

Figure 4.0.3: tank filled of water, at TU Delft laboratory, to dive piles under water ;

In order to reach moisture content values above fiber saturation point during tests (water saturated condition), the wooden piles were stored in wet conditions for the pre-processing purpose in a container outside the laboratory (Fig. 4.0.3).

At the end, for three segments that were tested, two disks were sawn (Fig.4.0.4):

- three 100 mm thick wooden disks sawn from a section of piles without knots, i.e. a clear wood section of the same pile segments.
- three 100 mm thick wooden disks were sawn from a section of piles with knots.

The six total disks were subsequently tested in compression, in water-saturated condition.

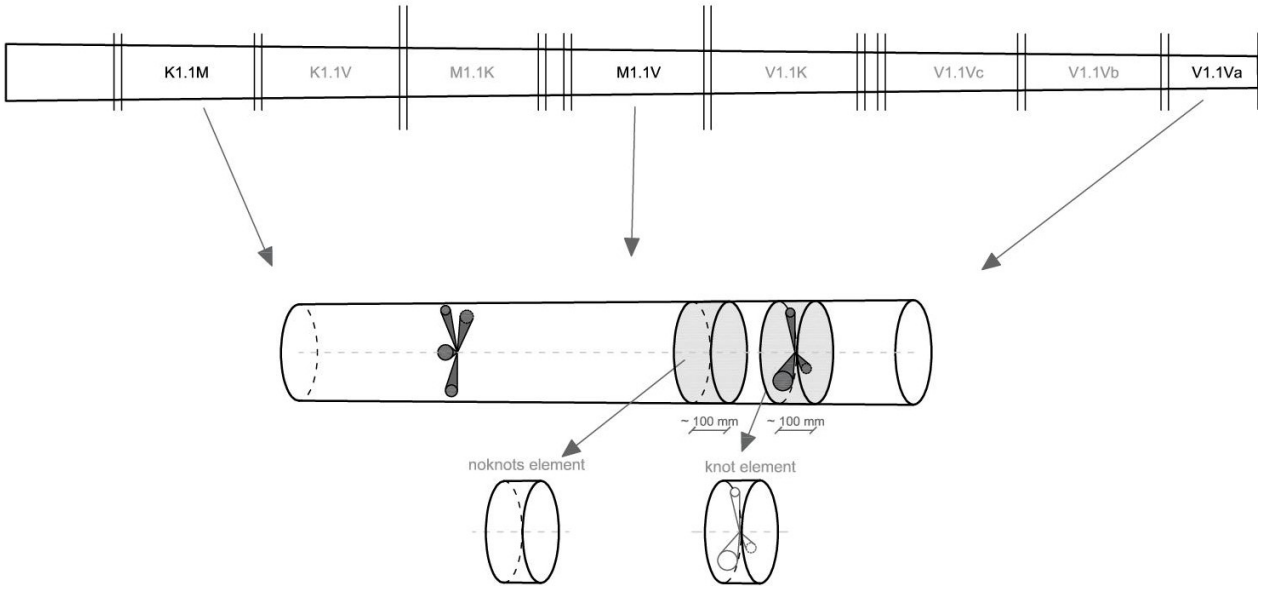

Figure 4.0.4: cutting of the disks with and without knots;

Figure 4.0.5: two wooden disks cut from segment M1.1V;

Figure 4.0.6: cutting procedure of the pile M1.1V;

Chapter 5

Methodology

The research is presented in a general framework where the main stages of the methodology are shown.

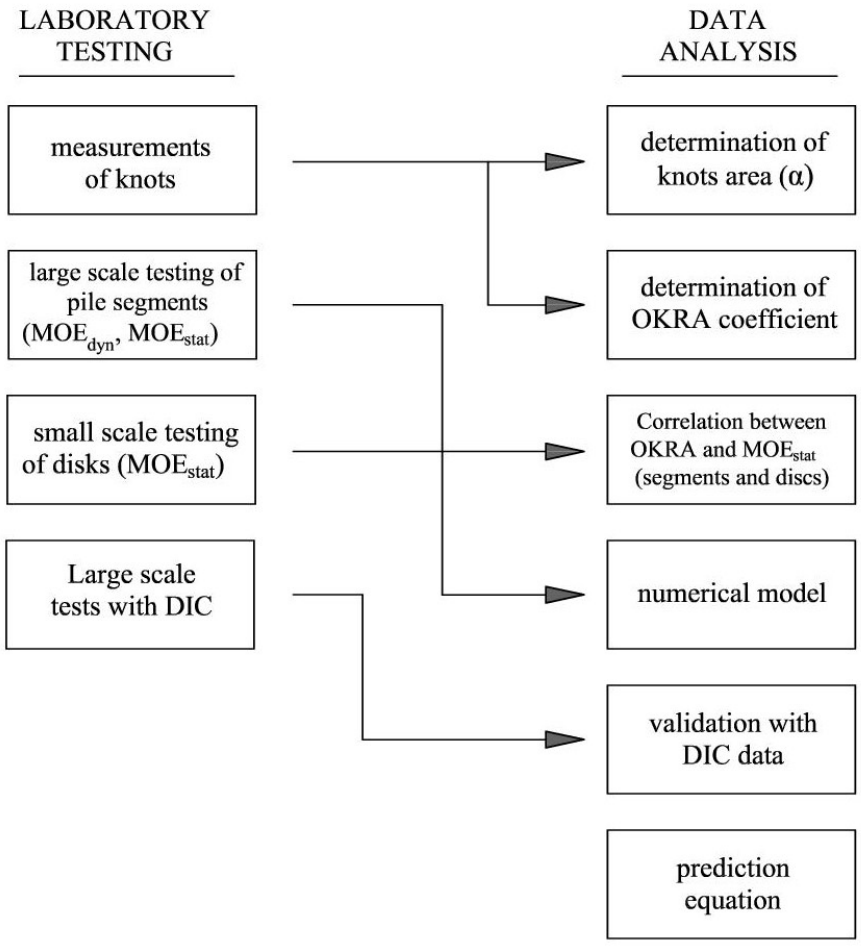

5.1 Knots Evaluation

5.1.1 Knots Measurement

The knots layout of timber piles was calculated considering both the diameter of the knot itself (d_1) and the diameter around the knot where fiber deviations were visible ($d_1 + \alpha d_1$)(Fig.5.1.1). With this method, the influence on the stiffness of zones where fibers are not parallel to the axial load could be taken into account.

For this reason, one of the aims of this thesis research is to evaluate the inclination of the fibers due to the presence of knots.

The coefficient α is a geometrical factor. It considers the size of the fibers deviation around a knot, and it is visually measured. In order to define α, 205 knots were analysed.

$$d_2 = d_1 + \alpha \cdot d_1 = d_1 \cdot (1 + \alpha)$$

where:
- d_2 *[mm] : diameter where fiber deviations are visible;*
- d_1 *[mm] : knot diameter;*
- α *[-] : coefficient that indicates the size of the fiber deviation around a knot;*

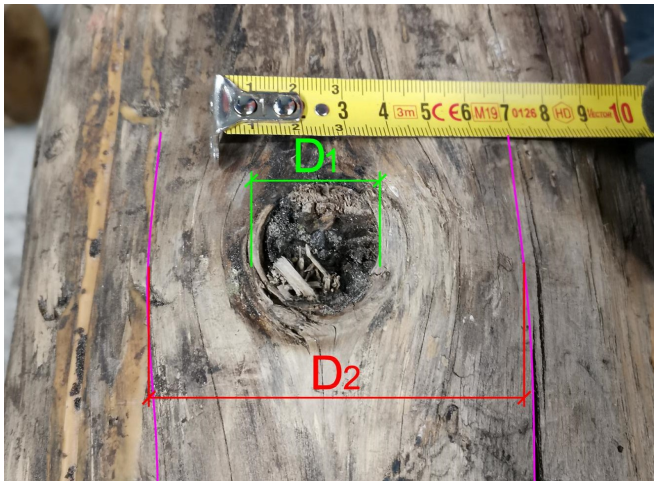

Figure 5.1.1: Knots size dimension d_1 and fibers deviation;

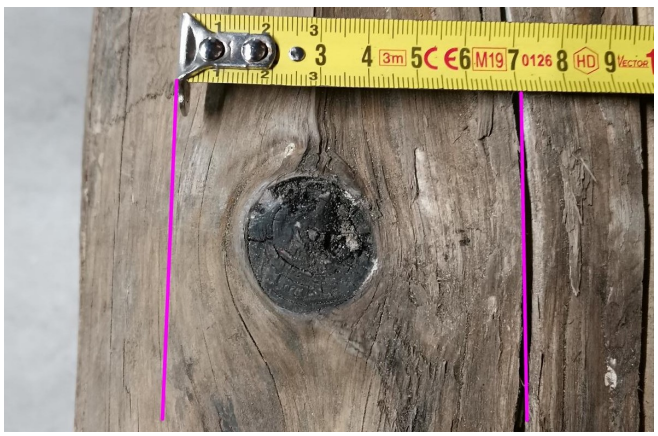

Figure 5.1.2: example of knot measurement taking into account the inclination of the fibers;

Procedure of measurement of the knots The following procedure was designed to create a standard to be followed for each segment (sample) and to obtain comparable measurements.
The knot size measurement procedure can be divided into 4 steps:

1. *Preparation of the sample* : first, sample was placed in a rigid and adequately illuminated support. These procedures were necessary for a correct evaluation of the position of knots on the surface of the pile.

2. *Identification of the sample head* : The side of the pile with the biggest circumference was considered (head of the sample). The position of knots was measured starting from the sample's head along the length of the segment.

3. *Position of the knot* : the distance from the origin of the reference system (sample's head) was evaluated for each knot.

4. *Knot size* : the size of a knot was measured taking into account the deviation of the fibers it generates.

Figure 5.1.3: 1)Preparation of the sample; 2)Identification of the sample head; 3)Position of the knot; 4)Knot size measurement.

5.1.1.1 Knots Ratio

The influence of the branch, which develops radially from the pith towards the outside of the trunk, is not measurable at every point. It would require the cutting of the trunk to assess its real influence whenever there is the presence of a branch. Therefore, it was necessary to assess their influence on the trunk without altering its integrity. To do this, the outer dimension of the knot in the tangential direction was taken, neglecting the real development of the branch in the radial direction (see figure 5.1.4).

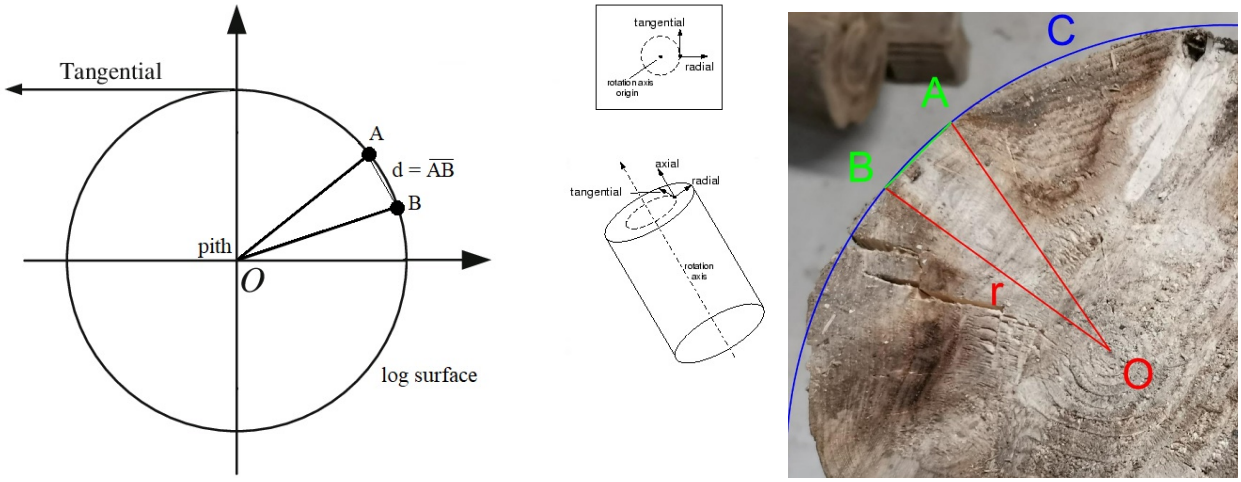

Figure 5.1.4: knot influence inside a pile section;

Since the value of the angle $A\hat{O}B$ is small, the dimension of the knot can be more easily measured through the segment AB (circumference string), because it is similar to the value of the arc of circumference d (see figure 5.1.4). The percentage of influence of the knot in the cross-section was obtained by dividing the value of the AB rope by the circumference of the pile.

By repeating the calculation for each knot present, the "knot ratio" (KR) is defined as the ratio between the sum of the diameters of knots in a branch whorl and the circumference of the pile in that whorl.

$$KR_i = \frac{\sum_{n=1}^{m} D_n}{C}$$

where:
- KR_i *[-] : KR of the cross-section number i;*
- D_n *[mm] : diameters of the knots;*
- C *[mm] : circumference of the cross-section;*

In 70% of the cases, the failure of a pile segment occured in the section with the highest number and/or bigger size of knots. On this basis, the maximum KR measured in a pile can only be used in relation to the compressive strength. However, knots in a pile occur in multiple cross-section and they can have relevant effects on the MOE of the entire segments. For this reason a knot calculation that takes into account the distribution of knots on the surface was used, in order to correctly estimate the influence on the MOE.

5.1.1.2 Overall Knots Area Ratio

The Overall Knots Area Ratio (OKR_A) is a factor to evaluate the presence of all knots along the external pile surface. Differently to the KR, the OKR_A is not based on a local analysis of a specific cross-section of the pile with bigger knots and/or larger number of knots, but it takes into account the area of knots along all the length of the pile. This global analysis is very important since the MOE is influenced by all the knots present in a pile and not just knots located in a specific cross-section. The OKR_A is defined as the ratio between the sum of the external area of knots on the surface of the pile and the external area of the pile.

$$OKR_A = \frac{\sum A_{kn,i}}{A_{ext,pile}} = \frac{\sum A_{kn,i}}{(2\pi \cdot r_{pile}) \cdot L_{pile}}$$

where:
- $A_{kn,i}$ *[mm^2] : external area of each knot on the surface of the pile;*
- r_{pile} *[mm] : radius of the pile taken into account;*
- L_{pile} *[mm] : length of the pile taken into account;*
- $2\pi r_{pile}$ *[mm] : circumference of the average pile cross-section;*

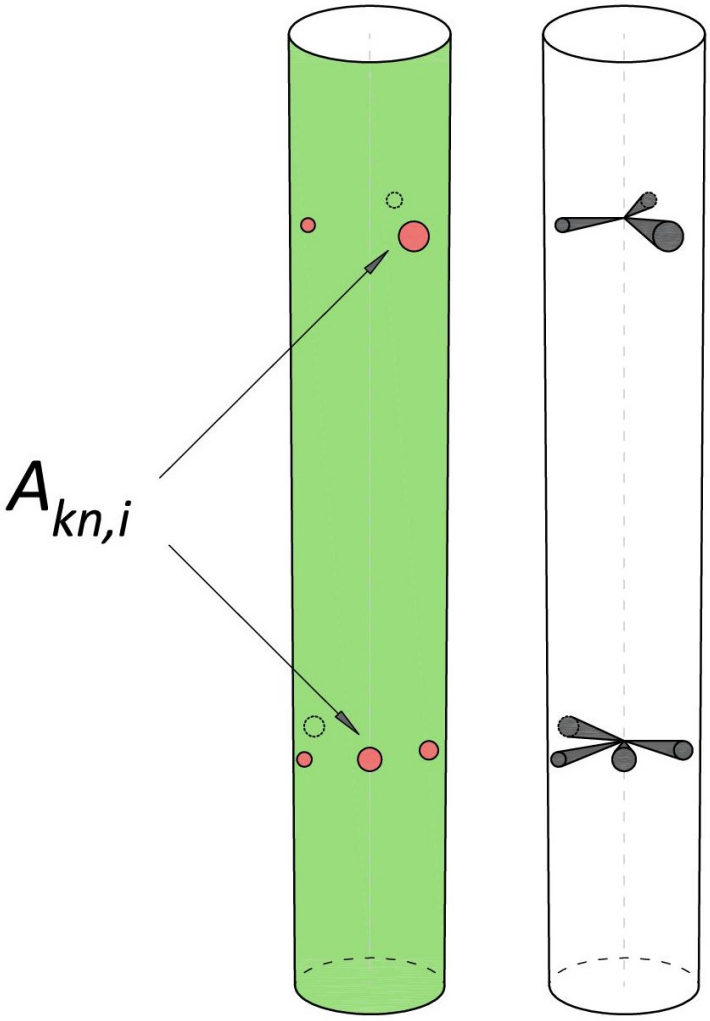

Figure 5.1.5: evaluation of OKR_A on a segment of a pile;

5.1.1.3 Overall Knots Volume Ratio

The Overall Knots Volume Ratio (OKR_V) is a factor to evaluate the presence of all knots on the volume of the entire segment of a pile. Differently to the OKR_A, OKR_V takes into account the development of knots into the pile as reported in paragraph 2.4.2. The OKR_V is defined as the ratio between the sum of the volume of knots into the pile and the entire volume of the pile.

$$OKR_V = \frac{\sum V_{kn,i}}{V_{pile}} = \frac{\sum V_{kn,i}}{(\pi \cdot r_{pile}^2) \cdot L_{pile}}$$

where:
- $V_{kn,i}$ *[mm^3] : volume of each knot;*
- r_{pile} *[mm] : radius of the pile taken into account;*
- L_{pile} *[mm] : length of the pile taken into account;*
- $\pi \cdot r_{pile}^2$ *[mm] : area of the average pile cross-section;*

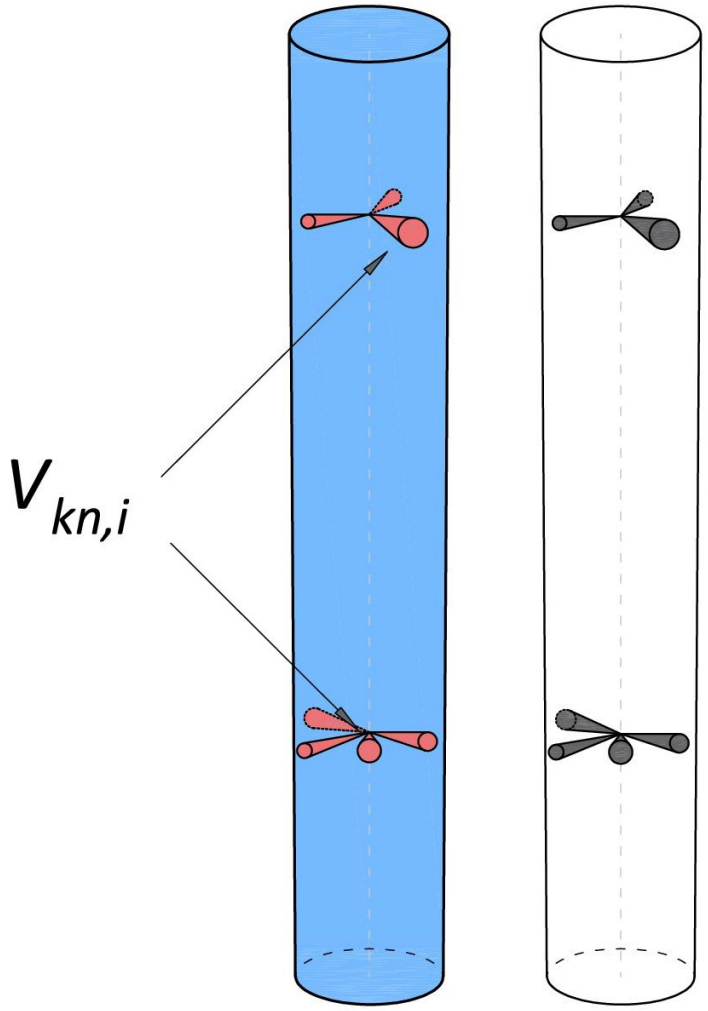

Figure 5.1.6: evaluation of OKR_V on a segment of a pile;

5.2 Determination of the mechanical properties of pile segments

In this paragraph, the stiffness of wooden piles is analysed through the determination of the modulus of elasticity (MOE). The timber piles studied in this thesis were tested with frequency response measurement with a MTG timber grader tool (to obtain the dynamic MOE) and with strain measurement derived by uniaxial compression test (to determine the static MOE). The tests were performed on 106 pile segments available.

5.2.1 Analysis of full-scale testing of pile segments

5.2.1.1 Determination of static modulus of elasticity

Mechanical testing was performed to determine the compressive strength ($f_{c0,wet}$) and the static modulus of elasticity ($MOE_{stat,wet}$) in wet condition. To this end, a displacement controlled set-up was used (Fig. 5.2.1), based on the standards EN 408 and EN 14251, where the specimens were subjected to an axial load in direction parallel to the fibers.

The tests were performed on the full length of the segment of the pile and locally considering a portion of the pile. Therefore, it is possible to distinguish the *Full-scale Analysis* (full length of piles) and the *Local Analysis* (portion of piles) that are described in the next chapters.

The compression test was carried out on a displacement control set-up where the wooden pile was placed between two parallel steel plates. The displacement between the two steel plates was monitored with four linear potentiometers placed on the four edges. The deformation of the wooden pile was measured with six linear potentiometers screwed on the pile. Four of them were placed on each side of the pile, 90 degrees from each other. The length of these four sensors was variable since it was equal to two-thirds of the length of the specimen. The other two sensors were placed on a surface with and without knot to evaluate the variation in terms of strain. The length of these two was set at 200 mm. For the test, a hinge was placed on top of the pile and in addition, a steel plate was placed between the pile and the hinge to have a uniformly distributed load on the pile. The following figure shows the set-up and the position of the sensors.

The compression test was carried out at a constant speed of 0.02 mm/s until the peak load was reached. The specimens were loaded to failure and the displacement was hence increased at higher speed until the cracks were visible.

The MOE can be evaluated by choosing two displacement steps that correspond with two different forces applied at the head of the pile. The inclination of the curve was the reference value to the calculation of the static MOE on the specific interval of data taken into account.

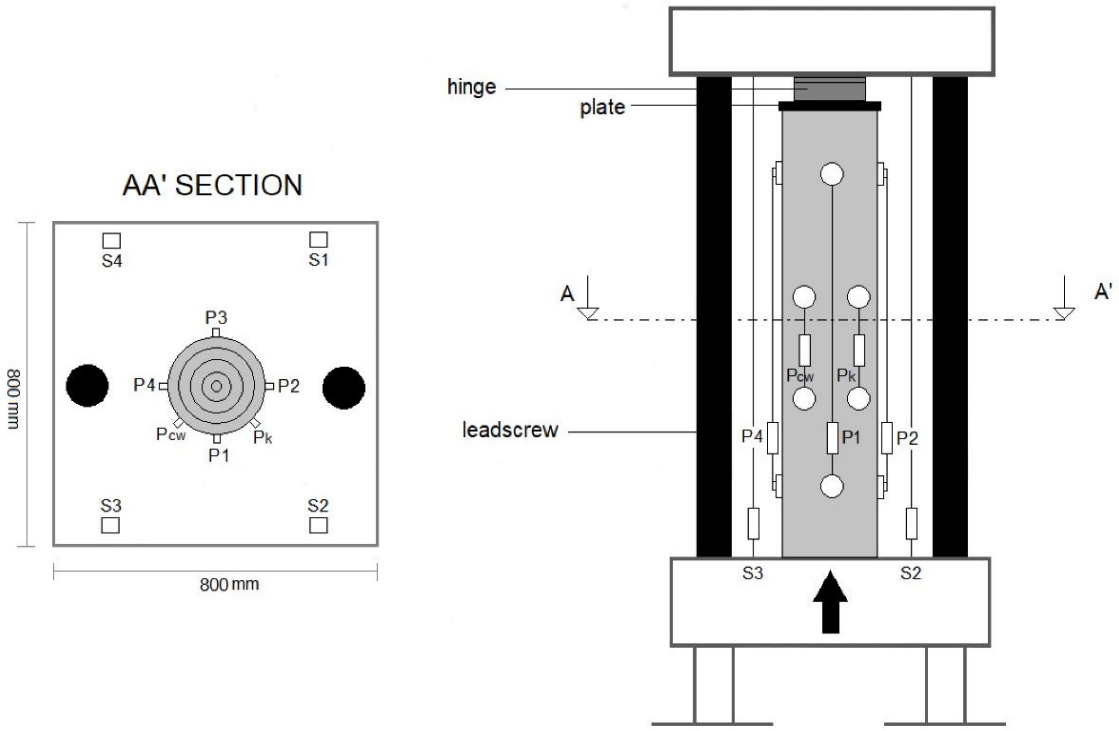

Figure 5.2.1: uniaxial compression test carried out at the TU Delft and position of the sensors [5];

Figure 5.2.2: example of unaxial compression test on a pile on the right and the position of a linear potentiometers around a knot area on the left;

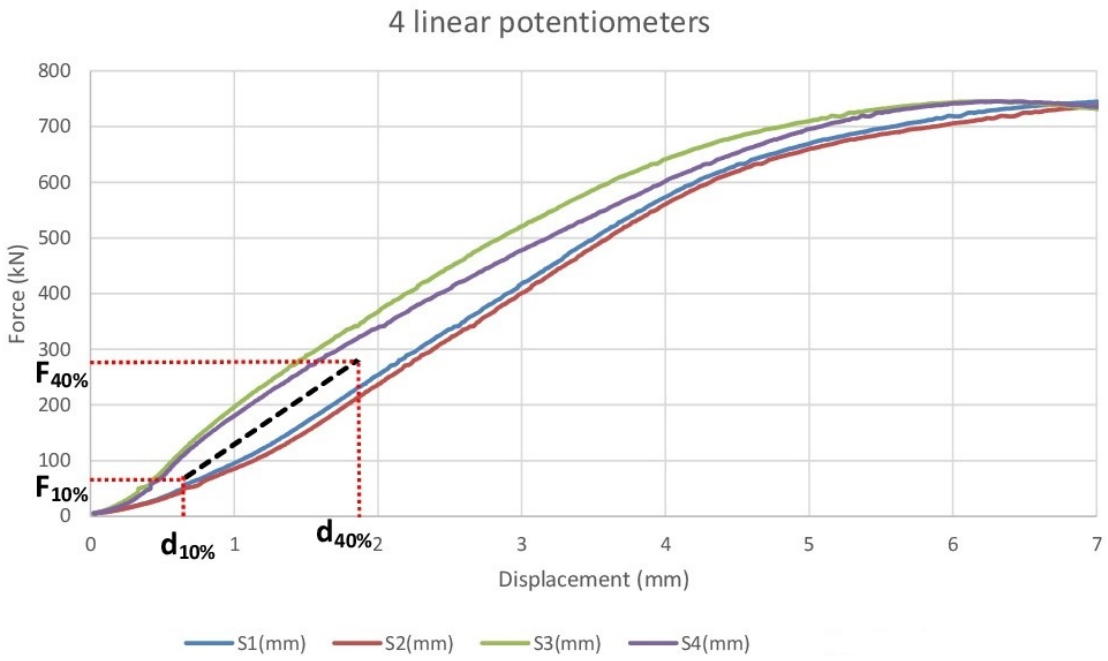

Figure 5.2.3: force-deformation curve of a unaxial compression test;

TheMOE_{stat} was calculated with the ratio between stress variation ($\Delta\sigma$) and strain variation ($\Delta\varepsilon$), between 10% and 40% in the slope of the linear elastic portion of the stress-strain curve, resulting from the four linear potentiometers attached on the pile:

$$MOE_{stat} = \frac{\Delta\sigma}{\Delta\varepsilon} = \frac{(\sigma_2 - \sigma_1)}{(\varepsilon_2 - \varepsilon_1)} = \frac{(F_2 - F_1)/A_r}{(L_2 - L_1)/L_0} = \frac{\Delta F}{\Delta L} \cdot \frac{L_0}{A_r}$$

where:
- ΔF *[N] : difference of load applied in two different steps;*
- ΔL *[mm] : variation of length of the linear potentiometers;*
- L_0 *[mm] : initial length of the linear potentiometers;*
- A *[mm^2] : average area of the pile;*

The piles were tested above fiber saturation point (wet conditions).

5.2.1.2 Determination of Dynamic modulus of Elasticity

Foundation piles work in a longitudinal way, due to the statical service loads (axial loads). The strain and integrity of a pile are measured calculating longitudinal stiffness, for this reason this is an important parameter to evaluate wooden foundation piles.

The presence of knots significantly affects the value of the MOE of a wooden foundation pile. Specifically, knots type, dimension, development inside the trunk, density, and distribution along the length of the pile influence the longitudinal stiffness.

The acoustic response is one of the most used methods to evaluate the MOE of a pile without altering its integrity. This can be calculated with a particular instrument that measures the MOE of an entire wooden pile, taking into account the presence of knots, the tapering of the pile and other parameters described below.

The frequency response measurement was carried out with MTG grader tool. First of all, the instrument was calibrated with a plastic bar that has standard properties.

After this, each specimen, before the compression test, was placed on two wooden sticks to avoid the influence of the floor. A mechanical impact was applied at the head of the pile with a hand-held hammer and the signal was recorded at the opposite side of the pile with the accelerometer.

Subsequently, the vibration signal was analysed in the software in the time domain and it was converted into the frequency domain using fast Fourier transformation (FFT). The first three eigenmodes were obtained from the resulting FFT spectra (Fig. 5.2.6).

Then, the MOE was calculated with the following equation:

$$v = \frac{2L}{\Delta t} \qquad MOE_{dyn} = v^2 \cdot \rho = 4\rho L^2 f^2$$

where:
- *L [mm] : length of the segment of the pile;*
- *t [s] : time measured between the start and the end of the acoustic signal;*
- *v [m/s] : velocity of the signal inside the pile;*
- *f [s/rad] : frequency of vibration of the pile;*
- *ρ [kg/m^3] : density of the pile;*

The dynamic measurement of the modulus of elasticity can vary due to multiple factors in a wooden foundation pile. These factors are, for example:

- material: Timber is a non-homogeneous material. The cross section has different densities through juvenile wood and mature wood. The natural variation of density can be found also along the length of the entire pile.
- knots: The presence of knots in timber piles influences the dynamic response. Knots have different densities and stiffness than clear wood. Moreover, knots cause deviation of the longitudinal fibers resulting in a variation of the response locally in the wooden pile.
- shape: A wooden pile derives from a tree. For this reason, the shape of a pile is tapered (larger on the head and smaller on the tip).

In order to take into account these aspects in a dynamic response evaluation, a numerical model was performed in paragraph 7.2.

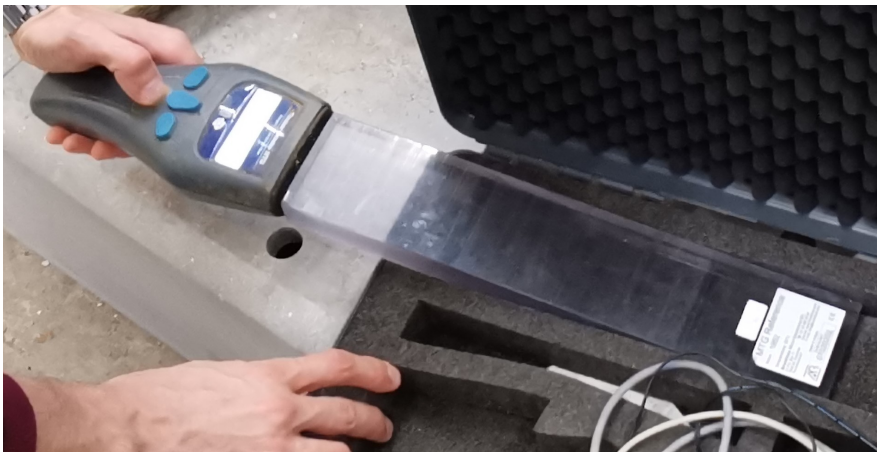

Figure 5.2.4: MTG grader tool calibration of the instrument;

Figure 5.2.5: MTG measurement of the dynamic response of a pile;

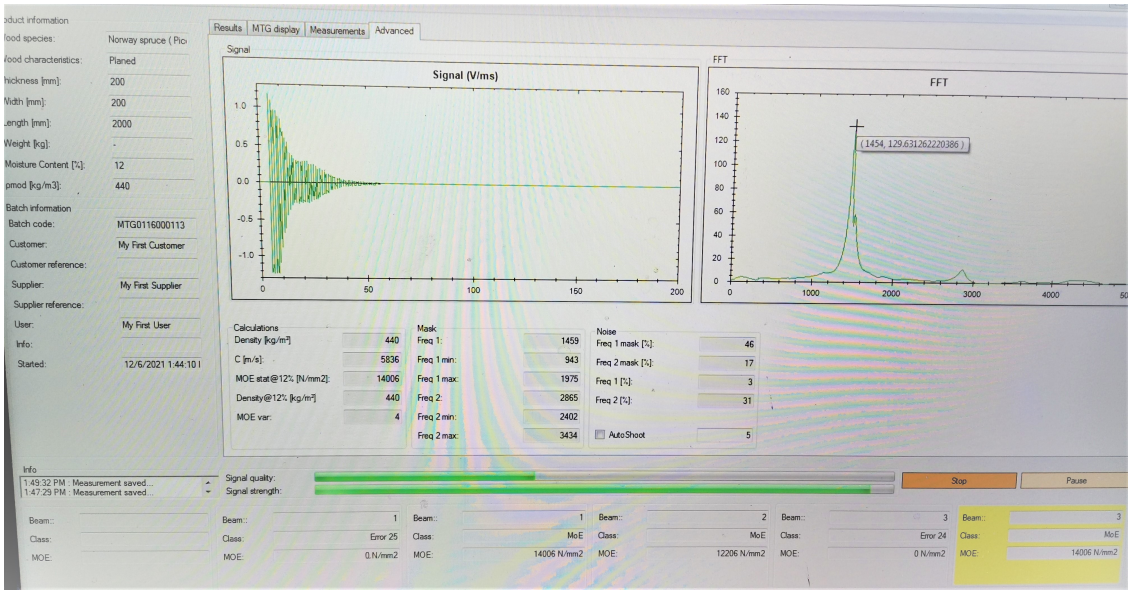

Figure 5.2.6: signal and FFT graph from a MTG measurement;

5.2.2 Local Analysis

5.2.2.1 Compression Tests on Disks

The global analysis of pile segments was validated by testing in total 6 disks:

- three 100 mm thick wooden disks sawn from a section of piles without knots, i.e. clear wood section of the same pile segments.;
- three 100 mm thick wooden disks were sawn from a section of piles with knots.

All the disks were subsequently tested in compression, in water-saturated condition.

Both the disks with and without knots were sawn with a length about 100 mm, since usually a branch whorl is visible over a length of 100 mm. This was also done for disks without knots in order to get comparable measures between the two categories of disks. Before the testing, the disk was levelled on the top and bottom surfaces, to have an uniformly distributed compression load.

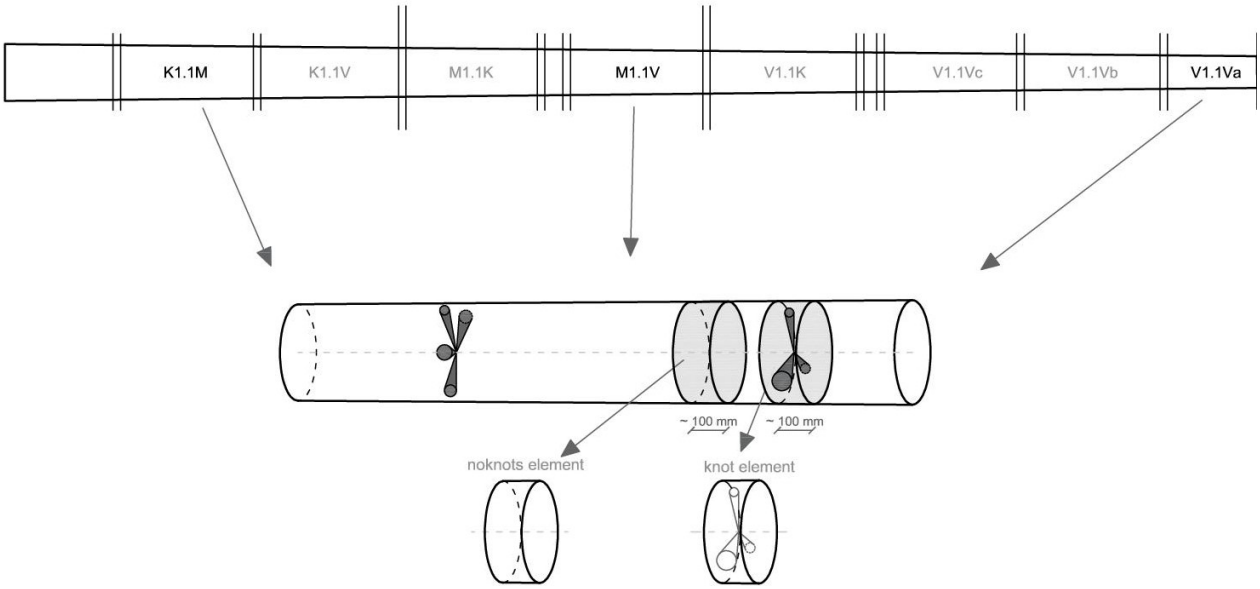

Figure 5.2.7: cutting of the disks with knots and without knots;

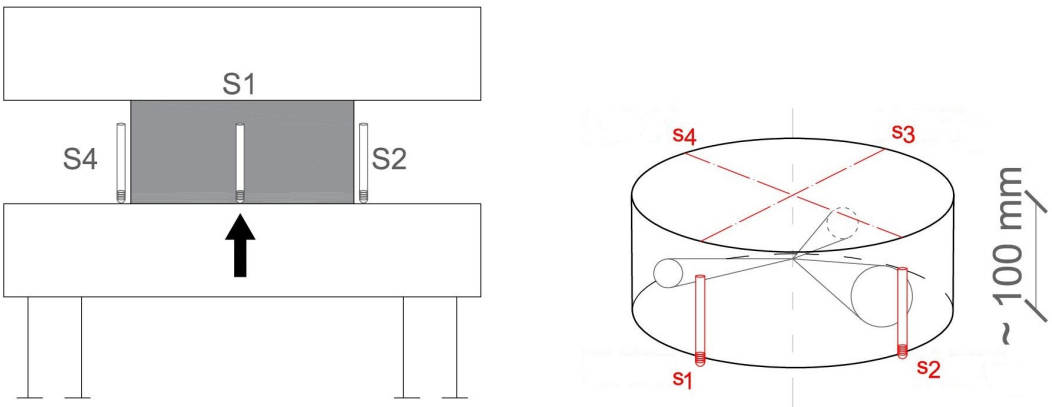

Figure 5.2.8: test layout of the toni technik machine for compression test on disks;

The disks were tested on the Toni Technik machine for compression tests. Four linear potentiometers were placed on the four side of the disks. The sensors have a length of 40 mm with a stroke of 2 mm (Fig. 6.3.1).

All the samples were tested above fiber saturation point ($\omega > 32\%$) with the aim to obtain comparable measurement.

In order to get precise value of the MOE, the test was carried out performing load cycles in elastic phase. Four load cycles were done for each disks. The MOE was calculated neglecting the first load cycle, where the load-displacement curve is affected by the adjustment of the specimen. Therefore, after the first load cycle, a more stable slope of the load-displacement curve was obtained, representing the actual stiffness of the material (Figure 5.2.9).

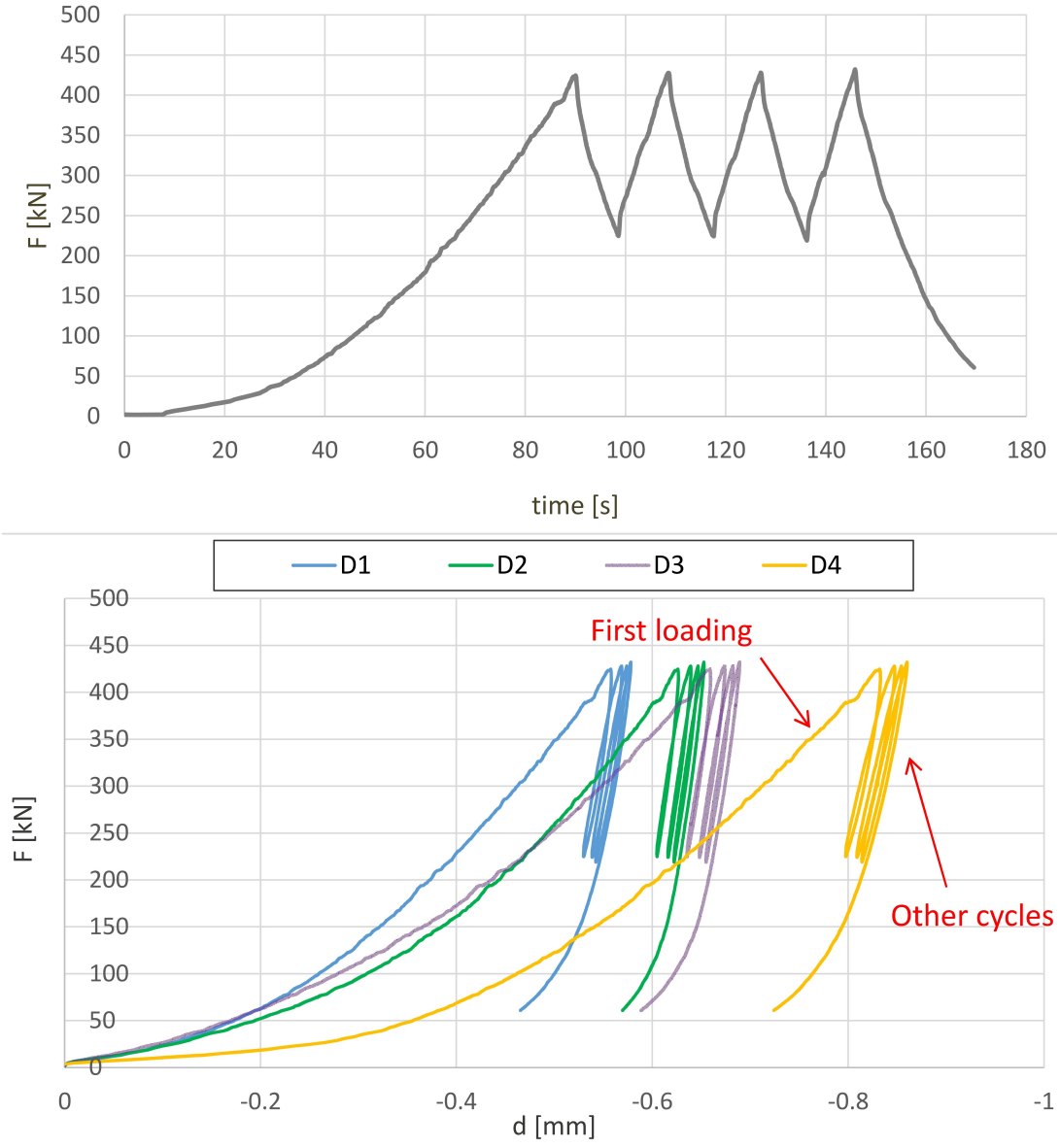

Figure 5.2.9: loading cycles of a compression test of a disk;

The average MOE_{stat} was calculated from the average stress-strain curve given by the four linear potentiometers attached to the disks.

$$\left(\frac{\Delta F}{\Delta d}\right)_{avg} = \left[\left(\frac{\Delta F}{\Delta d}\right)_{D1} + \left(\frac{\Delta F}{\Delta d}\right)_{D2} + \left(\frac{\Delta F}{\Delta d}\right)_{D3} + \left(\frac{\Delta F}{\Delta d}\right)_{D4}\right]/4$$

Every MOE of a different linear potentiometers was calculated considering the first three load cycle of the compression test:

- a = fist load cycle;
- b = second load cycle;
- c = third load cycle.

$$\left(\frac{\Delta F}{\Delta d}\right)_{Di} = \left[\left(\frac{\Delta F}{\Delta d}\right)_{Di,a} + \left(\frac{\Delta F}{\Delta d}\right)_{Di,b} + \left(\frac{\Delta F}{\Delta d}\right)_{Di,c}\right]/3$$

In the end, the MOE of the disk can be evaluated as:

$$MOE_{stat} = \left(\frac{\Delta F}{\Delta d}\right)_{avg} \cdot \frac{h_{sample}}{A_{sample}}$$

where:
- ΔF *[N] : difference of load applied in two different steps;*
- Δd *[mm] : variation of length of the linear potentiometers;*
- h_{sample} *[mm] : initial height of the sample;*
- A_{sample} *[mm^2] : area of the load application;*

5.3 Influence of knots on the MOE

The influence of knots on the MOE of timber piles was evaluated observing how the MOE was influenced by different OKR:

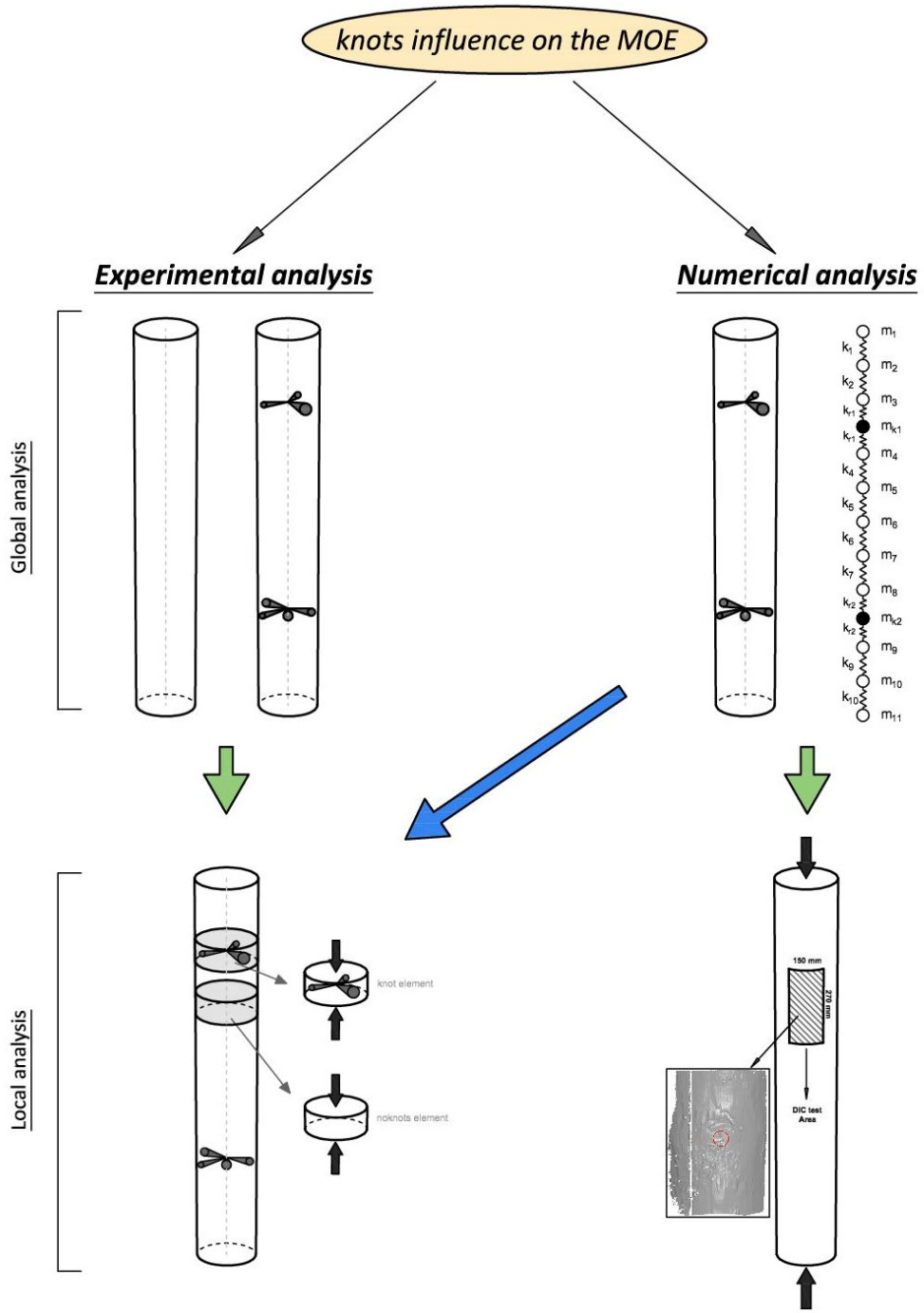

First of all, an experimental analysis was done comparing piles without knots and piles with knots. The values of the MOE were confirmed with local analysis on disks of the piles. In particular, the MOE was measured with the static measurement performing uniaxial compression test (on piles and disks of the pile) and dynamic measurement (on piles).
Then, a numerical model was created to confirm the experimental evidence. In order to create this model, some hypotheses were formulated and a DIC test was performed to verify these hypotheses. Then, results of the numerical model and results of the experimental analysis were compared. Both the analyses are described in the following sections.

5.3.1 Experimental Analysis

In order to analyse the influence of knots on the MOE, it was necessary to obtain a correlation between pile segments without knots (no knots "nk") and pile segments with knots ("k"). This comparison was performed considering 106 tested pile segments.

Pile segments without knots ($OKR = 0$) and with different values of OKR were compared. Four classes were created depending on OKR, describing the influence of knots on the MOE by comparing pile segments with and without knots (called reference piles).
In this analysis, only 5 pile segments without knots were available. Therefore, in order to validate the MOE of the five reference piles, 3 disks were sawn from sections of piles without knots and tested in compression.

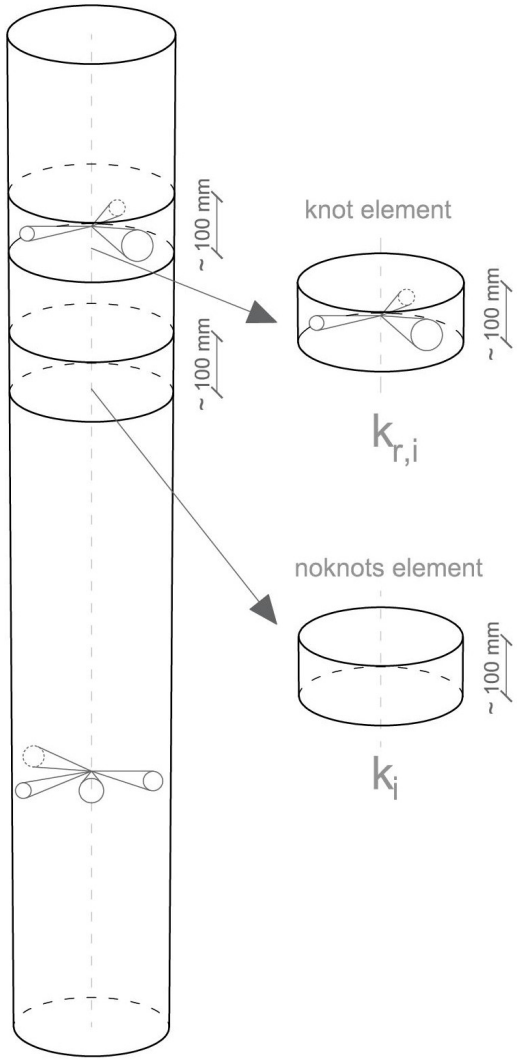

Figure 5.3.1: two wooden disks were cut for each of the 3 piles tested. The first one was sawn from a section of piles with knots, the second one was sawn from a section of piles without knots;

The MOE obtained from the tests were correlated to the OKR by using a linear regression analysis.

$$\overline{y} = \beta_0 + \beta_1 x \implies MOE = \beta_0 + \beta_1 OKR \qquad ; \qquad MSE = \frac{1}{n}\sum_{i=1}^{n}(y_i - \overline{y})^2$$

where:
- β_i *[-] : factor of linear regression analysis;*
- y_i *[-] : real value attended;*
- x *[-] : independent variable;*
- n *[-] : number of samples tested;*
- MSE *[-] : Mean Squared Error;*

Meanwhile, the comparisons between 5 classes were done using average values that have different kind of variability in results. A Gaussian and normalyzed distribution of the data was considered for a great number of data, and t-student distribution was considered for a small number of specimen. Therefore, the error can be estimated calculating a standard deviation as follows:

$$S_{dev} = \sqrt{\frac{\sum(y_i - y)^2}{n-1}}$$

where:
- S_{dev} *[-] : standard deviation;*
- y_i *[-] : real value attended;*
- y *[-] : estimated value;*
- n *[-] : number of samples tested;*

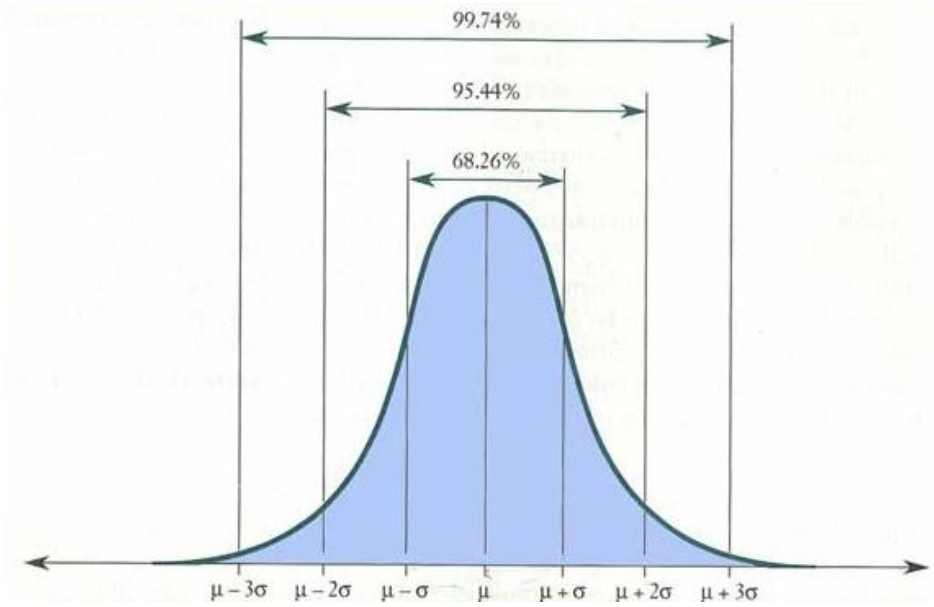

Figure 5.3.2: gaussian distribution of a set of data;

5.3.2 Numerical Analysis

The numerical model was performed to predict the dynamic response of wooden piles with and without knots. In the model, the presence of knots and the tapered shape of the pile were taken into account to understand the influence of these factors on the MOE.

The numerical model analyses the natural frequencies of a wooden pile with a theoretical method. This is the case of a freely imposed beam undamped:

$$m\ddot{u} + ku = 0$$

To find an harmonic solution to this problem, it was assumed that:

$$\overline{u} = \overline{X} sin(\omega t)$$

Replacing the harmonic response in the equations of motion, it was obtained:

$$-MX\omega^2 sin(\omega t) + KX sin(\omega t) = 0 \implies KX = \omega^2 MX$$

The vectors u and scalars λ, that fulfill a matrix equation of the form $Ku = \lambda Mu$, are called "generalized eigenvectors" and "generalized eigenvalues" of the equation. The values of λ, that fulfill $KX = \lambda MX$, are related to the natural frequencies by $\omega_i = \sqrt{\lambda_i}$. The vectors X are the "mode shapes" of the system. These are the initial displacements that allow the mass to vibrate harmonically.

Therefore, a freely imposed beam has the following eigenvalues (see fig.5.3.4) [33]:

$$\omega_0 = 0 \qquad \omega_1 = \sqrt{\frac{EA}{mL}} \qquad \omega_2 = 2 \cdot \sqrt{\frac{EA}{mL}} \qquad \omega_3 = 3 \cdot \sqrt{\frac{EA}{mL}} \qquad \dots$$

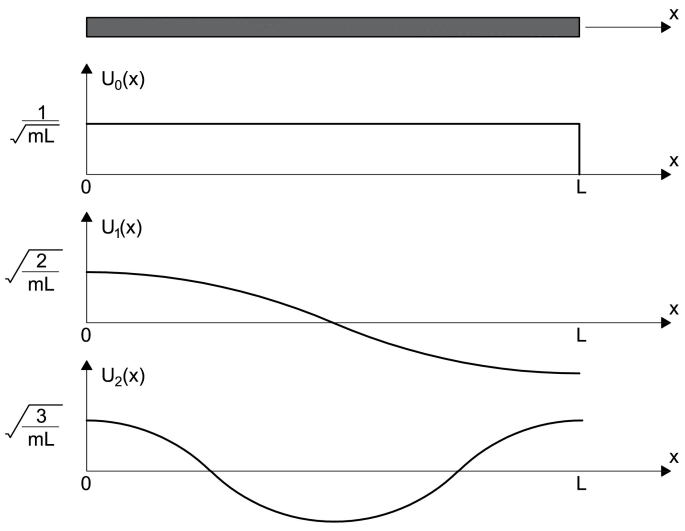

Figure 5.3.3: Mode shapes of free-free beam in axial vibration;

The wooden pile was subdivided into n segments with a specific mass taking into account the tapering of the pile. Each mass is connected with the following mass in series with springs. In the pile without knots, all the springs have the same stiffness. In the pile with knots, the springs represent a low stiffness (the equations was obtained from the analysis in chapter 7.2.1).

$$k_{nk} = \frac{E_{nk} \cdot A_{res}}{L_{elem}} = \frac{E_{nk} \cdot A_{tot}}{L_{elem}} \qquad k_{kn} = \frac{E_{nk} \cdot A_{res}}{\phi_{kn,max}} = \frac{E_{nk} \cdot A_{tot} \cdot (1 - KR)}{\phi_{kn,max}}$$

where:
- E_{nk} *[N/mm^2] : modulus of elasticity of no knots element;*
- A_{res} *[mm^2] : resistance area;*
- A_{tot} *[mm^2] : total area of the cross section considered;*
- L_{elem} *[mm] : length of the no knots element;*
- E_{nk} *[N/mm^2] : modulus of elasticity of wood without knots;*
- A_{res} *[mm^2] : resistance area;*
- A_{tot} *[mm^2] : total area of the cross-section considered;*
- KR *[-] : factors that takes into account the presence of knots in the cross-section;*
- $\phi_{kn,max}$ *[mm] : maximum size dimension of knots in the cross-section;*

The matrices of the system made up of material properties. The mass matrix is a (n x n) diagonal matrix. The stiffness matrix is a symmetrical matrix containing only the values of the stiffness of the springs. This matrix is also a (n x n) matrix, where n is equal to the number of masses.

$$\overline{\overline{M}} = \begin{bmatrix} m & 0 & \dots & \dots & \dots & \dots & \dots \\ 0 & m & 0 & \dots & \dots & \dots & \dots \\ \dots & \dots & \dots & \dots & \dots & \dots & \dots \\ \dots & \dots & 0 & m_k & 0 & \dots & \dots \\ \dots & \dots & \dots & \dots & \dots & \dots & \dots \\ \dots & \dots & \dots & \dots & 0 & m & 0 \\ \dots & \dots & \dots & \dots & \dots & 0 & m \end{bmatrix}$$

where m_k is the mass of the segment of the pile with the presence of knots.

$$\overline{\overline{K}} = \begin{bmatrix} k_1 & -k_1 & 0 & \dots & \dots & \dots & \dots & \dots & \dots \\ -k_1 & (k_1 + k_2) & -k_2 & 0 & \dots & \dots & \dots & \dots & \dots \\ 0 & -k_2 & (k_2 + k_3) & -k_3 & 0 & \dots & \dots & \dots & \dots \\ \dots & \dots & \dots & \dots & \dots & \dots & \dots & \dots & \dots \\ \dots & \dots & \dots & \dots & -k_r & 2 \cdot k_r & -k_r & \dots & \dots \\ \dots & \dots & \dots & \dots & \dots & \dots & \dots & \dots & \dots \\ \dots & \dots & \dots & \dots & \dots & \dots & -k_{n-2} & (k_{n-2} + k_{n-1}) & -k_{n-1} \\ \dots & \dots & \dots & \dots & \dots & \dots & \dots & -k_{n-1} & k_n \end{bmatrix}$$

where k_r is the stiffness of the spring between segments of the pile with the presence of knots.

The springs of the part with knots have different stiffness than the part without knots. This variation takes into account the presence of knots in a cross-section.
The lower stiffness value of sections with knots than sections without knots was verified performing a test with high accuracy on the surface of a wooden pile (DIC test par. 5.3.2.1).

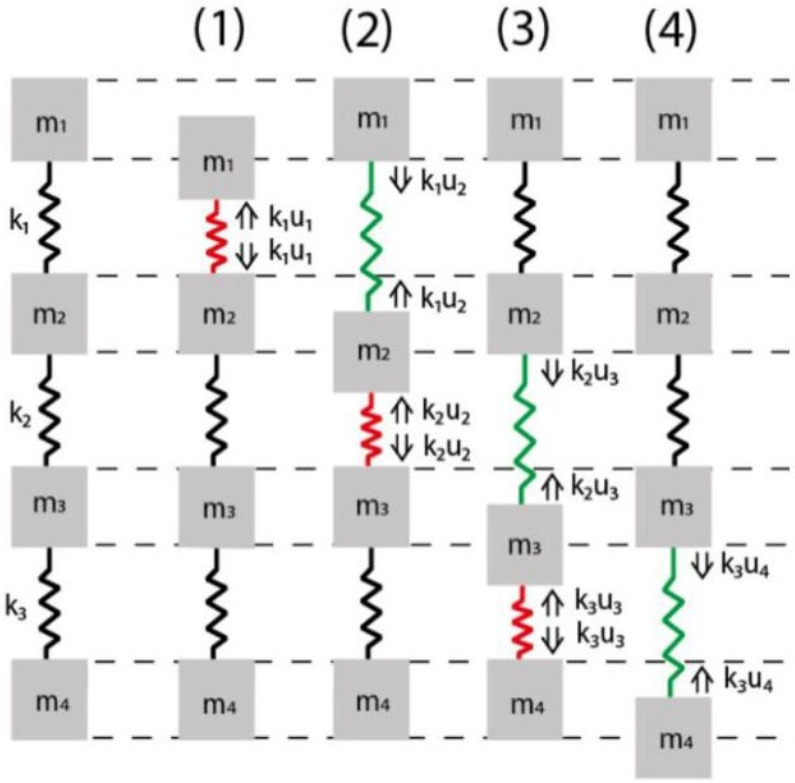

Figure 5.3.4: Freely imposed mass-spring system subdivided in 4 segment;

5.3.2.1 DIC Test

DIC (Digital Image Correlation) test was carried out on the surface of the pile to analyzed the behaviour of knots area during a compression test. The test has the aim of verifying if the real stiffness of a knot can be obtained considering the low stiffness of wood where the fibers deviate.

The instruments used to conduct the compression test with DIC were the following: parts of camera, lenses, calibration tables, lighting, and GOM software for image acquisition and processing.

The test was performed as follows:

1. A surface of 270x150 mm was chosen for the analysis. The surface included a knot area and no knot area with the aim of analyzing the stiffness around the knot during a compression test. First of all, a wooden surface of the pile was painted with a white paint. Then, a black random dotted layer was sprayed on the white surface (Figure 5.3.5). The dotted pattern has the aim of getting a mesh on which the measurement of the deformation is based.

2. The images were acquired with a system of 2 cameras with lenses of 12 MPx, chosen according to the availability of the instruments provided by TU Delft. In particular, the lenses correspond to a measuring volume of 280x200x180 according with the measurement of the analyzed surface (Figure 5.3.6). In order to get more accurate images, the images were acquired in specific conditions using polarized lights.

Figure 5.3.5: Painting of the pile surface;

ARAMIS Adjustable 12M

Lens	Range MV width* / mm	Measuring volume name	MV / mm³	Camera frame	Camera angle	Measuring distance / mm	Slider distance	Clear width /mm	Calibration object	Distance ring / mm	Aperture	Dual LED	Reference point size / mm	Touch probe (PM x)
Titanar B 75 mm	20 - 155 / 295	**20**	20x15x4	500/800	25	291	90	150	CQ40/MV38	50	22	10°	0.4	-
		35	35x25x10	500/800	25	345	114	235	CQ40/MV38	20	22	10°	0.4	-
		70	70x50x40	500/800	25	512	188	410	CQ40/MV60	10	22	10°	0.4	-
		110	110x80x80	500/800	25	697	270	605	CP40/MV100	-	22	10°	0.4	-
		180	180x130x130	800	25	1045	424	950	CP40/MV170	-	16	10°	0.4	-
		250	250x180x180	800	25	1396	580	1305	CP40/MV320	-	11	10°	0.8	1.5
Schneider 50 mm	30 - 245 / 440	**35**	35x25x10	500/800	25	233	64	155	CQ40/MV38	20	22	10°	0.4	-
		70	70x50x30	500/800	25	345	114	275	CQ40/MV60	10	16	10°	0.4	-
		120	120x90x70	500/800	25	512	188	455	CP40/MV170	-	16	10°	0.4	-
		170	170x130x80	500/800	25	697	270	640	CP40/MV170	-	11	10°	0.4	-
		280	280x200x180	800	25	1058	430	1000	CP40/MV320	-	11	10°	0.8	1.5
		370	370x280x240	800	25	1396	580	1335	CP40/MV320	-	8	10°	1.5	3

Figure 5.3.6: Lenses ARAMIS adjustable 12M with its specific conditions of work;

The cameras system has this specific set-up (figure 5.3.7):

(a) Polarizing filter of the left camera;

(b) Polarizing Filter of the led lamp left;

(c) Polarizing Filter of the led lamp right;

(d) Polarizing filter of the right camera;

Before testing, the system needed to be calibrated using a specific calibration table. The procedure described in GOM manual was followed.
The results of the calibration are shown by GOM software resulting in a mesh size of 21 Pixels with 16 Pixels of distance between the centres of the mesh. The final accuracy was 0.039 Pixels = 0.01mm that corresponds to an error of about 15% on the final results on the strains.

3. The pile selected for the test was positioned on the bottom plate of the compression test machine and linear potentiometers were placed on the surface of the pile. The setting used for the linear potentiometers is described on chapter 5.2.1.1. The deformations were measured during the test both with DIC and linear potentiometer, to validate the reliability of the DIC results.

   The pile was tested in compression and the cameras of the DIC system acquired subsequent images for each load step (approximately 200 images every 10 minutes).

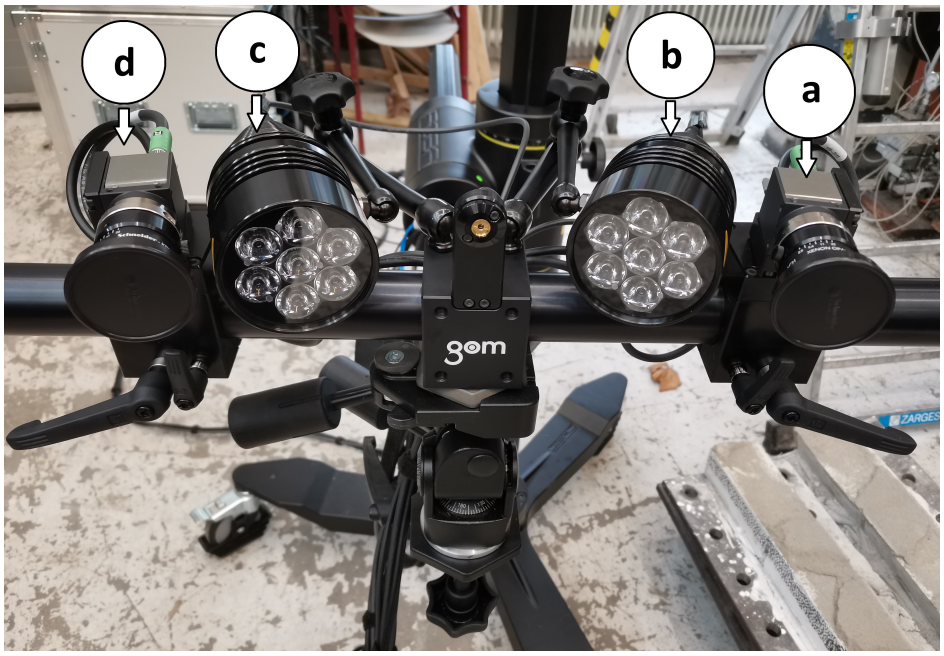

Figure 5.3.7: DIC cameras setting;

Figure 5.3.8: DIC cameras calibration;

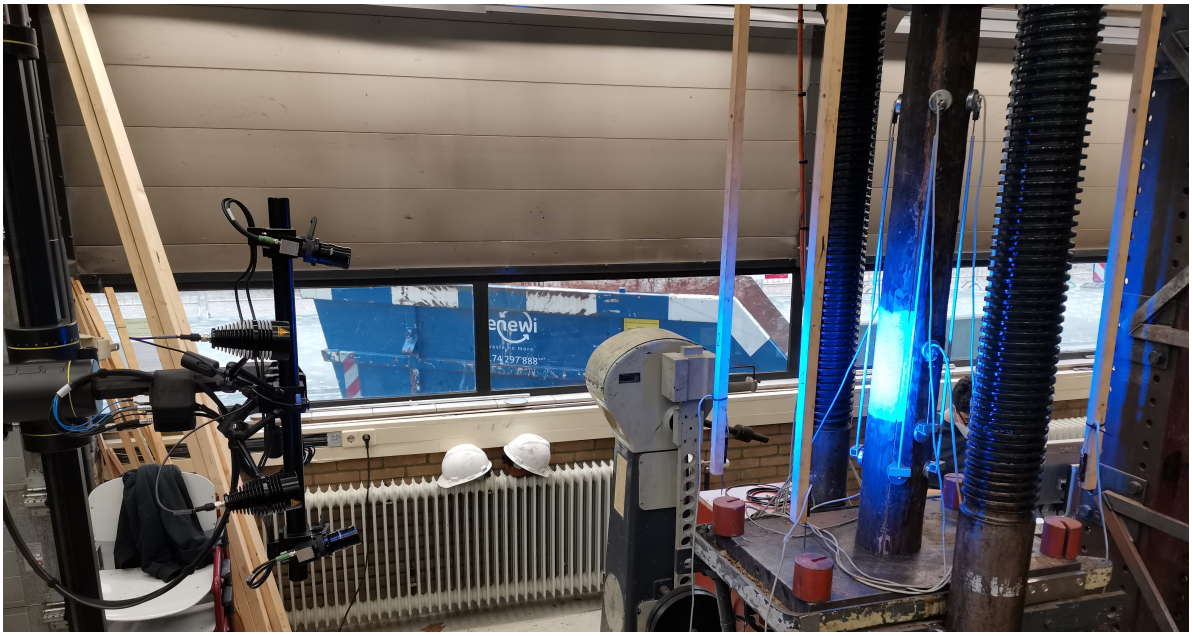

Figure 5.3.9: Compression test on a pile segment. The deformations are measured around a knot area with DIC;

4. The data was analysed using software GOM. The software creates a three dimensional model (3D mesh) by analyzing the speckled surface before the test. Then, the software gives the deformation measurements for each moment of the test by analyzing sequent images acquired during the compression test. The strains of the section of the pile with knots and the section without knots were calculated with the following equation:

$$\Delta\varepsilon = \frac{L_2 - L_1}{L_0} = \frac{\Delta L}{L_0}$$

where:
- $\Delta\varepsilon$ *[-] : strain between two points in two load steps;*
- L_0 *[mm] : original distance between two points;*
- L_1 *[mm] : distance between two points at load step 1;*
- L_2 *[mm] : distance between two points at load step 2.*

The variation in strain between the different areas of the surface leads to a variation of the stiffness on the knot area:

$$MOE = \frac{\Delta\sigma}{\Delta\varepsilon}$$

where:
- $\Delta\sigma$ *[Mpa] : the variation in stress between two load steps;*
- $\Delta\varepsilon$ *[%] : strain of a length for two different load steps;*

The variation on the MOE around a knot area obtained with DIC test was necessary to verify if the real stiffness of a knot can be obtained considering the low stiffness of wood where the fibers deviate. This assumption was used also in the determination of the stiffness of the numerical model (par. 5.3.2).

5.4 Prediction Model

5.4.1 Modelling of the MOE based on density and OKR

In order to predict the value of the MOE of a pile segments with knots, a prediction model was developed considering the influence of knots on the MOE of wooden foundations pile segments.

The value of the MOE of piles without knots, called MOE_{nk}, was considered. The final equation was obtained by reducing the MOE_{nk} of the presence of knots.

$$MOE_k \quad \Longrightarrow \quad f(MOE_{nk})$$

First of all, the value of MOE_{nk} was calculated with a linear regression analysis performed on the 5 segments without knots. The MOE_{nk} depends on the different density of segments.

$$MOE_{nk} = C_1 \cdot \rho_{nk} + C_{1k}$$

where:
- C_1,C_{1k} *[-] : factors obtained from a linear regression analysis;*
- ρ_{nk} *[kg/m^3] : density the pile segments without knots;*

Then, the presence of knots was taken into account using OKR.

$$MOE_k = MOE_{nk} \cdot (1 - C_2 OKR)$$

where:
- C_2, *[-] : the factor representing the influence of knots on the MOE;*
- OKR *[-] : factor representing the presence of knots in segments of piles;*

The equation was proposed with the aim of predict the MOE of a wooden foundation pile, by knowing the MOE of the wood without knots and the knots layout in a new designed wooden foundation pile.

Chapter 6

Results

6.1 Knots Evaluation

6.1.1 Relationship between d_1 and α

The coefficient α, that is determined by visual measurements, is shown in Table 6.1. It is possible to observe that larger knots contributed less to fiber deviation, while smaller knots contributed more. In the tip of a pile, where knots were found more frequently, a knot had a more severe influence on the fiber deviation and implying an alteration of the modulus of elasticity.

$$d_2 = d_1 \cdot (1 + \alpha)$$

The tip-parts of piles have less deviation of the fibers compared with its knot dimension. However, the head and middle parts have a higher deformation of the fibers compared with their knot size.

In order to analyse the correlation between d_1 and α, 5 classes were created depending on the size of knot d_1 (Table 6.1). The average value of α was calculated for each class; by considering a normal distribution of the data, the correspondent standard deviation is $S_{dev} = 0.27$ (shown on the figure 6.1.1).

The coefficient α decrease while the size of knot (d_1) increases (Figure 6.1.1). This leads to the conclusion that, in proportion, at the increase of the dimension of a knot the deviation of the fibers around a knot area decrease.

class of knots	α [-]	note
A	1.12	$d_1 \leq 15mm$
B	1.19	$16mm \leq d_1 \leq 20mm$
C	0.97	$21mm \leq d_1 \leq 25mm$
D	0.93	$26mm \leq d_1 \leq 30mm$
E	0.86	$31mm \leq d1$

Table 6.1: 5 class of knots are shown;

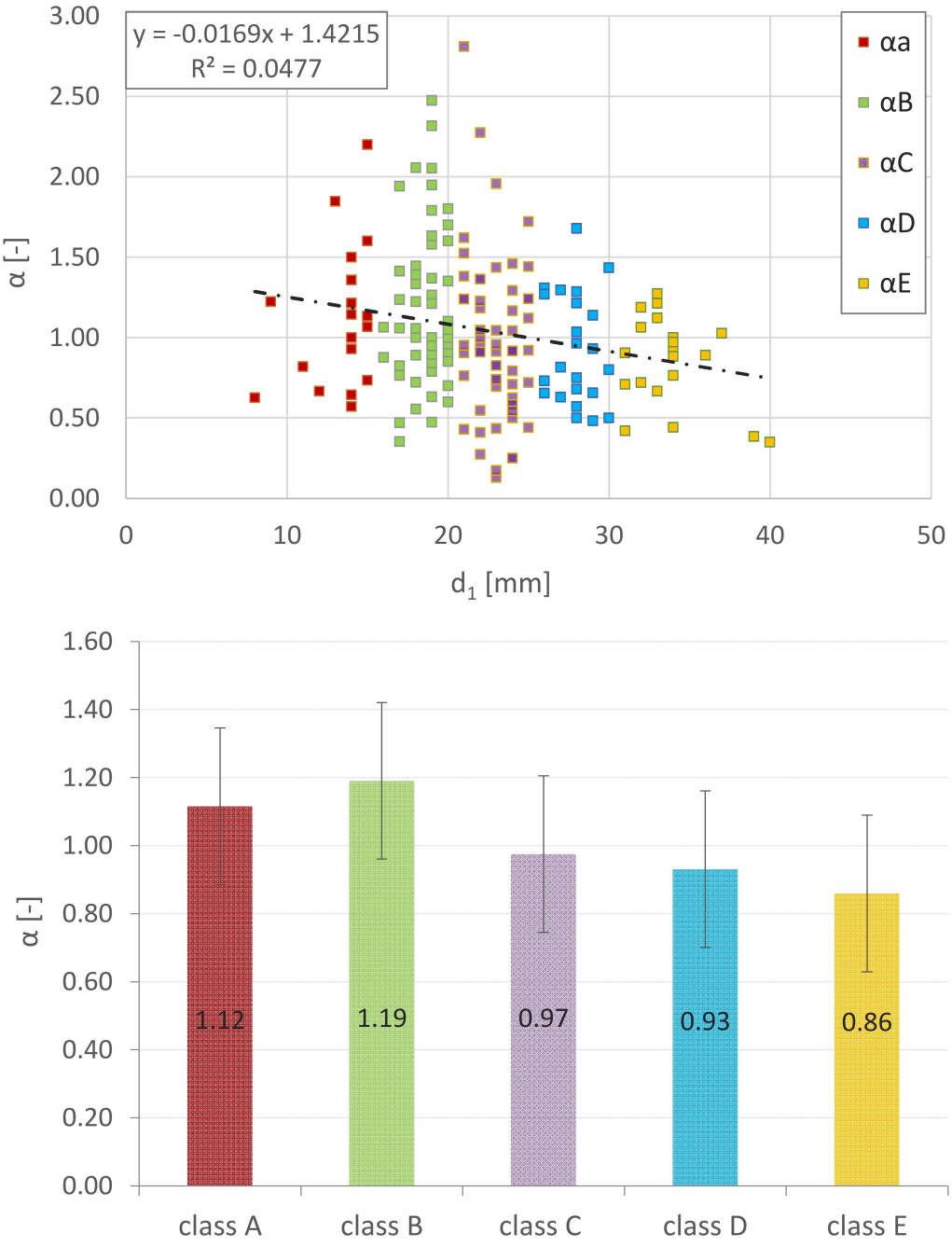

Figure 6.1.1: variation of α at the increase of d_1;

6.1.2 KR along the length of a pile

It was interesting to show the knots layout along the length of a pile with the aim of knowing which were the segments of a pile with higher knots presence.

The variation of KR values was plotted along the length of each full pile. Taking the segments in the right order, it was possible to evaluate the value of KR of an entire pile. Considering the KR measurement of each segment of a pile, the trend of KR along the length of the full pile was showed.

KR values increases from the head to the tip of the pile and the frequency of cross-sections with knots becomes higher towards the tip-part. These behaviours could be caused by two different causes:

- In the upper part of a tree (the tip of the pile), more branches are present (Figure 6.1.4).
- The KR increase due to the tapering nature of a growing tree, and the head of the pile becomes bigger than the tip. This causes a decrease of the circumference "C" of the pile on the tip and a resulting increase of KR value.

$$KR = \frac{\sum D_i}{C}$$

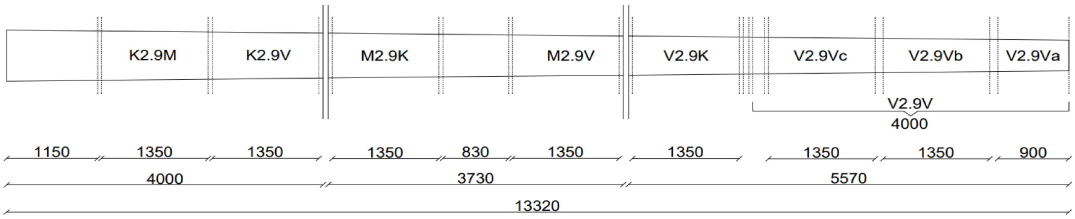

Figure 6.1.2: segments subdivision of pile OAM 2.9;

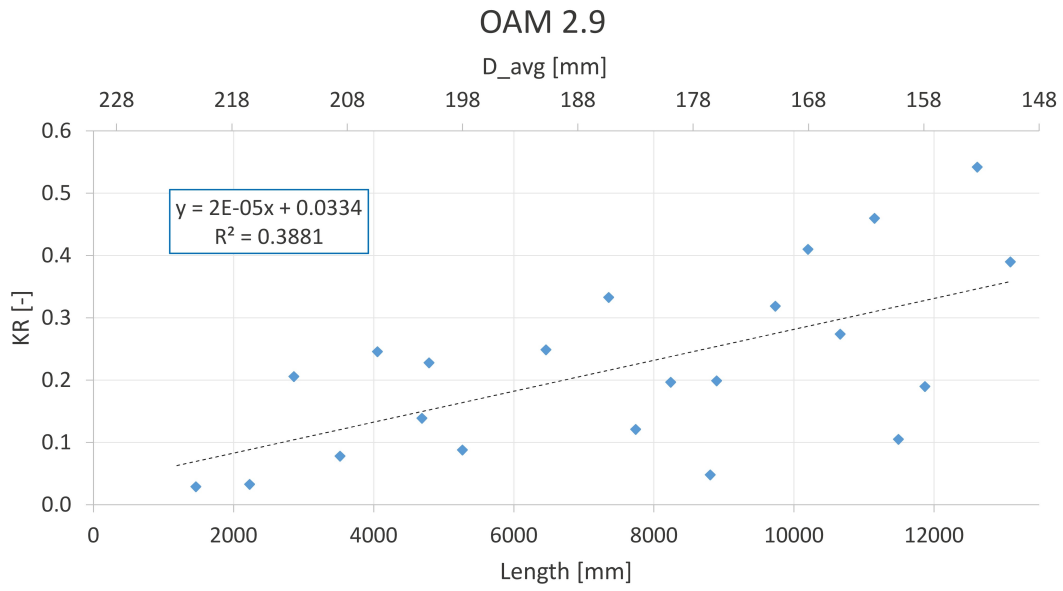

Figure 6.1.3: KR along the length of pile OAM 2.9;

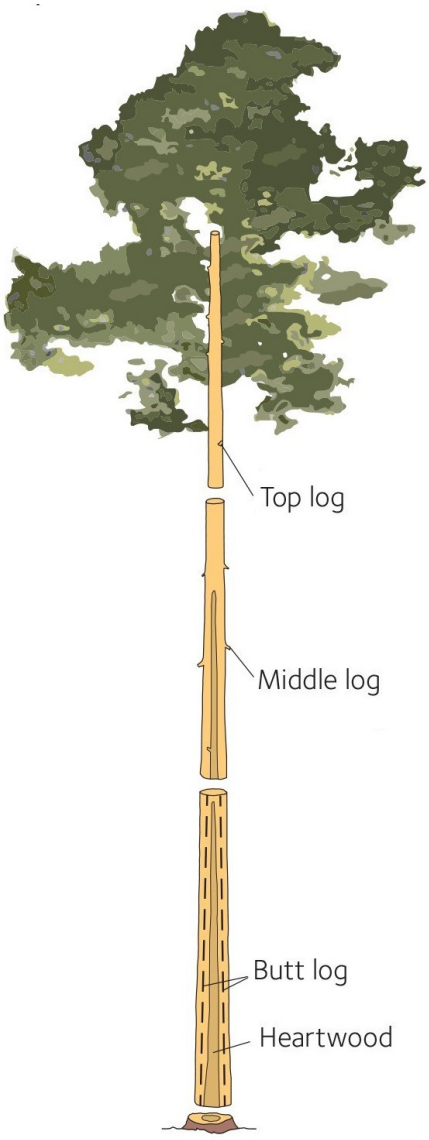

Figure 6.1.4: longitudinal section of a tree;

The other pile considered in this analysis are: OAM1.1, OAM1.4, OAM2.1, OAM2.8, OAM2.9 , OAM2.10. The steps followed to measure the KR along the pile length are the same as for pile 2.9. The results are shown in appendix A.

6.2 Mechanical properties

On the next step, the segments of pile stored at TU Delft were tested with the methods described on section 5.2.1. 106 segments were tested with compression tests and frequency response measurements in order to evaluate the mechanical properties.

Mechanical properties were obtained for the head, middle and tip parts. Generally, both the MOE dynamic and static, show a decrease from the head to the tip of each pile (Fig. 6.2). This led to the conclusion that the MOE could be influenced by knots presence. However, also the larger presence of juvenile wood, especially in tips, could contribute to the decrease of stiffness.

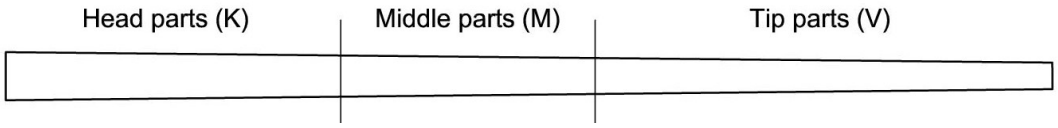

Figure 6.2.1: The three parts of a pile;

	MOE_{stat} [Mpa]	MOE_{dyn} [Mpa]
Head parts	10590	11180
Middle parts	9950	10500
Tip parts	8460	9000

Table 6.2: mechanical properties in head, middle and tip parts;

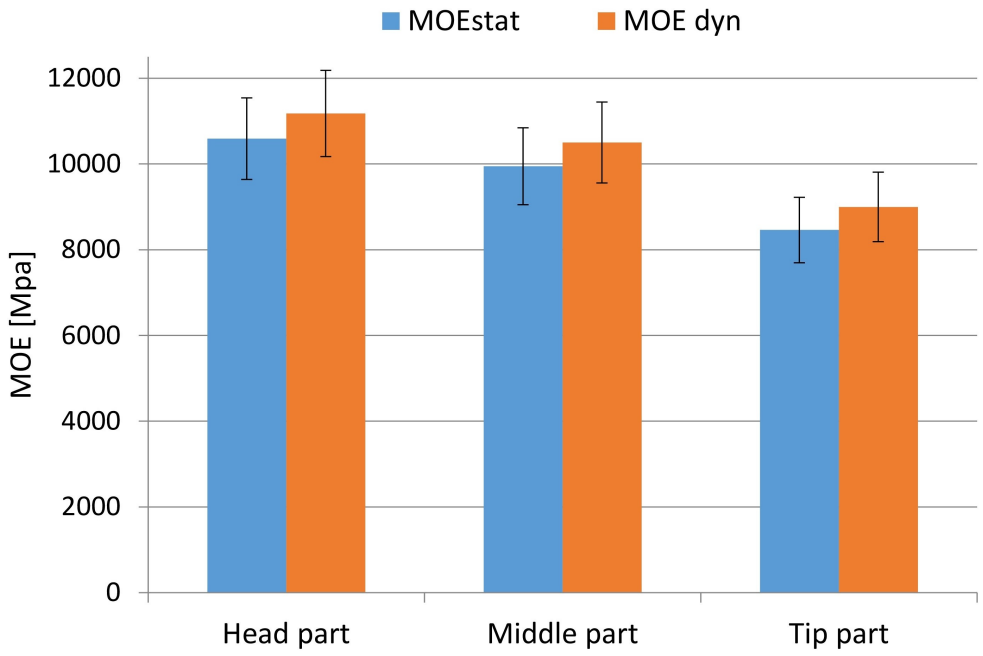

Figure 6.2.2: mechanical properties in head, middle and tip parts;

6.3 Experimental Analysis

6.3.1 MOE of Reference : without knots

Wood is a natural material, consequently a pile has some defects inside. In particular, in this research defects as knots were taken into account. Two different types of wooden piles were considered: the wooden piles without knots and the wooden piles with knots.

The aim of this research was to analyse the influence of knots on the mechanical properties (specifically on the MOE). Therefore, it was necessary to get a value of the MOE that can represent the MOE of the parts of a pile without knots ($MOE_{nk} = \text{"}MOE\ no\ knots\text{"}$).

The MOE_{nk} was determined based on the results from the compression tests of 5 pile segments in which no knots were visible. However, this value could be influenced by other aspects such as geometry imperfections, cracks, resin pockets in the pile, factors that are common in timber piles but that can lead to an alteration of the MOE.

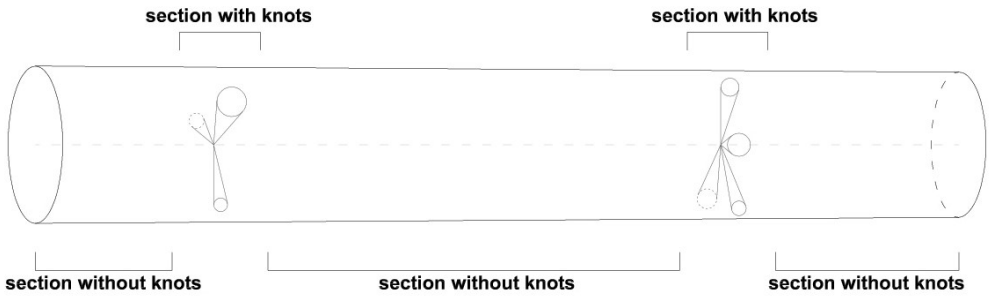

Figure 6.3.1: two different kinds of wood inside a trunk;

However, neglecting these factors, it was assumed that the average modulus of elasticity of pile segments without knots can be used as a reference value for MOE_{nk}:

$$MOE_{nk} = MOE_{pile,nk}$$

In this way, the value of the MOE of timber piles without knots was defined as MOE_{nk}.

In order to get a single reference value of MOE_{nk}, the average MOE of the aforementioned five piles without knots were determined in Table 6.3.

segments ID	knots	MOE_{dyn} [Mpa]	MOE_{static} [Mpa]
K 2.9 M	no	11800	11500
K 2.7 M	no	12900	12150
K 2.11 M	no	12750	12400
K 3.10 M	no	10850	10350
K 3.12 M	no	11600	11700
average		11980	11620

Table 6.3: values of the MOE of the 5 piles tested in this thesis research;

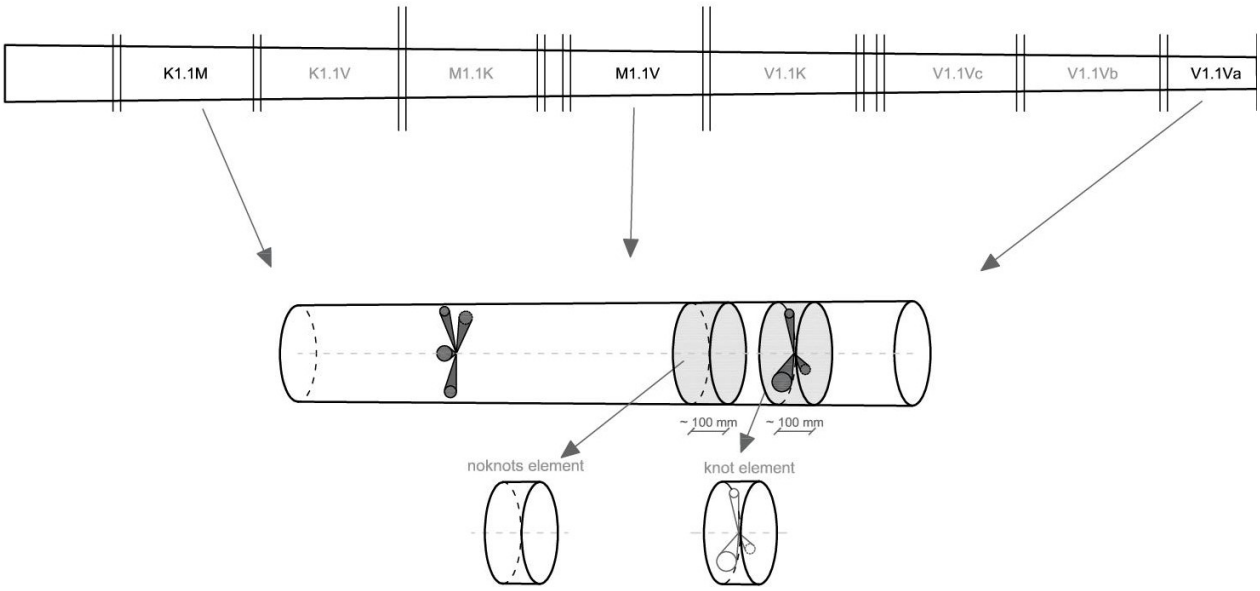

Figure 6.3.2: cutting of the disks with knots and without knots;

Figure 6.3.3: example of a compression test on disks M1.1V with knots;

However, these values obtained for the 5 pile segments, were validated with three disks sawn from the pile OAM 1.1 and then tested in compression to get the MOE_{nk}. Three pile segments were chosen (K1.1M, M1.1V and V1.1Va) to be tested.

The MOE of the disks without knots correspond to the MOE of the pile segments without knots (MOE_{nk}) described before. For disks K1.1M and M1.1V without knots, the value of the MOE is similar to the value of the piles without knots ($MOE_{pile,nk}$). For this reason, the assumption $MOE_{nk} = MOE_{pile,nk}$ was correct.

pile	**nk / k**	**C [mm]**	MOE_{disk} **[Mpa]**	$MOE_{pile,nk}$ **[Mpa]**
K1.1M	nk	750	11700	11600
M1.1V	nk	650	11700	11600
V1.1Va	nk	450	8050	no reference

Table 6.4: comparison between the MOE obtained from the disks and the average MOE available from the piles without knots;

The value of the MOE_{nk} of the V1.1Va was different to the reference $MOE_{pile,nk}$ due to its different composition of wood in a cross-section on the tip-part compared with head-part or middle-part. These last two parts of a pile are composed of similar percentage of heartwood, juvenile wood and sapwood. However, the tip-part is composed of more juvenile causing less stiffness of the sections without knots (Figure 2.2.2).
Unfortunately, there were not tip-parts of a pile available without knots. Therefore, there were not reference piles to get a comparable value of $MOE_{pile,nk}$ for the tip-parts.

In order to understand the differences between timber piles with knots and timber piles without knots, three other disks were cut. The three disks represent a section of the timber piles with knots (fig.6.3.2). In this way, the variation on the MOE and in the density was calculated.

pile	knots	C $[mm]$	height $[mm]$	m_ω [g]	m_{dry} [g]	ω [%]	MOE_{disks} [Mpa]
K1.1M	no	765	98.5	2560	1800	42%	11700
K1.1M	yes	790	97.5	2930	2060	42%	9260
M1.1V	no	640	100	1860	1260	47%	11700
M1.1V	yes	685	97	2220	1490	49%	7110
V1.1Va	no	457	97	880	610	43%	8050
V1.1Va	yes	465	100	1070	750	42%	5300

Table 6.5: Data of the disks before testing;

The variation on density of knots was investigated from disks in order to get a coefficient of increment of the density due to the presence of knots in a cross-section.

First of all, drying condition was studied. The variation of mass in the disk with knots was calculated considering the conical shape of knots.

$$V_{disk} = \pi R^2 \cdot h = \frac{C^2 \cdot h}{4\pi} \qquad ; \qquad V_{knot} = \frac{1}{3}\pi r_{kn}^2 \cdot R = \frac{C \cdot d_{kn}^2}{24}$$

where:
- *C [mm] : circumference of the disk;*
- *h [mm] : height of the disk;*
- *r_{kn} [mm] : radius of knot;*
- *d_{kn} [mm] : diameter of knot;*

A system of two equations and two variables can be written by considering the knots volume and the volume of the disk:

$$\begin{cases} m_{knots} = \rho_{nk} \cdot (V_{tot} - V_{knots}) + \rho_k \cdot V_{knots} \\ m_{noknots} = \rho_{nk} \cdot V_{tot} \end{cases}$$

where:
- *ρ_{nk} [kg/m^3] : density of wood without knots;*
- *ρ_k [kg/m^3] : density of wood with knots;*

pile	nk / k	C [mm]	height [mm]	m_{dry} [g]	V_{knot} $[m^3]$	ρ_{dry}	$\rho/\rho_{dry,nk}$
K1.1M	nk	765	98.5	1800		390	
K1.1M	k	790	97.5	2060	$4.64 \cdot 10^{-4}$	730	1.85
M1.1V	nk	640	100.0	1260		390	
M1.1V	k	685	97.0	1490	$4.01 \cdot 10^{-4}$	600	1.55
V1.1Va	nk	460	97.0	610		380	
V1.1Va	k	465	100.0	750	$3.02 \cdot 10^{-4}$	700	1.84
average						$[kg/m^3]$	1.75

Table 6.6: calculation of the increment on dry density of the MOE;

An average factor of 1.75 is shown. It means that the density of the knots can be 1.75 times major than the density of the wood without knots in dry conditions. These results are in accordance with the literature [25] where a factor of 2.0 was found.

It was not possible to follow the same procedures in wet conditions due to the uncertain value of water inside the cells that made wooden disks [14].

In order to get an approximate factor of densities increase in wet conditions, a generic assumption was done. The disk with and without knots were assumed with the same volume (same moisture content), and the factor of increase was evaluated considering the increment of mass due to only the knots presence.

$$\frac{m_{wet,knots}}{m_{wet,noknots}} = \frac{\rho_{wet,k}}{\rho_{wet,nk}}$$

pile	nk / k	C [mm]	height [mm]	m_{wet} [g]	V_{knot} $[m^3]$	$\rho_{wet,k}/\rho_{wet,nk}$
K1.1M	nk	765	98.5	2560		
K1.1M	k	790	97.5	2930	$4.64 \cdot 10^{-4}$	1.15
M1.1V	nk	640	100.0	1860		
M1.1V	k	685	97.0	2220	$4.01 \cdot 10^{-4}$	1.20
V1.1Va	nk	460	97.0	880		
V1.1Va	k	465	100.0	1070	$3.02 \cdot 10^{-4}$	1.22
average						1.19

Table 6.7: calculation of the increment on wet density of the MOE;

This lead to the conclusion that the increment on the density of knots in wet condition can be about 20% of the value of wood without knots.

For future analysis, it is suggested to develop the research on local analysis with the aim of better understand the real value of the MOE of wood with and without knots and the increment in density of the knots in dry and wet conditions.

Chapter 7

Analysis

7.1 Experimental Analysis

7.1.1 Knots influence on the MOE

In the previous chapters, the possible influence of knots on the MOE is shown. The knots inside a pile can significantly alter the values of dynamic and static MOE. Therefore, it was necessary to have a correlation between the knots layout and mechanical properties of piles.

The influence of knots on mechanical properties was analyzed on the 106 piles available. Knots were considered in three different ways (paragraph 5.1.1):

- KR : the ratio between the sum of the diameters of knots in a section and the circumference of the pile in that section;
- OKR_A : the ratio between the sum of the external area of knots on the surface of the pile and the external area of the pile;
- OKR_V : the ratio between the sum of the volume of knots into the pile and the entire volume of the pile.

However, the MOE can be altered by all the knots along its length; therefore, the KR is not representative of knots layout because it considers the influence of knots on a single cross-section. Furthermore, OKR_A and OKR_V are more representative of knots layout in a pile because they take into account all the knots in a pile.

The head parts and middle parts are characterized by a low value of OKR_A and high values of MOE opposite to the tips that are characterized by higher OKR_A and lower MOE values. The relationship between the MOE and knots layout was showed in fig. 7.1.1 and 7.1.2.

The comparison between fig. 7.1.1 and 7.1.2, shows that factor OKR_A has a higher correlation with the variation of the MOE due to a $R^2 = 0.3159$ rather than a $OKR_V = 0.2461$. R^2 is the coefficient of determination, it represents the proportion of the variation in the dependent variable that is predictable from the independent variable. However, it was necessary to consider that OKR_V cannot be accurate as it weighs the real shape of knots inside a pile starting from its center. In reality, a knot does not have a perfect conical shape and the branches develop irregularly and not always from the centre of the cross-section.

For this reason, the OKR_A is more reliable to measure the real influence of knots on a segment of a pile as it considers the outer dimension of the knots on the external surface of a pile.

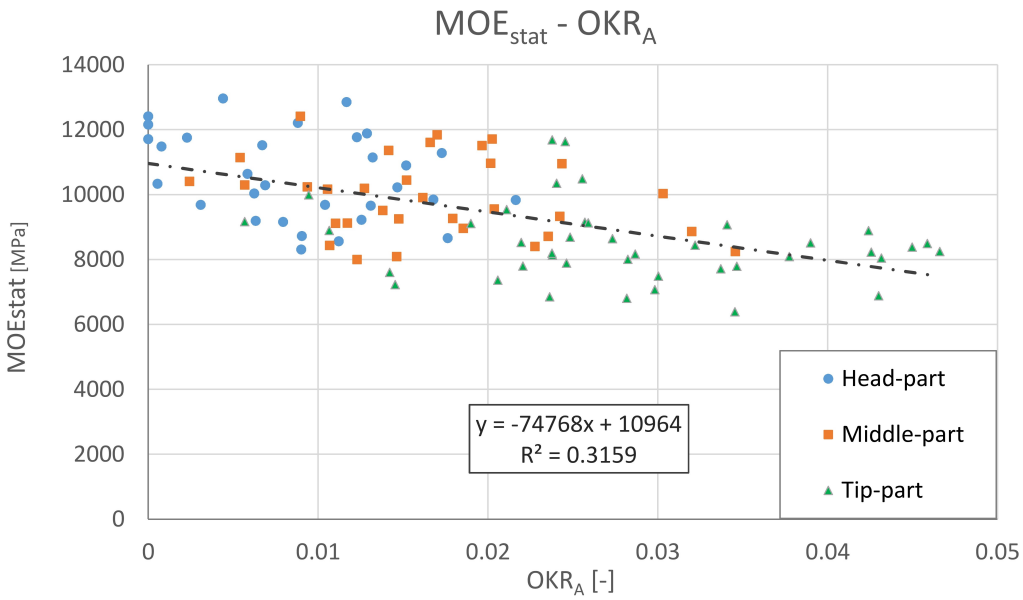

Figure 7.1.1: correlation between the MOE and OKR_A values: the blue points are the head parts of the piles, the orange points are the middle parts of the piles, the green points are the tip parts of the piles.

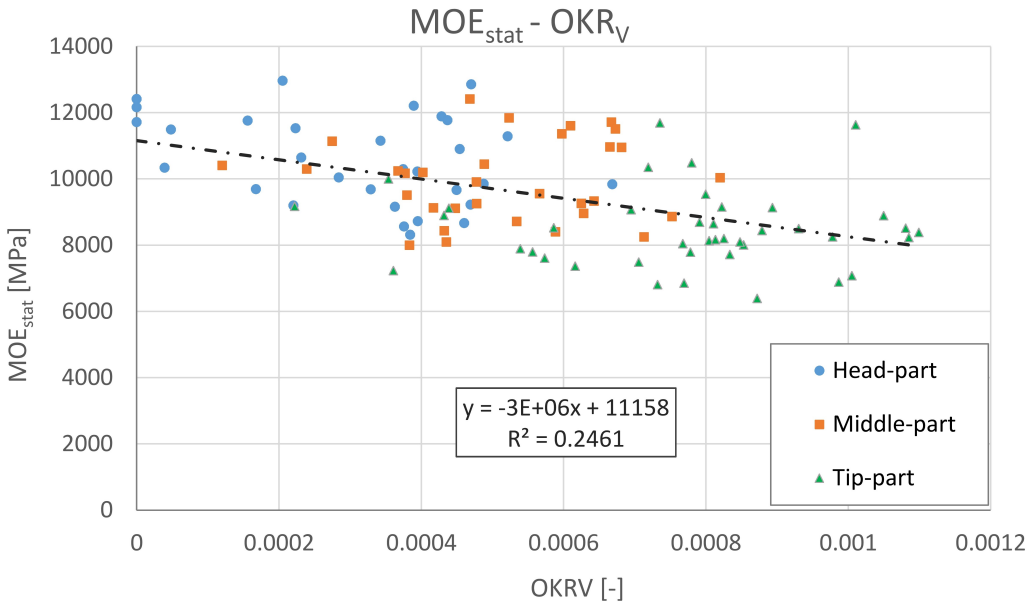

Figure 7.1.2: correlation between the MOE and OKR_V values: the blue points are the head parts of the piles, the orange points are the middle parts of the piles, the green points are the tip parts of the piles.

Then, all the piles were graded based on their knots layout taken into account with OKR_A. Four classes were created:

- class 1 : piles with $OKR_A < 0.010$;
- class 2 : piles with $0.010 < OKR_A < 0.017$;
- class 3 : piles with $0.017 < OKR_A < 0.014$;
- class 2 : piles with $0.024 < OKR_A$;

The average value of the static MOE was calculated for each class and then compared with the value of the MOE_{nk}. A general reduction of the MOE was shown in accordance with the trend of figure 7.1.1. The reduction between piles without knots and piles with knots is evident and its values are shown in the table below.

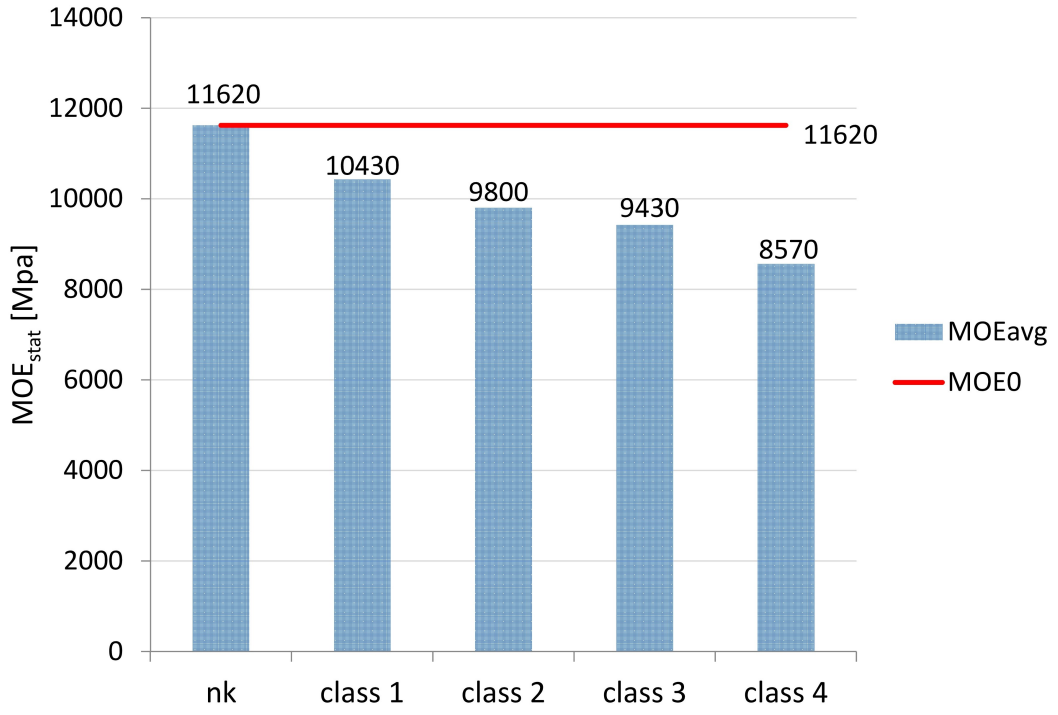

Figure 7.1.3: variation on the MOE for each class of piles with different values of OKR_A;

class	MOE_{avg}	MOE_{nk}	**reduction** [%]
nk	11620	11620	0
class 1	10430	11620	10
class 2	9800	11620	16
class 3	9430	11620	19
class 4	8570	11620	26

Table 7.1: Results of the comparison between piles with knots and without knots;

7.1.2 MOE along the length of a pile

It was interesting to analyze how the MOE value varies through the length of an entire wooden foundation pile because knots usually are more present on the tip-parts than the head parts.

In order to obtain a correlation, different pile were selected (OAM1.1, OAM1.4, OAM2.1, OAM2.8, OAM2.9, OAM2.10). All these piles were composed by eight segments that were cut before the compression tests. MOE values obtained from tests were plotted along the length of the same pile, with the aim of evaluating the variation of the MOE from the head parts to the tip parts of the piles.

A decrease of the MOEs values can be observed in the whole length of a pile, but a more significant reduction happens on the two ends (V2.1Vb and V2.1Va). There can be two reasons for this phenomenon:

- *Tapering* : The pile is tapered and the lower circumference on the tip increases the influence that knots have on both the cross-section and the stiffness.
- *Juvenile wood* : a pile has more juvenile wood in the top parts due to the natural grows of the tree. The higher percentage of juvenile wood leads to low values of stiffness (Fig.2.2.2).

In figure 7.1.4, the variation of the MOE along the length of the pile 2.1 is reported. Further analysis are shown in appendix B.

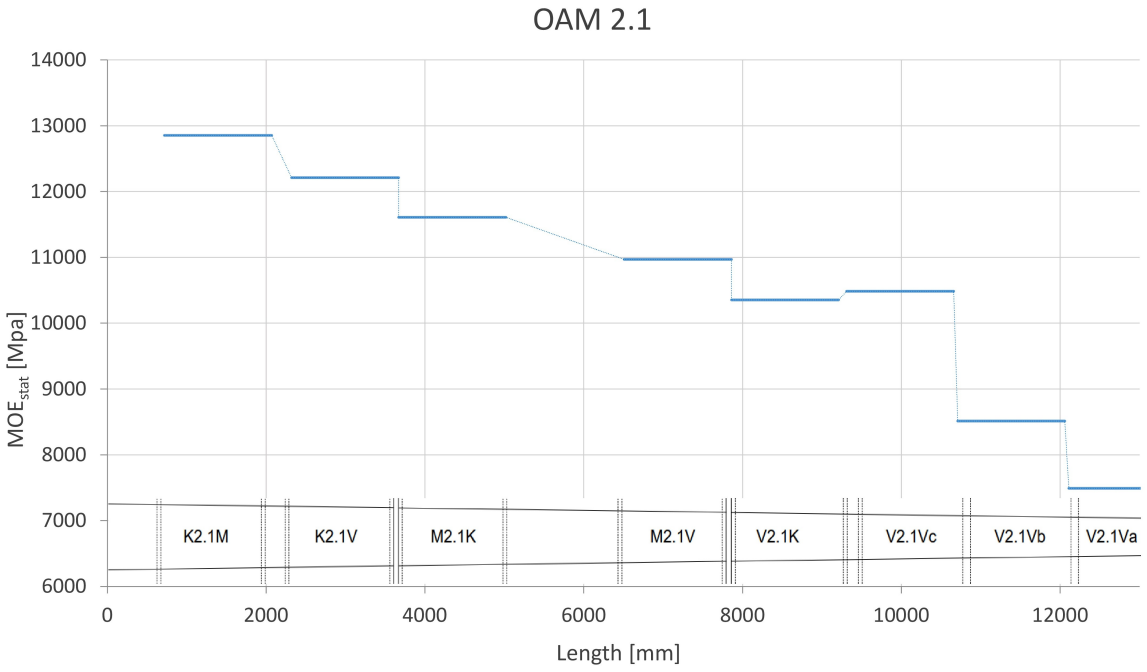

Figure 7.1.4: variations of the MOE in the whole length of the pile OAM 2.1.

7.2 Numerical Analysis

A numerical analysis to simulate the acoustic response of a pile was performed, with the aim to verify if knots are the most influence factor on the variation on the MOE of a pile segment.

The dynamic MOE value can vary for multiple factors that were taken into account during the numerical analysis, such as:

- tapering of the pile: the shape changes along the length of the pile and this causes variation on the acoustic response;
- presence of knots: the presence of knots changes the density and the stiffness locally in the pile.

7.2.1 Numerical Model

In order to verify the high influence of knots on the MOE of a pile segments, a numerical model to estimate the dynamic response of wooden piles with knots was performed using *Matlab* software.

Data set used for the final calibration was made of comparable piles in terms of density, length and diameter. These parameters are relevant to calculate the dynamic MOE (par. 5.2.1.2):

$$MOE_{dyn} = 4 \cdot \rho \cdot L^2 \cdot f^2$$

Several parameters can influence the acoustic response of wooden piles due to the natural origin of timber. It is important to take into account the main parameters that influence the MOE value, such as:

- density and diameter;
- tapering;
- influence of knots on the stiffness and density of a cross-sections;
- knots layout.

All these parameters were considered during the development of the numerical model, in order to have an accurate estimation of the dynamic response of a wooden pile.

7.2.1.1 Hypothesis

To model the stiffness of the parts with and without knots of a pile, two main hypotheses were developed to simulate the real behaviour of a pile:

- MOE of sections without knots: the stiffness value of sections without knots is unknown for each pile. As it is necessary for the evaluation of the acoustic response of a pile to get a reference value of this stiffness, it was assumed:

$$MOE_{nk} = MOE_{pile,nk}$$

where:
- MOE_{nk} *[Mpa] : modulus of elasticity of sections without knots;*
- $MOE_{pile,nk}$ *[Mpa] : modulus of elasticity of a pile without knots;*

The MOE of segments without knots was assumed be equal to the MOE of a pile without knots with the same geometrical characteristic (par. 6.3.1).

- Influence of knots on the stiffness: it was assume that the resistance area is equal to the total area removing the percentage of knots present in a cross-section (figure 7.2.1).

$$A_{res} = A_{tot} \cdot (1 - KR)$$

where:
- A_{res} *[mm^2] : resistance area. Wood area that reacts to the longitudinal load;*
- A_{tot} *[mm^2] : total area (cross-section area);*
- KR *[-] : factor that represent the presence of knots on the cross-section;*

Both hypothesis were necessary to create the model. Therefore, the latter was verify later in the thesis using the DIC test to prove reliability of the model (the first hypothesis was confirmed by the tests on disks par. 6.3.1).

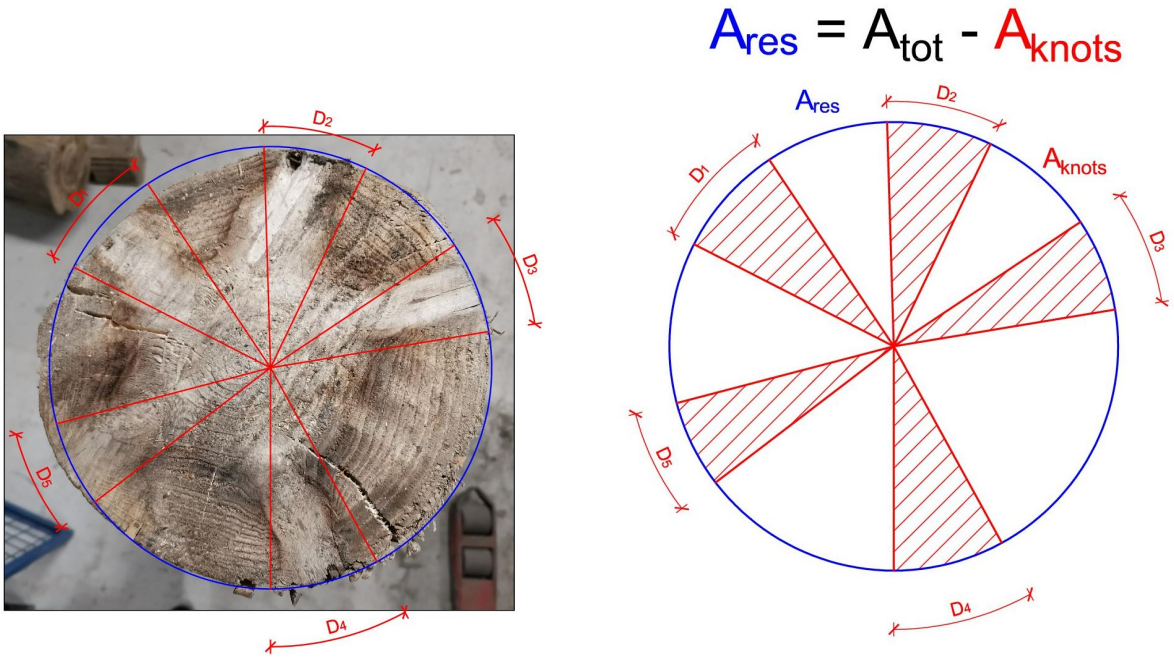

Figure 7.2.1: resistance area of a cross-section with knots;

7.2.1.2 Discretization of the pile

The pile is made of portions with and without knots. Hence, segments of the pile have to be subdivided in parts that have different characteristics. Moreover, the parts of segment depend on how many subdivisions of the problem are needed (discretization of the problem).

$$L_{elem} = \frac{L_{tot} - \sum D_{kn,i}}{n}$$

where:
- L_{tot} *[m] : total length of the segment of pile;*
- $D_{kn,i}$ *[m] : sum of the height of cross-section with knots;*
- n *[-] : number of subdivision of the segment length net of knots;*

The parts of segment have a truncated cone shape due to the tapering of the pile. When a cross-section with knots occurs, a special element needs to be added to the model with different characteristics than the rest of the pile. This part takes the same dimension of the size of knots in that cross-section (fig. 7.2.2).

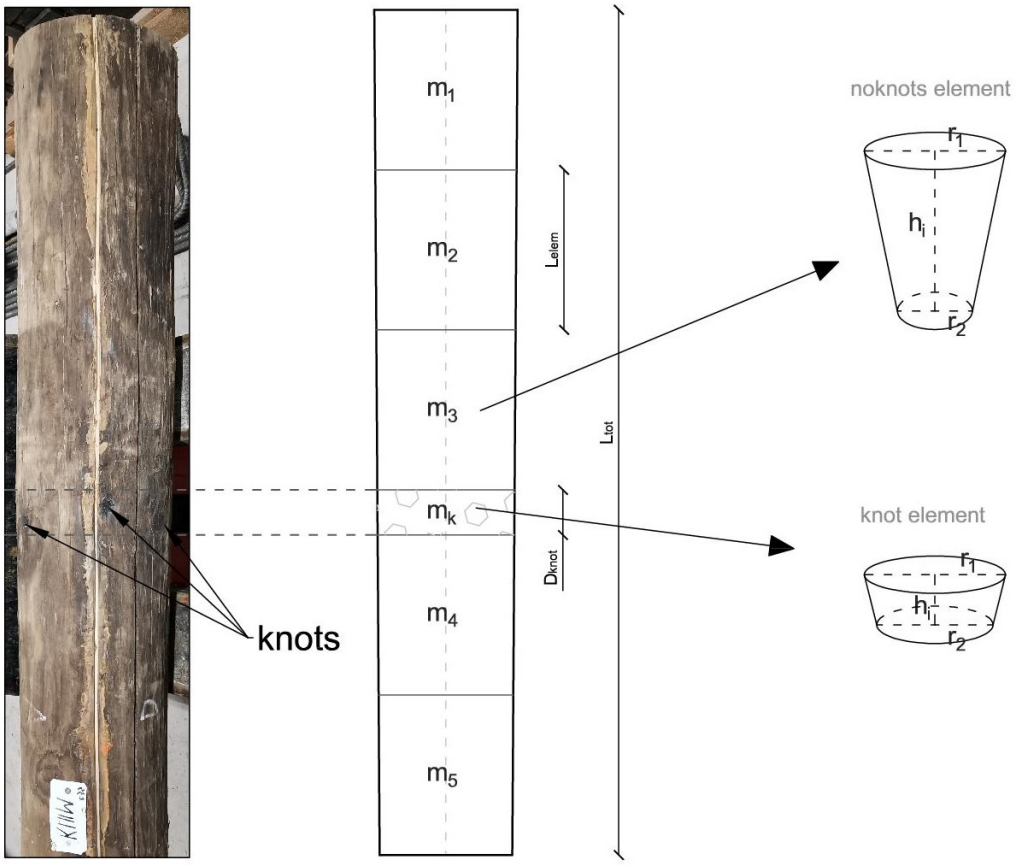

Figure 7.2.2: discretization of the segments of a pile in parts;

7.2.1.3 No Knots Element

The parts of the segments without knots were called "*no knots elements*". It was assumed that these elements are made of one material only that has the mechanical features of wood without knots (ρ_{nk}, MOE_{nk}).

The volume of no knots elements was calculated as a truncated cone due to its tapering (figure 7.2.3):

$$V_{elem} = V_{nk} = \frac{1}{3} \cdot \pi \cdot h \cdot (r_1^2 + r_1 r_2 + r_2^2)$$

where:
- h *[m] : height of the no knots element ;*
- r_1 *[m] : maximum radius between the two faces;*
- r_2 *[m] : minimum radius between the two faces;*

In order to get the masses matrix, the mass of each element can be evaluated as:

$$m_{nk} = V_{elem} \cdot \rho_{nk} = V_{nk} \cdot \rho_{nk}$$

where:
- V_{elem} *[m^3] : volume of the element of model considered ;*
- V_{nk} *[m^3] : volume of the no knots element;*
- ρ_{nk} *[kg/m^3] : density of the no knots part;*

Elements in the model are connected using springs that replicate the real stiffness of the pile in each part. Each one has a different stiffness value due to the tapering of the pile and the presence of knots. In general, the stiffness of a spring is calculated as:

$$k_{elem} = \frac{EA}{L}$$

where:
- E *[N/mm^2] : modulus of elasticity of the spring;*
- A *[mm^2] : resistance area;*
- L *[mm] : length of the spring;*

In case of sections without knots, the resistance area is the same as the total area:

$$k_{nk} = \frac{E_{nk} \cdot A_{res}}{L_{elem}} = \frac{E_{nk} \cdot A_{tot}}{L_{elem}}$$

where:
- E_{nk} *[N/mm^2] : modulus of elasticity of no knots element;*
- A_{res} *[mm^2] : resistance area;*
- A_{tot} *[mm^2] : total area of the cross section considered;*
- L_{elem} *[mm] : length of the no knots element;*

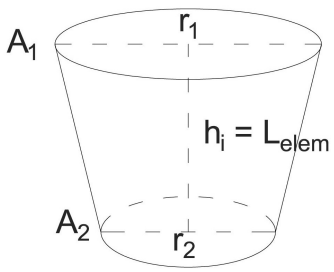

Figure 7.2.3: geometry of no knots element;

7.2.1.4 Knots Element

The parts of the segments without knots was called "*knots elements*". These elements have different characteristics compared with no knots elements and it was necessary to define how knots influence mechanical behaviour in terms of mass and stiffness.

The presence of knots can be evaluated considering its conical shape in terms of mass and volume. The mass of knots elements was calculated by adding the mass of each knot to the mass of wood without knots, netted of knots volume as in the following equation:

$$m_{elem} = m_{kn} = (V_{elem} - V_{kn}) \cdot \rho_{nk} + V_k \cdot \rho_k$$

where:
- V_{elem} *[m^3] : volume of the element of model considered ;*
- V_k *[m^3] : sum of the volume of each knot in the cross-section considered;*
- ρ_{nk} *[kg/m^3] : density of the no knots part;*
- ρ_k *[kg/m^3] : density of knots;*

The volume of a knot can be similarly calculated considering the conical shape:

$$V = \frac{1}{3} \cdot A \cdot h$$

Assuming that all knots are round knots and taking into account that a knot start from the centre of a cross-section, the equation above can be rewritten as:

$$V_{knot} = \frac{1}{3} \cdot \pi r_{knot} \cdot R_{pile}$$

where:
- r_{knot} *[mm] : external radius of the knot on the pile surface;*
- R_{pile} *[mm] : distance between pith and bark of a pile that correspond to the radius of the pile;*

In particular, the volume of knots is evaluable as:

$$V_{k,i} = \frac{1}{3} \cdot \pi \phi_i^2 \cdot R \qquad \Longrightarrow \qquad V_k = \sum_{i=1}^{n} V_{k,i}$$

where:
- $V_{k,i}$ *[m^3] : volume of a single knot;*
- V_k *[m^3] : sum of the volume of each knot in the cross-section considered;*
- ϕ_i *[m] : size of each knot;*
- R *[m] : radius of the pile on the cross-section considered;*

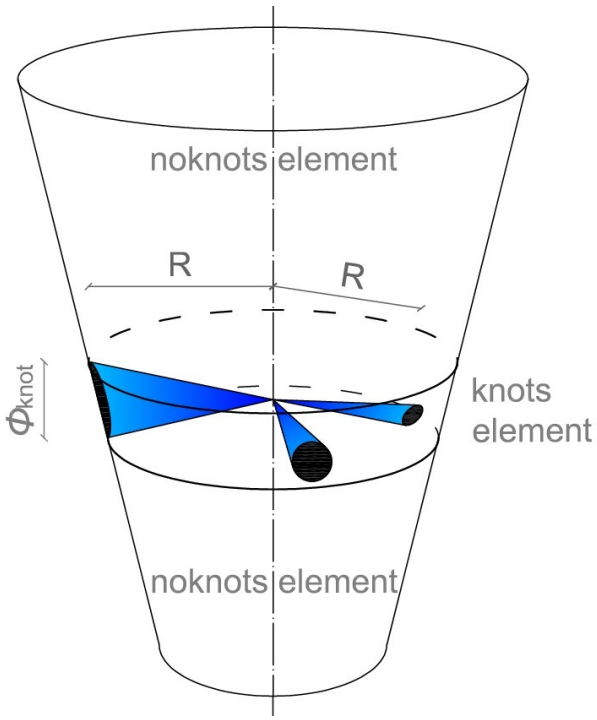

Figure 7.2.4: presence of knots inside the knots element;

Elements in the model were connected with springs that replicate the real stiffness of the pile in each part. Each one has a different stiffness value due to the tapering of the pile and the presence of knots. In general, the stiffness of a spring is evaluated as:

$$k_{elem} = \frac{EA}{L}$$

where:
- E *[N/mm^2] : modulus of elasticity of the spring;*
- A *[mm^2] : resistance area;*
- L *[mm] : length of the spring;*

In the case of knots element, the presence of knots significantly influences the stiffness of springs due to the inclination of the fibers. Since wooden piles are subjected to the axial loads parallel to the longitudinal direction of the fibers, knots alter the angle between load and fiber direction, causing a reduction of the stiffness. This can be evaluated with a reduction of the resistance area of the cross-section considering the presence of knots with the usage of KR:

$$k_{kn} = \frac{E_{nk} \cdot A_{res}}{\phi_{kn,max}} = \frac{E_{nk} \cdot A_{tot} \cdot (1 - KR)}{\phi_{kn,max}}$$

where:
- E_{nk} *[N/mm^2] : modulus of elasticity of wood without knots;*
- A_{res} *[mm^2] : resistance area;*
- A_{tot} *[mm^2] : total area of the cross-section considered;*
- KR *[-] : factors that takes into account the presence of knots in the cross-section;*
- $\phi_{kn,max}$ *[mm] : maximum size dimension of knots in the cross-section;*

In particular, when a section with knots occurs the spring of the model between knots element and no knots element is composed of two different types of springs, as shown in figure 7.2.5. This is due to the masses of the model being located at the center of gravity of elements and the spring includes a part of no knots element and a part of knots element.

$$k_{kn} = \frac{E_{nk} \cdot A_{avg} \cdot (1 - KR)}{\phi_{kn,max}/2} \qquad ; \qquad k_{nk} = \frac{E_{nk} \cdot A_{avg}}{L_{elem}/2}$$

where:
- E_{nk} *[N/mm^2] : modulus of elasticity of wood without knots;*
- A_{avg} *[mm^2] : average area between consecutive elements;*
- KR *[-] : factors that takes into account the presence of knots in the cross-section;*
- $\phi_{kn,max}/2$ *[mm] : maximum size dimension of knots in the cross-section subdivided by two;*
- $L_{elem}/2$ *[mm] : length of no knots element subdivided by two;*

The sum in series of the two stiffness is:

$$k_r = \frac{k_{nk} \cdot k_k}{k_{nk} + k_k}$$

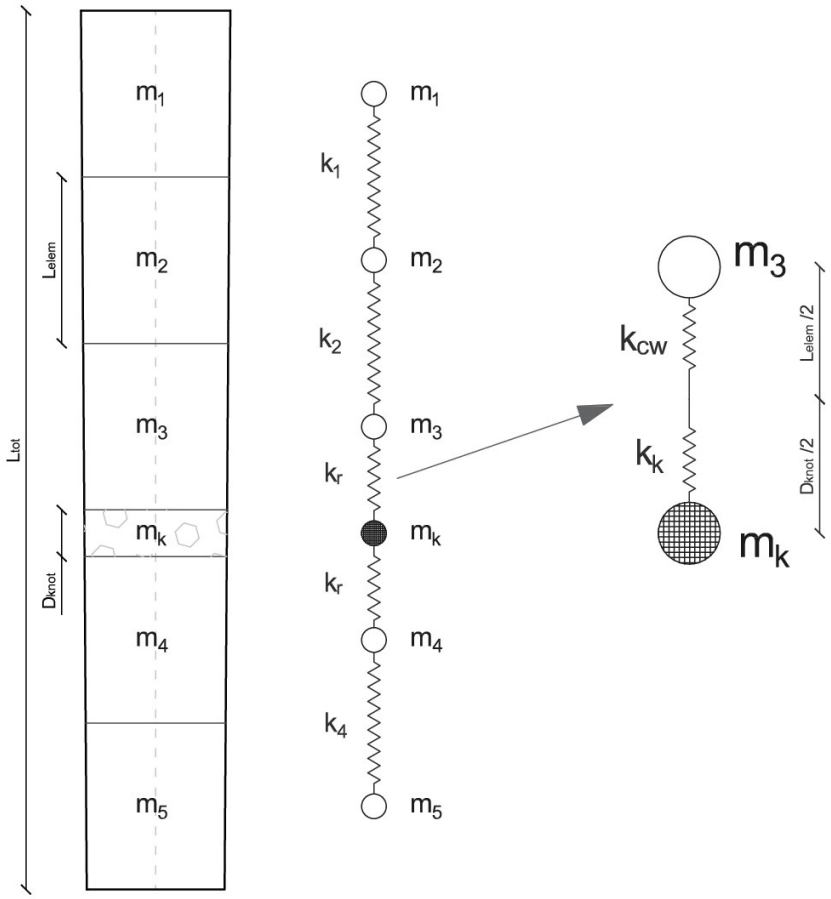

Figure 7.2.5: example of evaluation of the spring stiffness between no knots and knot elements;

7.2.1.5 Resolution of the System

In order to find the natural frequencies of wooden piles, the numerical model has to be formulated in a problem of eigenvectors and eigenvalues:

$$\overline{\overline{K}} \cdot \overline{X} = \lambda \cdot \overline{\overline{M}} \cdot \overline{X}$$

where λ is the eigenvalue, X is the eigenvector, K is the matrix of the stiffness and M is the matrix of the masses.

For a system with two masses, or more generally two degrees of freedom, M and K are 2x2 matrices. In a system with n degrees of freedom, they are nxn matrices.

$$\overline{\overline{M}}_{nxn} = \begin{bmatrix} m & 0 & \dots & \dots & \dots & \dots & \dots \\ 0 & m & 0 & \dots & \dots & \dots & \dots \\ \dots & \dots & \dots & \dots & \dots & \dots & \dots \\ \dots & \dots & 0 & m_k & 0 & \dots & \dots \\ \dots & \dots & \dots & \dots & \dots & \dots & \dots \\ \dots & \dots & \dots & \dots & 0 & m & 0 \\ \dots & \dots & \dots & \dots & \dots & 0 & m \end{bmatrix}$$

where m_k is the mass of the part with knots.

$$\overline{\overline{K}}_{nxn} = \begin{bmatrix} k_1 & -k_1 & 0 & \dots & \dots & \dots & \dots & \dots & \dots \\ -k_1 & (k_1+k_2) & -k_2 & 0 & \dots & \dots & \dots & \dots & \dots \\ 0 & -k_2 & (k_2+k_3) & -k_3 & 0 & \dots & \dots & \dots & \dots \\ \dots & \dots & \dots & \dots & \dots & \dots & \dots & \dots & \dots \\ \dots & \dots & \dots & \dots & -k_r & 2\cdot k_r & -k_r & \dots & \dots \\ \dots & \dots & \dots & \dots & \dots & \dots & \dots & \dots & \dots \\ \dots & \dots & \dots & \dots & \dots & \dots & -k_{n-2} & (k_{n-2}+k_{n-1}) & -k_{n-1} \\ \dots & \dots & \dots & \dots & \dots & \dots & \dots & -k_{n-1} & k_n \end{bmatrix}$$

where k_r is the stiffness of the part with knots.

The system gives solutions in terms of eigenvalues λ. From these factors the angular and the vibration frequencies of the pile, are evaluable as:

$$\omega[\frac{rad}{s}] \quad = \quad \sqrt{\lambda} \qquad \Longrightarrow \qquad f[Hz] \quad = \quad \frac{\omega}{2\pi}$$

In the end, the MOE value is obtained from the first shapes mode, that is the first natural frequencies different to zero (f=[0 f_1 f_2 f_3 ... f_n]) as shown in figure 7.2.6. The MOE was evaluated with the following equation:

$$MOE_{mod} = 4 \cdot \rho \cdot f^2 \cdot L^2$$

where:
- *L [mm] : length of the segment of the pile;*
- *f [s/rad] : frequency of vibration of the pile;*
- *ρ [kg/m^3] : density of the pile;*

Further, to check the accuracy of the model, the MOE obtained was compared with the dynamic MOE measurement from MTG grader tool. As close the two values are, as more precise is the prediction of the model. Comparisons were plotted in the following paragraph.

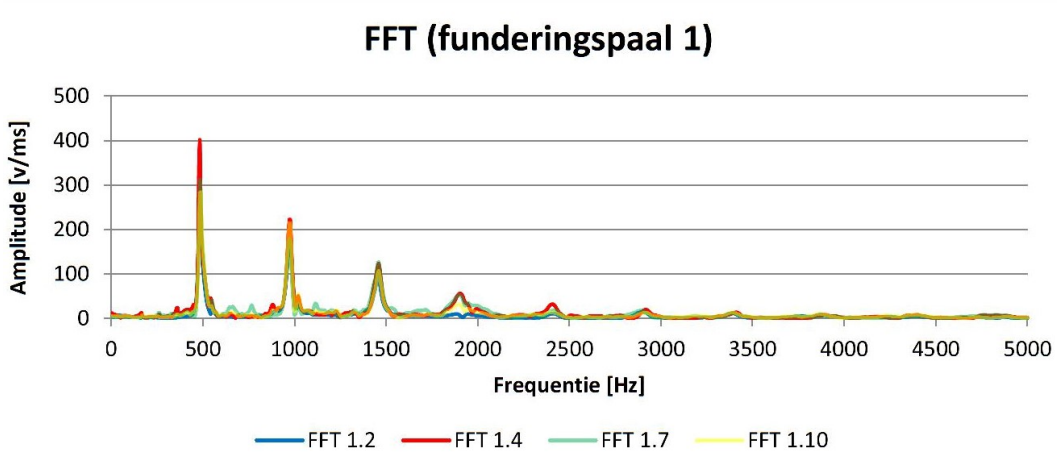

Figure 7.2.6: example of Fast Fourier Transformation (FFT) in frequency domain [33];

7.2.2 Calibration of the model

A numerical model made of masses and springs, can represent the acoustic response of a wooden pile well. Unfortunately, many factors contribute to obtain wrong results, such as different dimensions of segments and the presence of knots. For this reason, the numerical model needed a calibration.

The calibration of the model was based on the hypothesis that the MOE of sections without knots is similar among pile with comparable characteristics. For this reason, the comparison between piles with and without knots was performed considering piles with comparable characteristics. Three groups of piles with similar density, length and diameter are created, then several steps are carried out to calibrate the model:

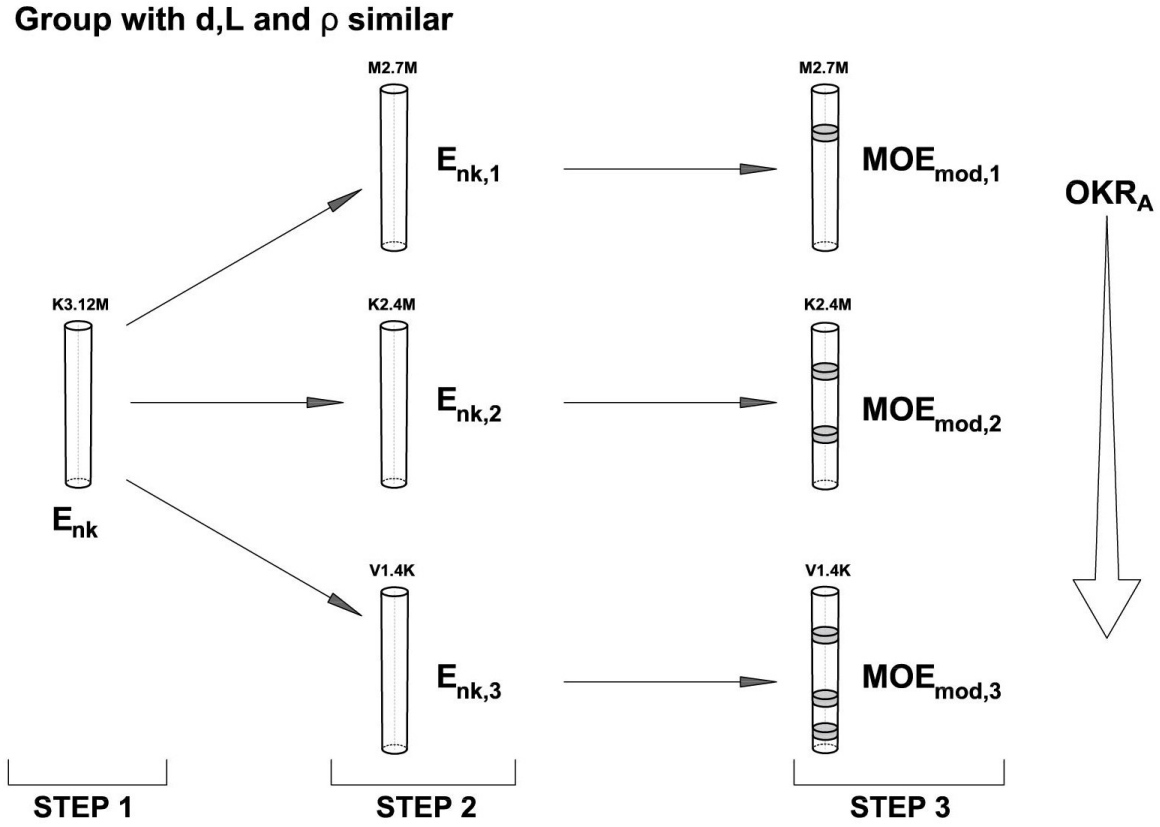

Figure 7.2.7: procedure for the calibration of the model;

1. In the first step, the modelling of a pile without knots was performed. The model was composed of springs which stiffness was calculated as an element without knots (as reported in the paragraph 7.2.3).

$$k_{nk} = \frac{E_{nk} \cdot A_{avg}}{L_{elem}}$$

The input value of the E_{nk} was the MOE_{dyn} measured on the entire segments due to the fact that the MOE of sections without knots (E_{nk}) was assumed similar to the MOE of a pile without knots ($MOE_{dyn,nk}$).

The output value of the model (MOE_{mod}) was the MOE of the segment without knots. This value must be similar to the MOE measured with MTG grader tool due to its dynamic behaviour. The MOE_{mod} of the pile without knots was called MOE_0 and it is the reference value used in the following steps.

$$MOE_{mod} = MOE_0$$

2. In the second step, another segment with similar diameter, length and density was considered. The new pile differs from the previous for the presence of knots, but it has a similar E_{nk} as its characteristics are alike. However, to obtain the precise E_{nk} correspondent to the features of the new pile, another model was made.
   The new segments was modelled without the presence of knots with the aim to obtain the correct E_{nk} value considering density, diameter and tapering of this specific pile. The output value of the model (MOE_1) was assumed as E_{nk} for the same segment model which simulates the presence of knots.

$$k_{nk} = \frac{E_{nk} \cdot A_{avg}}{L_{elem}} = \frac{MOE_0 \cdot A_{avg}}{L_{elem}} \qquad \Longrightarrow \qquad MOE_{mod} = MOE_1$$

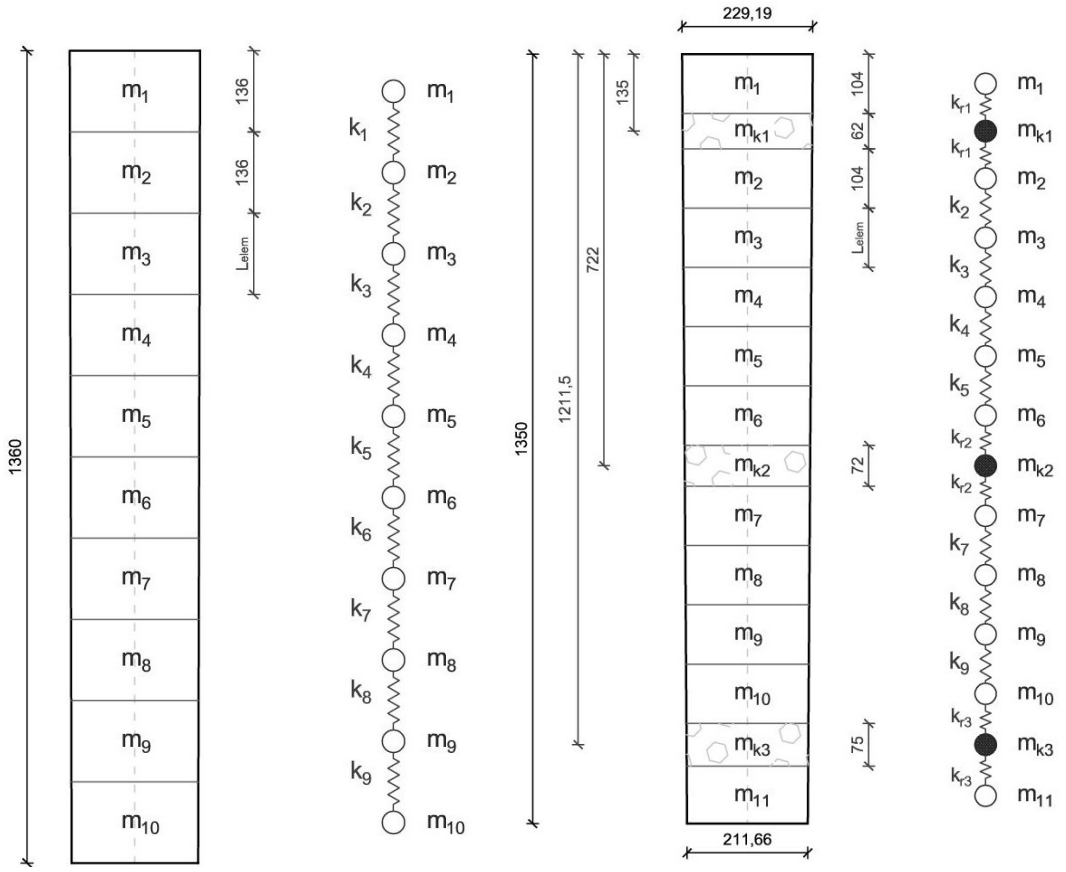

Figure 7.2.8: step 1 (on the left): example of the modelling of a pile without knots; step 3 (on the right): example of the modelling of a pile with knots;

segment	D [mm]	ρ $[kg/m^3]$	ρ_k $[kg/m^3]$	L [mm]	KR [-]	OKR_A [-]
K3.12M	**215**	**450**	**-**	**1360**	**-**	**0.00**
M2.7M nk	212	430	-	1350		
M2.7M	212	430	860	1350	0,12	$2.4 \cdot 10^{-3}$
K2.8M nk	213	420	-	1350		
K2.8M	213	420	840	1350	0,18/0,14/0,05	$1.0 \cdot 10^{-2}$
M2.4M nk	218	360	-	1350		
M2.4M	218	360	720	1350	0,27/0,18/0,07	$1.3 \cdot 10^{-2}$
V1.4K nk	221	370	-	1350		
V1.4K	221	370	740	1350	0,55/0,46/0,26	$4.7 \cdot 10^{-2}$
K2.9M	**220**	**460**	**-**	**1350**	**-**	**0.00**
M1.10M nk	224	420	-	1350		
M1.10M	224	420	840	1350	0,32/0,17	$1.4 \cdot 10^{-2}$
K3.10M	**213**	**310**	**-**	**1360**	**-**	**0.00**
K2.8V nk	209	390	-	1350		
K2.8V	209	390	780	1350	0,24/0,19/0,18	$1.3 \cdot 10^{-2}$
M1.1K nk	225	320	-	1350		
M1.1K	225	320	640	1350	0,36/0,27	$1.5 \cdot 10^{-2}$
V1.4Vc nk	201	350	-	1350		
V1.4Vc	201	350	700	1350	0,42/0,42/0,27/0,16	$4.3 \cdot 10^{-2}$

Table 7.2: input data of each segment. Segments are subdivided into 3 groups;

3. In the last step, the presence of knots was modelled. Knots have different densities which lead to more weight of the element with knots than the element without knots. Moreover, knots reduce the stiffness of that cross-section due to a smaller resistance area. The two effects were considered as reported in the previous paragraph (par. 7.2.1.1):

$$V_{kn,i} = \frac{1}{3} \cdot \pi \phi_i^2 \cdot R \qquad k_{kn} = \frac{E_{nk} \cdot A_{avg} \cdot (1 - KR)}{\phi_{kn,max}/2} = \frac{MOE_1 \cdot A_{avg} \cdot (1 - KR)}{\phi_{kn,max}/2}$$

$$MOE_{mod} = MOE_2 \qquad \Longrightarrow \qquad MOE_2 \sim MOE_{dyn}$$

The output value is the acoustic response of the segment (MOE_2). The output value must be similar to the dynamic MOE of the pile with knots measured with MTG grader tool.

Three groups of segments were created for the calibrations. Groups are made of piles with similar density, length and diameter. All the steps described above were followed for each group considering the density of knots 2 times the density of wood without knots.
In the following table are reported:

- *Step 1*: the pile of reference (bold);
- *Step 2*: similar piles with knots, but modelled without knots;
- *Step 3*: piles of the second step modelled with knots.

segment	MOE_{dyn} [Mpa]	E_{nk} [Mpa]	MOE_{mod} [Mpa]	Δ mod/dyn
K3.12M	**11600**	**11600**	**11450**	**1.10%**
M2.7M nk	-	11450	11400	-
M2.7M	10995	11400	11200	2.70%
K2.8M nk	-	11450	11300	-
K2.8M	10324	11300	10900	5.40%
M2.4M nk	-	11450	11200	-
M2.4M	10900	11200	10650	2.40%
V1.4K nk	-	11450	11100	-
V1.4K	8850	11100	9450	6.90%
K2.9M	**11800**	**11800**	**11750**	**0.60%**
M1.10M nk	-	11750	11550	-
M1.10M	10554	11550	10800	2.30%
K3.10M	**10850**	**10850**	**10850**	**0.10%**
K2.8V nk	-	10850	10600	-
K2.8V	9791	10600	10050	2.60%
M1.1K nk	-	10850	10550	-
M1.1K	10297	10550	9850	4.30%
V1.4Vc nk	-	10850	10400	-
V1.4Vc	8003	10400	9100	13.80%

Table 7.3: input and output data of the model;

Results show the accuracy of the model. All the predicted $MOE_{mod} = MOE_2$ are compared with MOE_{dyn}, and their variation is reported in % in the last column of table 7.3. The error is lower in a pile with low values of KR (less presence of knots) than a pile with high values of KR (high presence of knots). The accuracy of the model is high because the error is often less than 10%.

Shapes mode can be also a factor to represent the accuracy of the model. Shapes mode of a freely imposed beam are reported in section 5.3.2. Solutions in terms of eigenvectors are shown in figure 7.2.9 and they display how shapes mode of the numerical model are similar to modes of a freely imposed beam (figure 5.3.4) but locally disturbed by knots presence.

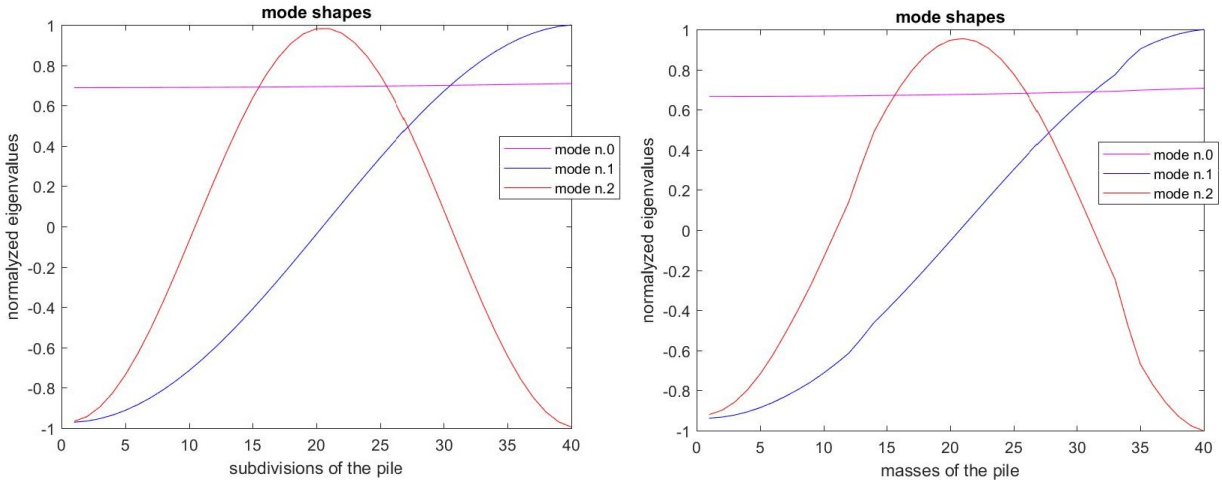

Figure 7.2.9: shapes mode of pile K3.12M on the left and M2.4M on the right;

Density Influence In order to evaluate the influence of the density on the dynamic MOE obtained from the model, two cases were analyzed:

- Density of wood without knots: the pile K3.12M (piles without knots) was modelled with different values of density to evaluate the variation on the acoustic response. It was observed that the MOE value does not change at the variation of the ρ_{nk} because the frequency decrease when density increase.

ρ_{nk} $[kg/m^3]$	E_{nk} [Mpa]	freq [rad/s]	MOE_{mod} [Mpa]
766	11600	1420	11460
600	11600	1610	11460
700	11600	1490	11460
800	11600	1390	11460
900	11600	1310	11460

Table 7.4: variation of the MOE due to the variation of the wood without knots density;

- Density of knots: the pile M2.4M was modelled with the same value of $\rho_{nk} = 760kg/m^3$ but different values of ρ_k with the aim of evaluating the influence of the knots density on the solutions of the model. It was observed that the MOE value has a small variation at the increase of the knots density. This happened because knots are smaller compared with the whole segment of the pile. Therefore, knots masses have a small influence on the solutions of the numerical model.

ρ_{nk} $[kg/m^3]$	ρ_k/ρ_{nk}	E_{nk} **[Mpa]**	**freq [rad/s]**	MOE_{mod} **[Mpa]**	Δ_{red} **knots [%]**
760	1	11200	1389	10720	0.0%
760	1.3	11200	1387	10680	0.3%
760	1.6	11200	1385	10650	0.6%
760	1.8	11200	1383	10630	0.8%
760	2	11200	1381	10610	1.0%

Table 7.5: the MOE variation due to change in knots density;

The numerical model depends on the stiffness and density of wooden piles as observed in tables above. However, when the density in the model changes, the final MOE calculated does not change due to the coinciding decrease of frequency. Moreover, the influence of knots density on the MOE is not high because of the smaller weight of knots than the entire pile. Therefore, the influence of density is less than the influence of the stiffness on the numerical model.

7.2.3 DIC test

In order to prove that the the resistance area is equal to the total area removing the percentage of knots presence in a cross-section, a DIC test was done on two piles, M2.1M and K3.12M, during a compression test. The aim was to evaluate the variation on the MOE of the knot area compared with the no knots area. The value of stiffness on the knot surface must be similar to the value of stiffness of no knots surface removing the percentage of knots presence on the cross-section.

$$k_{kn} = \frac{MOE_{nk} \cdot A_{res}}{L_{elem}} = \frac{MOE_{nk} \cdot A_{tot} \cdot (1 - KR)}{L_{elem}} = \frac{MOE_k \cdot A_{tot}}{L_{elem}}$$

where:
- MOE_{nk} *[Mpa] : modulus of elasticity of wood without knots;*
- MOE_k *[Mpa] : modulus of elasticity of wood with knots;*
- A_{res} *[mm^2] : resistance area of the cross-sections;*
- A_{tot} *[mm^2] : total area of the cross-sections;*
- KR *[-] : factors that takes into account the presence of knots in the cross-section;*
- L_{elem} *[mm] : length of the element;*

It is possible to rewrite the previous hypothesis of the model to automatically verify it by proving the reliability of the new hypothesis:

$$A_{res} = A_{tot} \cdot (1 - KR) \qquad \Longrightarrow \qquad MOE_k = MOE_{nk} \cdot (1 - KR)$$

To obtain the variation of the MOE between parts of the pile with and without knots, two areas of the analyzed surface were individuated. The first one was the area of the knot; it was individuated through a visual inspection on GOM mesh of the area where major deformations occur. The second area was selected where no deformation due to knots presence occurs.

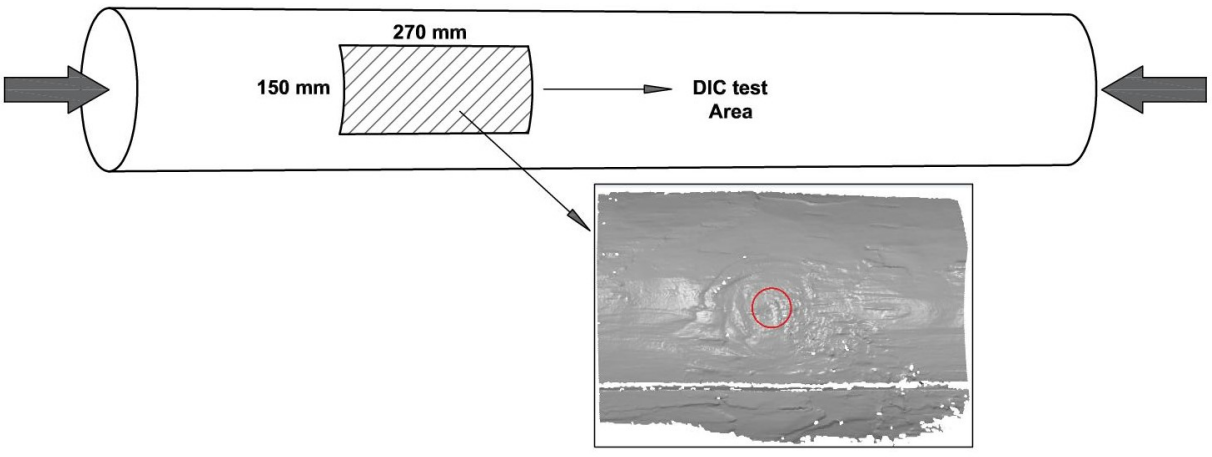

Figure 7.2.10: 3D mesh on software GOM around the knot;

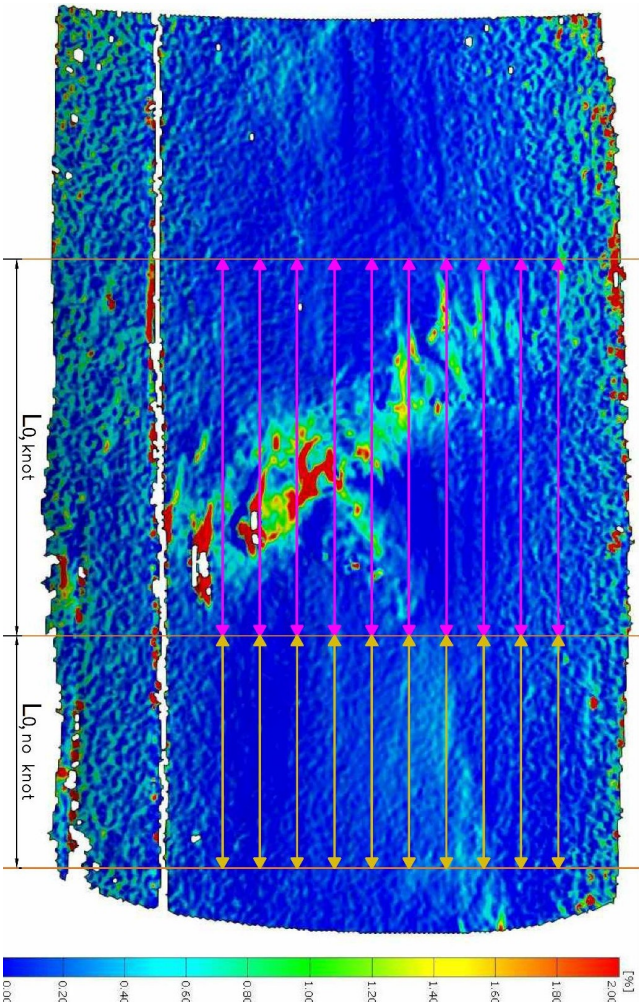

Figure 7.2.11: knots area in the middle of the figure and no knots area on bottom part;

In both areas, two points were selected on the ends and their distance was studied during the compression test. These represent a "virtual" linear potentiometers that displays the displacement of the no knots and knot area.

In order to obtain comparable values, the variation of the stiffness was chosen in elastic phase between two load steps (figure 7.2.12). It was assumed that the increase of stress between the two load steps was constant on knots and no knots area. This leads to the conclusion that if the stress is constant between two load steps, stiffness is inversely related to strains. Therefore, a decrease in stiffness causes an increment of strains on the considered surface.

$$MOE_{DIC} = \frac{\Delta\sigma}{\Delta\varepsilon_{avg}}$$

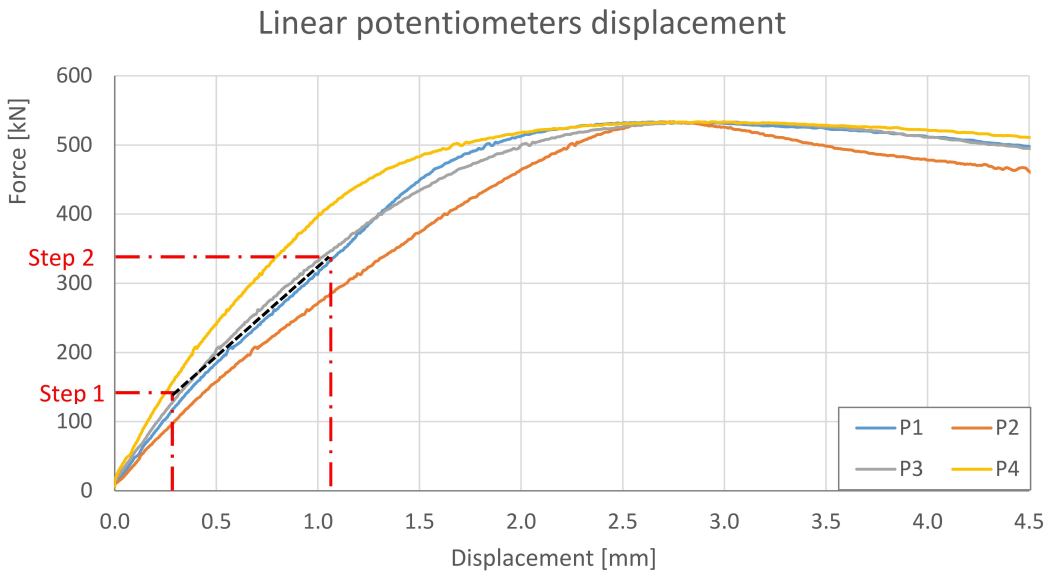

Figure 7.2.12: two load steps selected;

pile code	**element type**	**KR** [-]	F_1 [kN]	F_2 [kN]	$\Delta\sigma_{12}$ [Mpa]	ε_{avg} [%]	MOE_{DIC} [Mpa]	MOE_{KR} [Mpa]
M2.1M	No knots		150	350	6.15	-0.061%	10100	
M2.1M	knots	0.27	150	350	6.15	-0.079%	7790	7400
M3.12K	No knots		200	380	6.11	-0.060%	10100	
M3.12K	knots	0.19	200	380	6.11	-0.072%	8540	8210

Table 7.6: Results of DIC analysis of piles M2.1M and M3.12K;

The strains were calculated as the average value of the strain of each length considered on the portion of the selected surface.

$$\Delta\varepsilon_{avg} = \sum_{i=1}^{n} \frac{L_{2,i} - L_{1,i}}{L_{0,i}}$$

where:
- $\Delta\varepsilon_{avg}$ *[-] : average strain of the area considered;*
- $L_{0,i}$ *[mm] : original distance between two points;*
- $L_{1,i}$ *[mm] : distance between two points at load step 1;*
- $L_{2,i}$ *[mm] : distance between two points at load step 2.*

The results shown an increase of the strain between the area with knots instead of the area without knots. This leads to the conclusion that the area with knots has a lower value of modulus of elasticity.

Then, the $MOE_{DIC,k}$ was compared with the MOE obtained multiplying the $MOE_{DIC,nk}$ for the percentage of knots presence, the hypothesis yet to verify. The two values were similar on both piles tested. Therefore, it was possible to assume that the resistance area of knots cross-section is the total area reduced by the area of knots in a cross-section.

$$MOE_{DIC,k} \cong MOE_{KR} = MOE_{DIC,nk} \cdot (1 - KR) \qquad \Longrightarrow \qquad A_{res} = A_{tot} \cdot (1 - KR)$$

Another correlation was found by studying where maximum strains deformations occur. Deviation in the fibers direction was noticed when analyzing the deformations around the knot area. Where the maximum strains occur, the stiffness of wood becomes lower because the strains was high. The width perpendicular to the longitudinal direction of the maximum strains was called $d_{2,DIC}$.

The $d_{2,DIC}$ was like the width of d_2 measured before the test. Because of this, d_2 can be a good estimator of knots influence due to the higher deformation during a compression test (deviation of the fibers) instead of d_1 (knots size).

$$d_{2,DIC} = 44.76mm \qquad\qquad d_2 = 45mm$$

In this research, DIC tests were performed only on 2 segments of pile. For this reason, the accuracy of results from the analysis above can be improved. In order to get more reliable results, more tests are suggested to be performed using DIC technology.

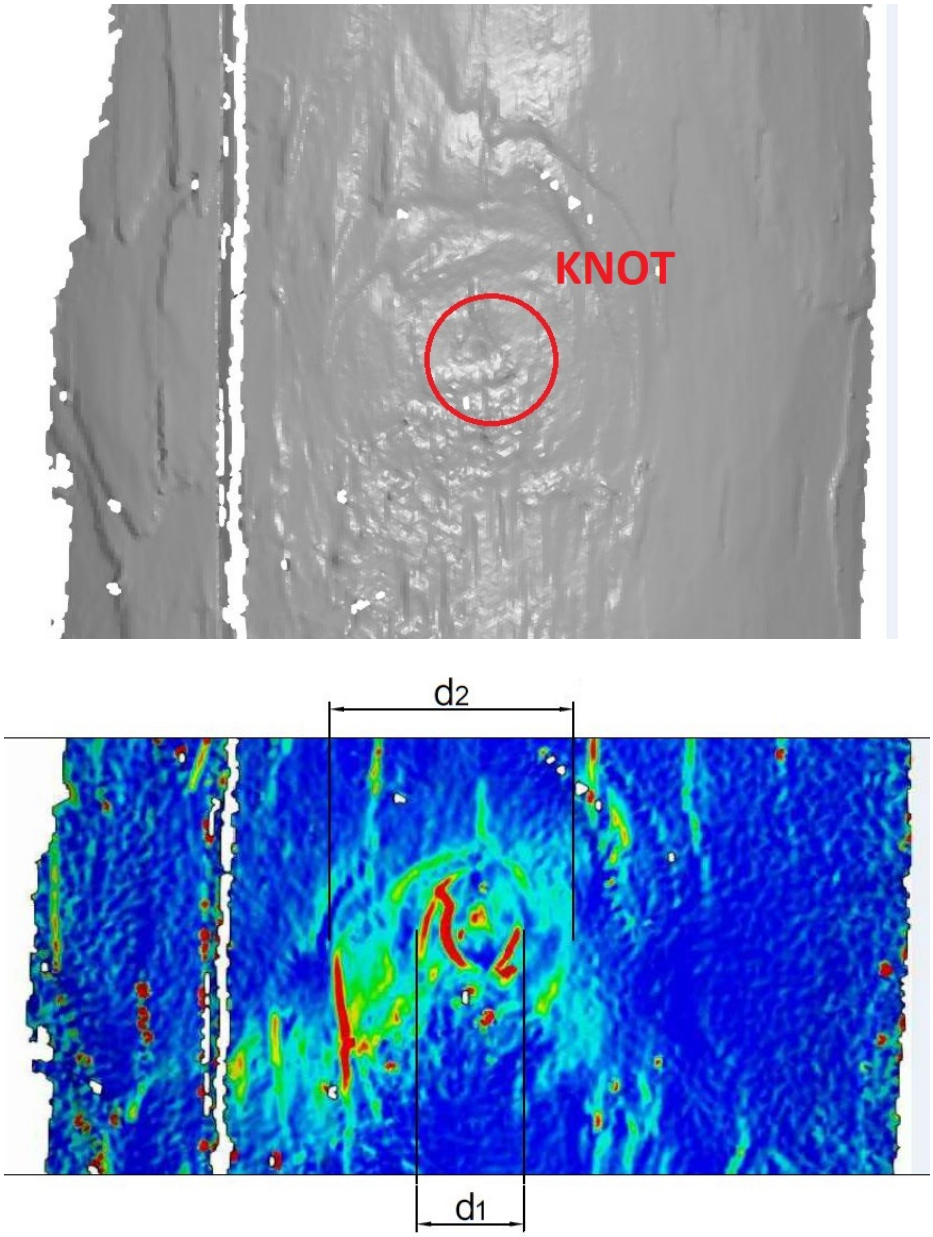

Figure 7.2.13: knots size dimension and strains of DIC test on pile M2.1M;

7.2.4 Application

In order to prove the reliability of the model, a comparison between real stiffness values of knots element and no knots element was done. The application has the aim to show that the MOE obtained by the model with theoretical evaluation is similar to the MOE obtained by the model using values of stiffness derived from local analyses.

The segments K1.1M, M1.1V and V1.1Va were modelled. Real values of the MOE of these piles were obtained from compression tests on disks (par. 6.3.1). Two different models were created considering a single value of E_{nk} obtained from compression test on the disk without knots ($MOE_{nk,disk}$) with the aim of further confirm that the resistance area is equal to the total area removing the percentage of knots present in a cross-section (figure 7.2.14):

1. The first model was performed by inserting the stiffness of no knots elements as $E_{nk} = MOE_{nk,disk}$. The stiffness of knots element was then modelled by reducing the total area of a cross-section of the knots area.

$$A_{res} = A_{tot}(1 - KR)$$

   The MOE obtained from the model was called $MOE_{mod,KR}$.

$$k_k = \frac{MOE_{nk,disk} \cdot A_{tot}(1 - KR)}{D_{knot}} \qquad \Longrightarrow \qquad MOE_{mod,KR}$$

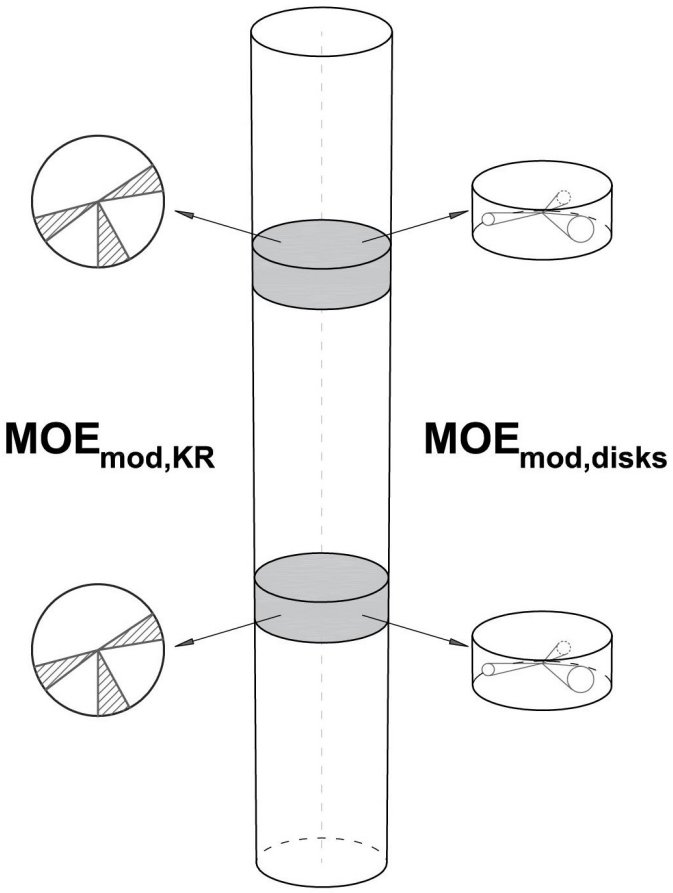

Figure 7.2.14: no knots element were modelled using theoretical evaluation (KR) and experimental evaluation (compression tests on disks);

2. The second model was performed by replacing the stiffness of knots elements with the real values of stiffness obtained from the compression test on the disk (table 7.7).

$$E_k = MOE_{k,disks}$$

The MOE obtained from the model was called $MOE_{mod,disks}$.

$$k_k = \frac{MOE_{k,disk} \cdot A_{tot}}{D_{knot}} \qquad \Longrightarrow \qquad MOE_{mod,disks}$$

The values of the MOE obtained from the two different models are similar. In general, the values of the $MOE_{mod,disks}$ is greater than $MOE_{mod,KR}$ due to the minimum contribution of the stiffness of knots in the cross-section instead of the absent contribution supposed before.

This application confirms that the MOE obtained from the model by using the resistance area rather than the real local values is correct. However, only three applications were performed. For this reason the accuracy of results can be improved. Future research can be done using this assumptions with the aim to confirm the numerical model using real values of the MOE obtained from local analysis.

pile ID	type	C [mm]	KR [-]	MOE_{disk} [Mpa]
K1.1M	nk	765	-	11720
K1.1M	k	790	0.37	9260
M1.1V	nk	640	-	11700
M1.1V	k	685	0.40	7110
V1.1Va	nk	460	-	8050
V1.1Va	k	465	0.47	5300

Table 7.7: characteristics of disks considered in the analysis;

pile ID	$MOE_{pile,dyn}$ [Mpa]	$MOE_{mod,KR}$ [Mpa]	$MOE_{mod,disk}$ [Mpa]
K1.1M	10570	11030	11280
M1.1V	10570	10540	10610
V1.1Va	7480	7000	7280

Table 7.8: the results of the first model on the left and the results of the second model on the right;

7.3 Prediction Equation

The aim of this research was to analyze the influence of knots on the MOE and to predict it in new designed piles. No equation has been previously developed in literature, and in order to give a first way to evaluate this influence, a prediction equation was performed.

In this thesis research emerged that the presence of knots in a cross-section is an important factor on the variation of the MOE. Another important factor is the density as it varies the MOE of the sections without knots (MOE_{nk}) in a pile. For these reasons, both factors were considered for the development of the prediction model.

A general approach was used considering the estimation theory with a 75% of the level of confidence (recommended in EN 14358). Based on this level of confidence, the sampling distribution (S) is probably included into the range [35]:

$$\mu_s - Z_c \cdot S_{dev} \leq S \leq \mu_s + Z_c \cdot S_{dev}$$

where:
- μ_s *[-] : predicted value of the linear analysis;*
- S *[-] : sampling distribution;*
- S_{dev} *[-] : standard deviation of the prediction model;*
- Z_c *[-] : factor based on the level of confidence;*

The distribution of the data was considered depending on the number of samples available in order to determine the standard error as reported in figure 7.3.1. The t-student distribution was used for small specimen available and normalyzed distribution for number of specimens $n \geq 60$. Therefore, the calculation of the MOE estimated is affected by an error:

$$\overline{y} = \beta_0 + \beta_1 x + \epsilon_{nk} = \beta_0 + \beta_1 x + Z_c \cdot S_{dev}$$

where:
- β_i *[-] : factor of linear regression analysis;*
- x *[-] : independent variable;*
- n *[-] : number of samples tested;*

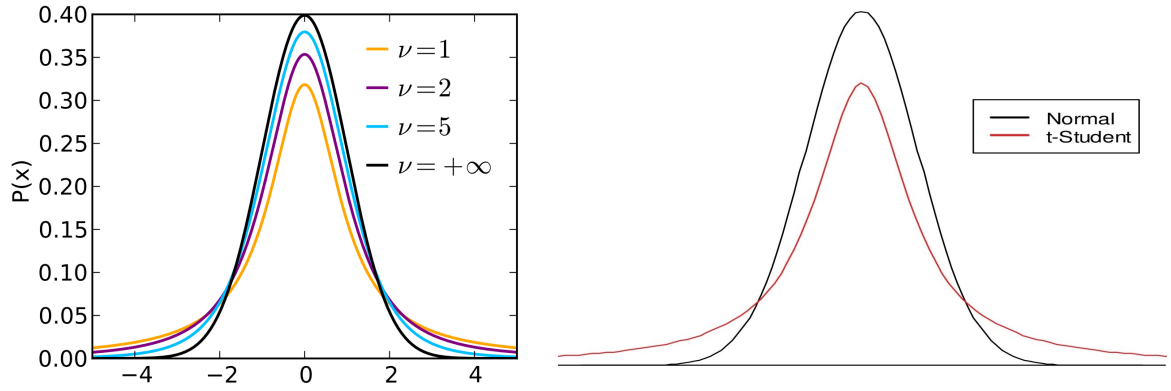

Figure 7.3.1: normalyzed and t-student distribution;

7.3.1 Stiffness piles without knot

In chapter 7.1.1, the variation on the MOE due to OKR_A is shown. To predict this variation, the MOE_{nk} needed to be calculated but it also varies with different densities. The 5 piles without knots were considered, and a linear regression analysis was done with the aim to obtain MOE_{nk} of reference valued based on dry density.
Future research can developed this type of analysis studying even more the MOE of segments without knots.

Wood above fiber saturation point have constant mechanical properties (figure 2.2.8) but the density varies when moisture content changes due to excess water in cells. The use of ρ_{wet} is wrong in these analyses because the weight of excess water does not contributes on stiffness of a pile. Therefore, the static MOE was related with the dry density with the aim to avoid the variation of ρ_{wet} due to the moisture content. The trend line of the linear regression was then analyzed on the 5 piles and plotted in figure 7.3.2.

$$MOE_{nk} = C_1 \cdot \rho_{dry} + C_{1k} = 10.52 \cdot \rho_{dry} + 6993 + \epsilon_{nk}$$

segments ID	knots	ρ_{wet}	ρ_{dry}	MOE_{dyn}	MOE_{static}
K 2.9 M	no	820	460	11820	11490
K 2.7 M	no	850	490	12870	12160
K 2.11 M	no	850	490	12760	12420
K 3.10 M	no	640	310	10860	10340
K 3.12 M	no	770	450	11600	11720

Table 7.9: data of the five piles without knots;

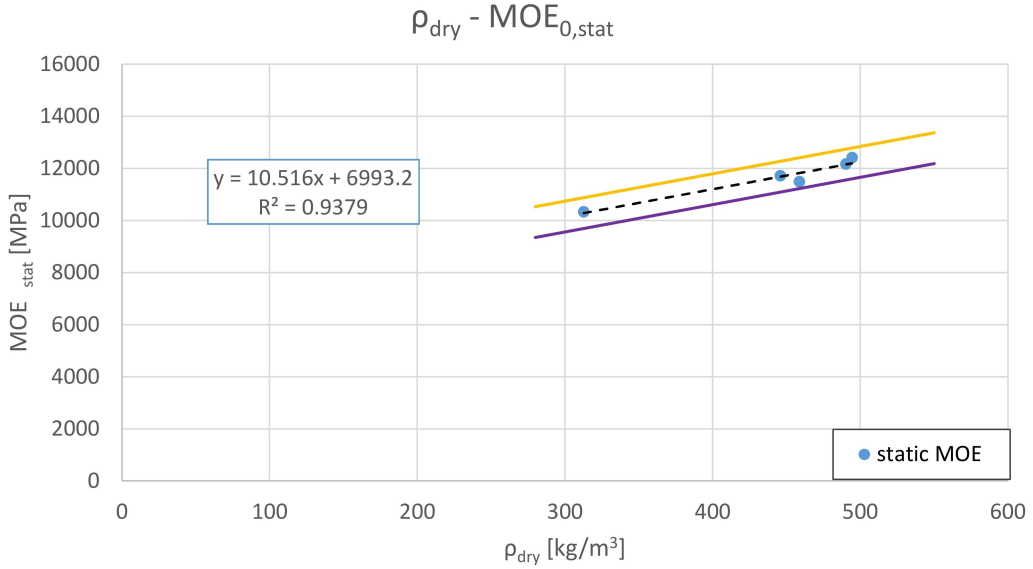

Figure 7.3.2: linear regression analysis of the 5 piles without knots. Yellow and purple lines represent the error of the trend line of the linear regression analysis;

The number of data available was five (< 60), therefore a t-student distribution was used for the evaluation of the standard error for this analysis. The number of the degree of freedom (d.o.f.) was:

$$\upsilon = N - 1 = 5 - 1 = 4$$

The Z_c value of 1.385 was selected considering 75% level of confidence and 4 d.o.f. (table 7.10).

The error was calculated multiplying the Z_c for the standard deviation as showed above [35].

$$S_{dev} = \sqrt{\frac{\sum(y_i - y)^2}{n-1}} = 430Mpa \qquad \Longrightarrow \qquad (N = 5) \quad \epsilon_{nk} = Z_c \cdot S_{dev} = 590Mpa$$

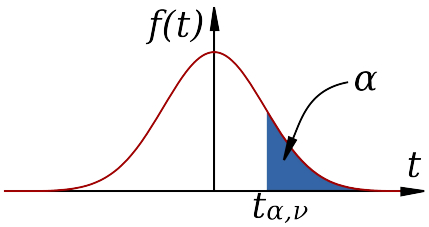

υ/(1-α)	0.8	**0.875**	0.9	0,95	0,975	0,99	0,995
1	1.376	2.653	3.078	6,314	12,706	31,821	63,657
2	1.061	1.680	1.886	2,920	4,303	6,965	9,925
3	0.978	1.473	1.638	2,353	3,182	4,541	5,841
4	0.941	**1.385**	1.533	2,132	2,776	3,747	4,604
5	0.920	1.337	1.476	2,015	2,571	3,365	4,032
6	0.906	1.307	1.440	1,943	2,447	3,143	3,707
7	0.896	1.285	1.415	1,895	2,365	2,998	3,499
8	0.889	1.270	1.397	1,860	2,306	2,896	3,355
9	0.883	1.258	1.383	1,833	2,262	2,821	3,250
10	0.879	1.249	1.372	1,812	2,228	2,764	3,169
20	0.860	1.209	1.325	1,725	2,086	2,528	2,845
30	0.854	1.196	1.310	1,697	2,042	2,457	2,750
40	0.851	1.190	1.303	1,684	2,021	2,423	2,704
60	0.848	1.184	1.296	1,671	2,000	2,390	2,660
100	0.846	1.179	1.290	1,660	1,984	2,364	2,626
∞	0.842	1.172	1.282	1,645	1,960	2,326	2,576

Table 7.10: values of Z_c based on the level of confidence of t-student distribution;

7.3.2 Stiffness piles with knots

With a known dry density it is possible to obtain a MOE_{nk} value. Subsequently, knots were modelled to further consider their influence. This was calculated by subtracting the MOE_{nk} to the percentage of knots $(1 - OKR_A)$ on the pile surface.

$$MOE_k = MOE_{nk} \cdot (1 - C_2 OKR_A)$$

The OKR_A was multiplied for a coefficient C_2 that represent the real influence of knots on the variation of the MOE. This coefficient was obtained optimizing the prediction model using a solver which minimizes the gap between the MOE predicted and real of the 106 piles available. The trend line of the prediction model has to be similar to the trend line of the real value of MOE_{stat} (figure 7.3.3). Indeed, both lines in figure 7.3.3 respect the previous law; therefore, they can be representative of the real variation of the MOE due to the presence of knots.

$$MOE_k = MOE_{nk} \cdot (1 - C_2 OKR_A) = MOE_{nk} \cdot (1 - 5.75 \cdot OKR_A)$$

$$MOE_k = (C_1 \cdot \rho_{dry} + C_{1k}) \cdot (1 - C_2 OKR_A) + \epsilon_k$$

where ϵ_k is the error that influence the prediction model of the MOE for different OKR_A values using 106 piles available for the development of the equation.

Another important characteristic of the equation has to be mentioned. When $OKR_A = 0$ the equation is the same of the prediction model for piles without knots ($MOE_{k=0} = MOE_{nk}$). Therefore, the proposed equation is representative of piles with and without knots.

Coefficient	Value	Note
C_1	10.52	trend line's inclination of piles without knots
C_{1k}	6993	trend line's intercept of piles without knots
C_2	5.75	minimize the gap between real and predicted values

Table 7.11: coefficient used on the prediction equation;

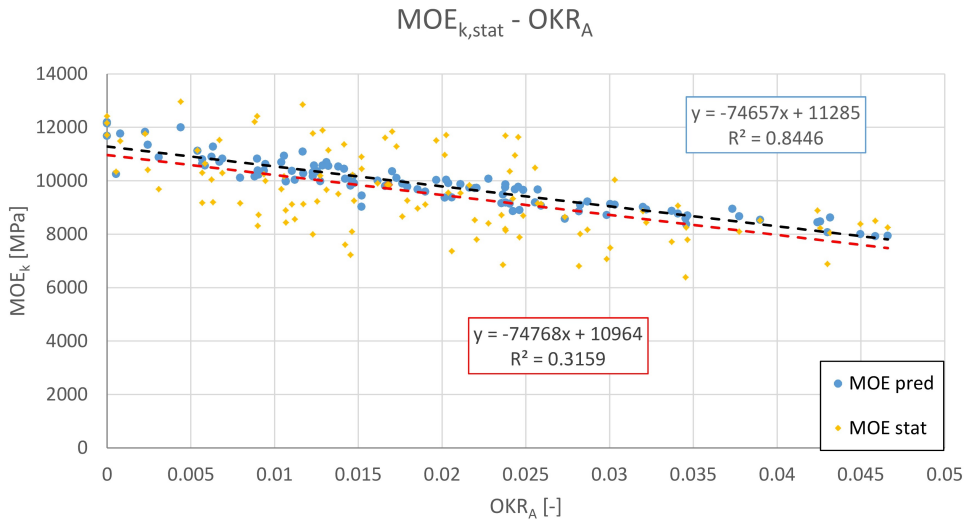

Figure 7.3.3: Plot of the predicted values (in blue and black) and real values (orange and red);

Considering the 106 piles available, the t-student distribution became a normalyzed standard distribution (figure 7.3.1). Therefore, the standard deviation and error were calculated with different value of Z_c based on the same level of confidence. The Z_c value for the 106 piles considered was 1.15, considering 75% level of confidence (table 7.12).

The error was calculated multiplying the standard deviation for the Z_c as showed above [35].

$$S_{dev} = \sqrt{\frac{\sum(y_i - y)^2}{n-1}} = 1210Mpa \qquad \Longrightarrow \qquad (N = 106) \quad \epsilon_{nk} = Z_c \cdot S_{dev} = 1390Mpa$$

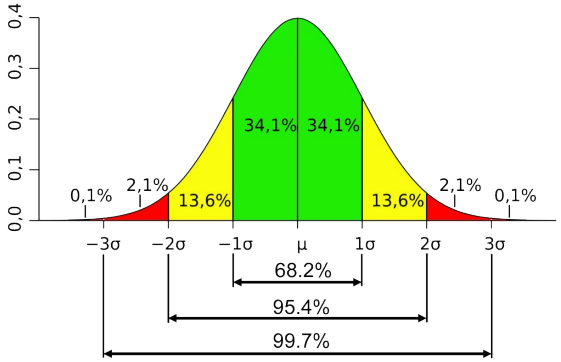

Z_c	0.00	0.01	0.02	0.03	0.04	**0.05**	0.06	0.07	0.08	0.09
0.0	0.0000	0.0040	0.0080	0.0120	0.0160	0.0199	0.0239	0.0279	0.0319	0.0359
0.1	0.0398	0.0438	0.0478	0.0517	0.0557	0.0596	0.0636	0.0675	0.0714	0.0754
0.2	0.0793	0.0832	0.0871	0.0910	0.0948	0.0987	0.1026	0.1064	0.1103	0.1141
0.3	0.1179	0.1217	0.1255	0.1293	0.1331	0.1368	0.1406	0.1443	0.1480	0.1517
0.4	0.1554	0.1591	0.1628	0.1664	0.1700	0.1736	0.1772	0.1808	0.1844	0.1879
0.5	0.1915	0.1950	0.1985	0.2019	0.2054	0.2088	0.2123	0.2157	0.2190	0.2224
0.6	0.2258	0.2291	0.2324	0.2357	0.2389	0.2422	0.2454	0.2486	0.2518	0.2549
0.7	0.2580	0.2612	0.2642	0.2673	0.2704	0.2734	0.2764	0.2794	0.2823	0.2852
0.8	0.2881	0.2910	0.2939	0.2967	0.2996	0.3023	0.3051	0.3079	0.3106	0.3133
0.9	0.3159	0.3186	0.3212	0.3238	0.3264	0.3289	0.3315	0.3340	0.3365	0.3389
1.0	0.3413	0.3438	0.3461	0.3485	0.3508	0.3531	0.3554	0.3577	0.3599	0.3621
1.1	0.3643	0.3665	0.3686	0.3708	0.3729	**0.3749**	0.3770	0.3790	0.3810	0.3830
1.2	0.3849	0.3869	0.3888	0.3907	0.3925	0.3944	0.3962	0.3980	0.3997	0.4015
1.3	0.4032	0.4049	0.4066	0.4082	0.4099	0.4115	0.4131	0.4147	0.4162	0.4177
1.4	0.4192	0.4207	0.4222	0.4236	0.4251	0.4265	0.4279	0.4292	0.4306	0.4319
1.5	0.4332	0.4345	0.4357	0.4370	0.4382	0.4394	0.4406	0.4418	0.4430	0.4441
1.6	0.4452	0.4463	0.4474	0.4485	0.4495	0.4505	0.4515	0.4525	0.4535	0.4545
1.7	0.4554	0.4564	0.4573	0.4582	0.4591	0.4599	0.4608	0.4616	0.4625	0.4633
1.8	0.4641	0.4649	0.4656	0.4664	0.4671	0.4678	0.4686	0.4693	0.4700	0.4706
1.9	0.4713	0.4719	0.4726	0.4732	0.4738	0.4744	0.4750	0.4756	0.4762	0.4767
2.0	0.4773	0.4778	0.4783	0.4788	0.4793	0.4798	0.4803	0.4808	0.4812	0.4817
...										

Table 7.12: values of Z_c based on the level of confidence of normalyzed standard distribution;

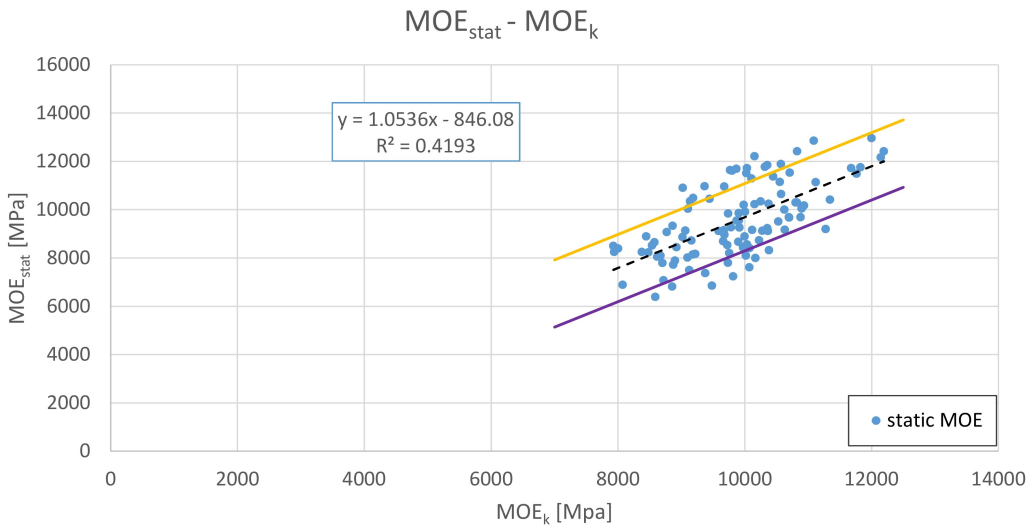

Figure 7.3.4: Accuracy of the model: predicted values and measured values were plotted. Yellow and purple lines represent the error of the trend line of a linear regression analysis;

The model developed above used 106 piles available on the TU Delft. Therefore, future research could use more piles to improve the accuracy of the prediction model. In particular, an higher number of piles without knots is necessary to improve the accuracy of the model.

7.3.3 Observation

In the end, the 4 classes of knots described in chapter 7.1.1 were further considered. In order to obtain a reduction of the MOE between different classes on the prediction model, a single value of density was considered $\rho_{dry} = 400kg/m^3$.

The reduction on the MOE from the average value of piles without knots increases with the increment of the presence of knots, as reported in the analysis (chapter 7.1.1). For this reason, this equation can represent a good model to predict the MOE of a wooden foundation piles by knowing the dry density and knots layout on the surface of the pile.

class of OKRA	MOE_{pred} **[Mpa]**	**reduction**
nk	11200	0%
1	10850	3%
2	10300	8%
3	9850	12%
4	9110	19%

Table 7.13: Values of the predicted MOE for different classes of OKR_A

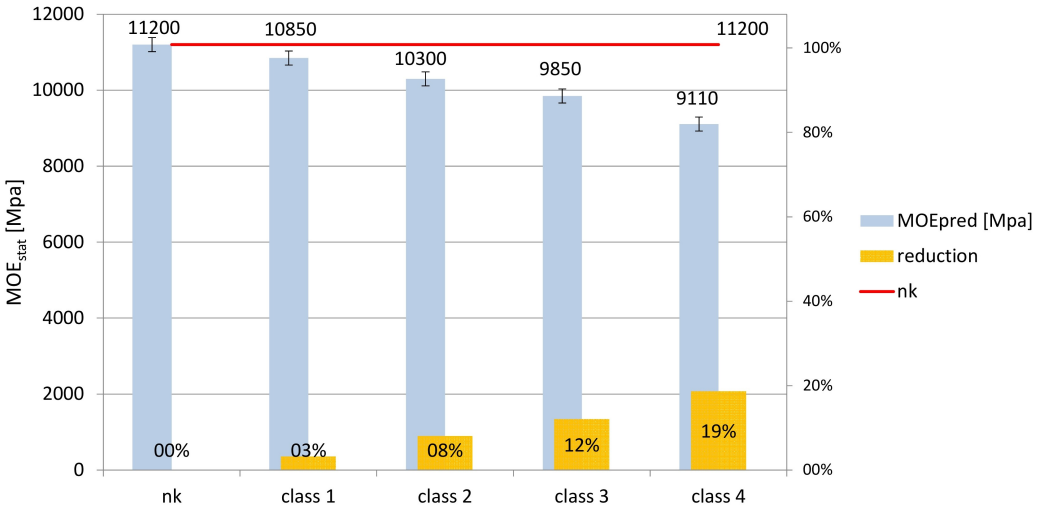

Figure 7.3.5: predicted MOE value for the 4 classes (blue) and the reduction from the no knot class (orange);

Chapter 8

Conclusion and Recommendation

The assessment of wooden foundation piles of bridges in Amsterdam has started to develop in recent years. The influence of knots on the modulus of elasticity was studied in this thesis as a part of the assessment framework of wooden piles.

For timber piles, one strength class based on visual grading is defined in Dutch standard NEN 5491 (2010). Therefore, several tests were performed using full-scale tests on pile segments and small-scale tests on disks with the aim to study the behaviour of knots in wooden foundation piles. The influence of knots on the MOE parallel to the grain was determined comparing the results of segments with and without knots.

The research showed that the presence of knots is not negligible and can significantly alter the MOE in longitudinal direction. In particular, the inclination of fibers around a knot area causes a relevant effect on the reduction of the MOE. The equivalent size of influence was estimated approximately as 1.5 times the diameter of the knot itself. Furthermore, the inclination of fibers considered with α results higher when the size of a knot d_1 is smaller.

The correlation between the MOE and the area around knots, where fibers deviate, is defined with a OKR_A. The OKR_A shows a better distribution of the data considering the presence of all knots in the entire surface of a pile (instead of KR) without requiring the study of the development of knots inside the trunk (necessary to calculate OKR_V).

Important correlations were found by comparing the MOE of piles with and without knots performing compression tests on full-scale analyses. 5 classes were created to show the decrease of the stiffness with the increase of OKR_A. The piles with knots have low values of the MOE for higher values of OKR_A. This could be related to a higher presence of knots in that section. Therefore, the presence of knots is a relevant factor for the variation of the MOE in a wooden foundation pile.

Local analyses were performed cutting 6 disks from three piles from sections with and without knots. Those disks were tested in compression to perform a small-scale analysis. A good correlation was observed between the MOE of pile segments and disks. In addition, this investigation has shown that the mechanical properties of wooden disks can be related to those of pile segments, opening up the possibility of further research on this topic.

The numerical model shows how the MOE of a pile is influenced by the knots area in a cross-section, the number of cross-sections and the knots layout. Furthermore, density of knots does not significantly affect the numerical MOE because knots represent small percentage of volume in a pile. The model confirms that the resistance area in a cross-section with knots is similar to the total area subtracted from the percentage of knots KR.

Digital Image Correlation (DIC) test was performed to better investigate the behaviour of knots on the variation of the MOE. DIC was used to analyze a small area around a knot, during a compression test of two pile segments. The results showed that the stiffness of a pile section with knots is lower than a section without knots. This led to the conclusion that the stiffness of knots is negligible in the longitudinal direction of a pile.

In the end, a prediction equation was developed by taking into account density and knots layout OKR_A that are the most important factor on the variation of the MOE in a wooden pile. The predicted values showed a good match with experimental results. In this way, it is possible to estimate the variation of the longitudinal MOE by knowing the density and the knots layout on the surface for a new designed pile.

These kinds of tests performed in this thesis research are the first in the assessment of wooden foundation piles. Therefore, further investigation can be done in the future to get more accurate correlations on the influence of knots on the MOE. In particular, some suggested topics to develop future research are the following:

- Small-scale tests show a good correlation with the MOE of pile segments. However, the MOE of sections without knots changes along the full-length of a pile in head, middle and tip-parts. Therefore, further research could be done to test more disks, in particular without knots, extracting the disks from different sections along the whole length of the piles.
- A better implementation of the prediction model can be obtained with more data. Therefore, more piles could be tested with the aim to calculate a more accurate equation. In particular, more piles without knots are necessary to obtain better accuracy.
- The increase of the density of knots is not exactly known when in wet conditions. Further research could be done to understand the increase of the density at different levels of moisture content ω. This analysis can improve the reliability of the evaluation of the acoustic response obtained from the numerical model.
- Lastly, to better understand the difference in the MOE of parts with and without knots, more local analyses could be done using DIC. This technique gave promising results. However, the behaviour of stiffness and strain around a knots area needs further research.

Appendix A

Knots along full length pile

In the following pages are reported the results of the data anlysis of the variation of the KR along the length of piles.

Batch	Code	KR_{max}	OKR_A	OKR_V
235	K1.1M	0.368	0.0168	0.000487
235	K1.1V	0.292	0.0152	0.000454
235	M1.1K	0.359	0.0152	0.000489
235	M1.1V	0.428	0.0242	0.000643
235	V1.1K	0.461	0.0273	0.000811
235	V1.1Vc	0.299	0.0107	0.000432
235	V1.1Vb	0.387	0.0238	0.000804
235	V1.1Va	0.629	0.0282	0.000732
235	K1.4M	0.217	0.0063	0.000220
235	M1.4K	0.299	0.0235	0.000534
235	M1.4V	0.465	0.0346	0.000713
235	V1.4K	0.55	0.0466	0.000978
235	V1.4Vc	0.424	0.0430	0.000986
235	V1.4Vb	0.255	0.0145	0.000361
235	V1.4Va	0.317	0.0282	0.000853
235	K2.1M	0.322	0.0117	0.000470
235	K2.1V	0.251	0.0088	0.000389
235	M2.1K	0.283	0.0166	0.000609
235	M2.1V	0.306	0.0202	0.000665
235	V2.1K	0.425	0.0240	0.000719
235	V2.1Vc	0.383	0.0256	0.000780
235	V2.1Vb	0.386	0.0390	0.001080
235	V2.1Va	0.606	0.0300	0.000705
235	K2.8M	0.181	0.0104	0.000329
235	K2.8V	0.24	0.0125	0.000469
235	M2.8K	0.225	0.0179	0.000625
235	M2.8V	0.41	0.0228	0.000589
235	V2.8K	0.246	0.0246	0.000539
235	V2.8Vc	0.272	0.0206	0.000616
235	V2.8Vb	0.32	0.0142	0.000573

Table A.1: values of knots ratio and overall knots ratio of segments of the batch 235;

Batch	Code	KR_{max}	OKR_A	OKR_V
235	K2.9M	0.033	0.0008	0.000048
235	K2.9V	0.206	0.0067	0.000223
235	M2.9K	0.246	0.0094	0.000367
235	M2.9V	0.333	0.0185	0.000628
235	V2.9K	0.199	0.0190	0.000439
235	V2.9Vc	0.41	0.0346	0.000778
235	V2.9Vb	0.46	0.0220	0.000586
235	V2.9Va	0.542	0.0426	0.001085
235	K2.10K	0.173	0.0023	0.000156
235	K2.10M	0.145	0.0044	0.000205
235	M2.10K	0.232	0.0090	0.000468
235	M2.10V	0.222	0.0054	0.000275
235	V2.10K	0.358	0.0245	0.001010
235	V2.10Vc	0.273	0.0095	0.000354
235	V2.10Vb	0.304	0.0211	0.000799
235	V2.10Va	0.386	0.0257	0.000822
235	K1.10M	0.146	0.0031	0.000168
235	M1.10M	0.319	0.0138	0.000380
235	V1.10M	0.374	0.0221	0.000556
235	K1.11M	0.221	0.0058	0.000231
235	M1.11M	0.244	0.0117	0.000417
235	V1.11M	0.452	0.0322	0.000879
235	K2.2M	0.292	0.0123	0.000437
235	M2.2M	0.351	0.0204	0.000566
235	V2.2M	0.538	0.0424	0.001050
235	K2.3M	0.345	0.0216	0.000668
235	M2.3M	0.315	0.0303	0.000820
235	V2.3M	0.46	0.0287	0.000813
235	K2.4M	0.249	0.0173	0.000521
235	M2.4M	0.267	0.0127	0.000402
235	V2.4M	0.457	0.0341	0.000695
235	K2.5M	0.377	0.0176	0.000460
235	M2.5M	0.366	0.0320	0.000752
235	V2.5M	0.41	0.0432	0.000767
235	K2.7M	0	0.0000	0.000000
235	M2.7M	0.117	0.0024	0.000120
235	V2.7M	0.18	0.0057	0.000222
235	K2.12M	0.223	0.0129	0.000428
235	M2.12M	0.223	0.0142	0.000597

Table A.2: values of knots ratio and overall knots ratio of segments of the batch 235;

Batch	Code	KR_{max}	OKR_A	OKR_V
449	K1.2M	0.265	0.0131	0.000449
449	M1.2M	0.371	0.0202	0.000667
449	V1.2M	0.273	0.0238	0.000735
449	K1.3M	0.207	0.0090	0.000395
449	M1.3M	0.284	0.0107	0.000432
449	V1.3M	0.509	0.0459	0.000930
449	K1.5M	0.191	0.0090	0.000384
449	M1.5M	0.293	0.0123	0.000383
449	V1.5M	0.545	0.0337	0.000833
449	K1.6M	0.254	0.0079	0.000363
449	M1.6M	0.289	0.0147	0.000478
449	V1.6M	0.325	0.0298	0.001005
449	K1.7M	0.23	0.0112	0.000376
449	M1.7M	0.322	0.0162	0.000477
449	V1.7M	0.406	0.0377	0.000848
449	K1.8M	0.182	0.0069	0.000374
449	M1.8M	0.185	0.0057	0.000239
449	V1.8M	0.348	0.0259	0.000893
449	M1.9M	0.321	0.0170	0.000523
449	V1.9M	0.337	0.0373	0.001020
449	K1.12M	0.203	0.0062	0.000284
449	M1.12M	0.354	0.0244	0.000681
449	V1.12M	0.353	0.0248	0.000791
449	K2.6M	0.133	0.0132	0.000343
449	M2.6M	0.233	0.0197	0.000673
449	V2.6M	0.252	0.0238	0.000825
449	K2.11M	0	0.0000	0.000000
449	M2.11M	0.227	0.0106	0.000377
449	V2.11M	0.215	0.0124	0.000452
449	K3.10M	0.033	0.0005	0.000039
449	M3.10M	0.217	0.0146	0.000435
449	V3.10M	0.437	0.0345	0.000872
449	K3.11M	0.237	0.0147	0.000394
449	V3.11M	0.515	0.0450	0.001099
449	K3.12M	0	0.0000	0.000000
449	M3.12M	0.206	0.0110	0.000448
449	V3.12M	0.403	0.0236	0.000769

Table A.3: values of knots ratio and overall knots ratio of segments of the batch 449;

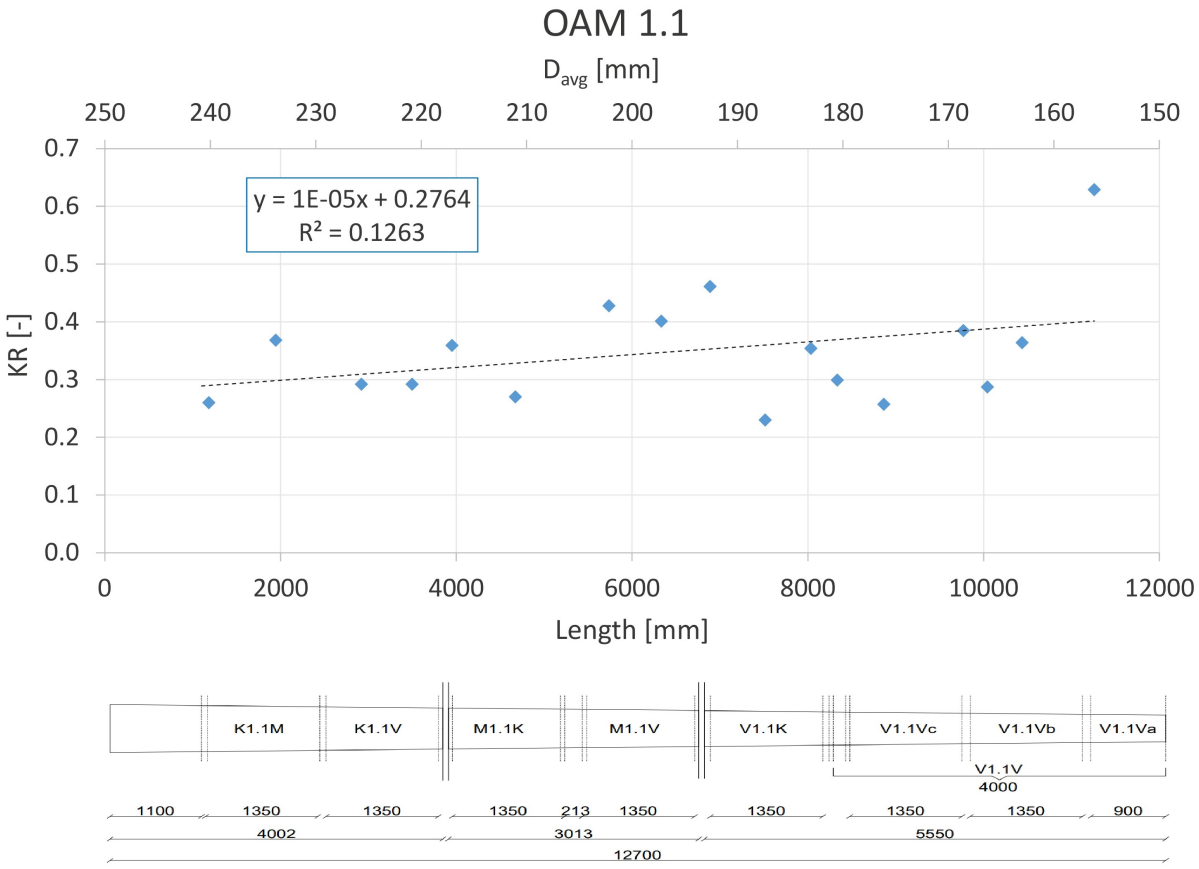

Figure A.0.1: KR trend of pile 1.1;

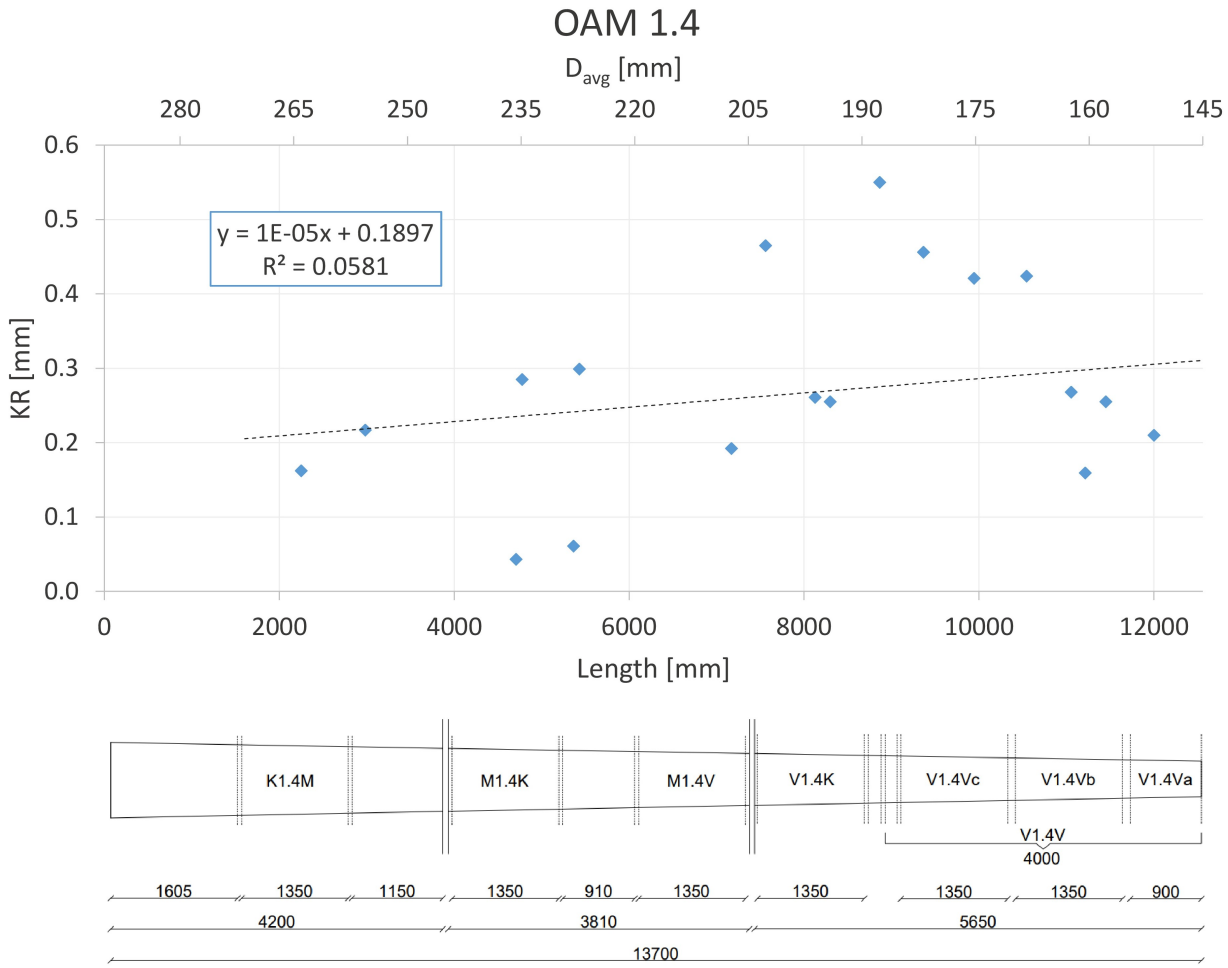

Figure A.0.2: KR trend of pile 1.4;

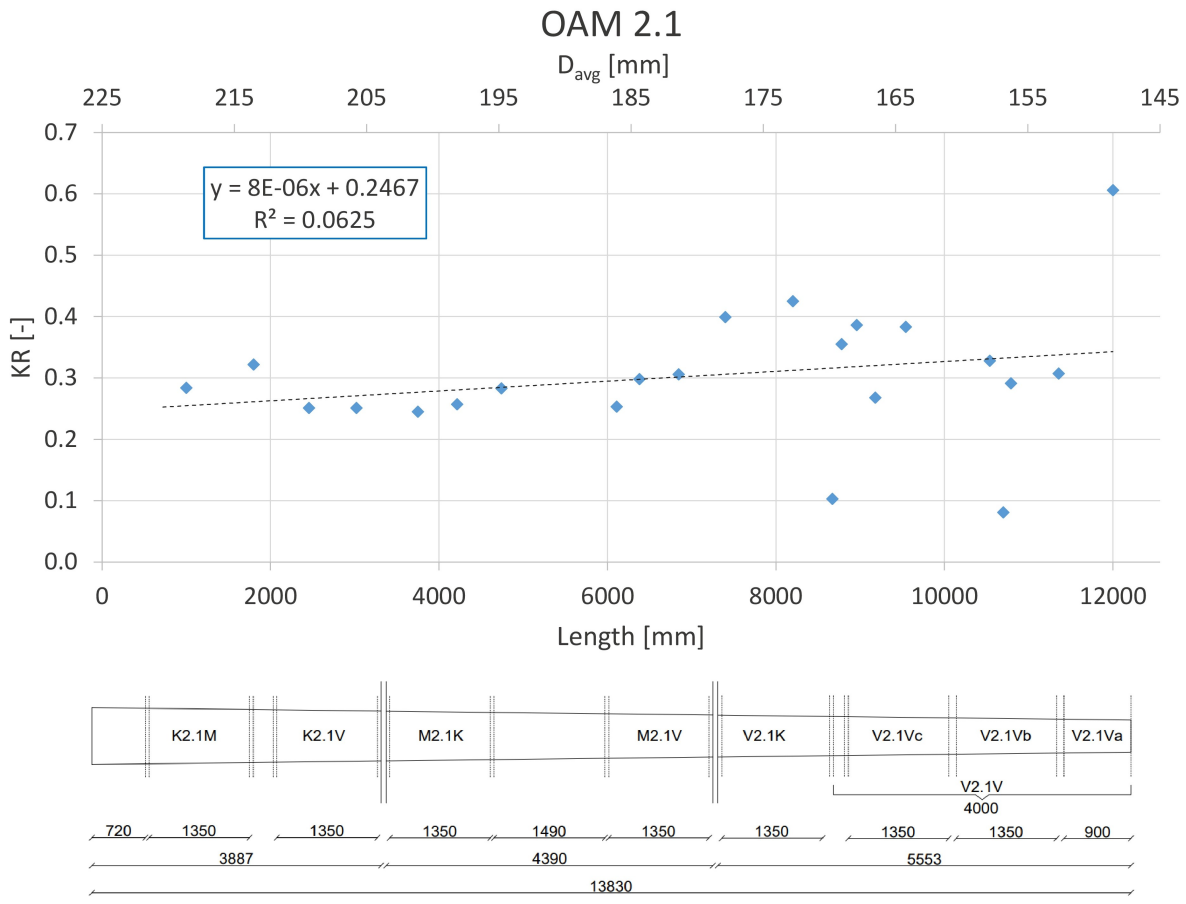

Figure A.0.3: KR trend of pile 2.1;

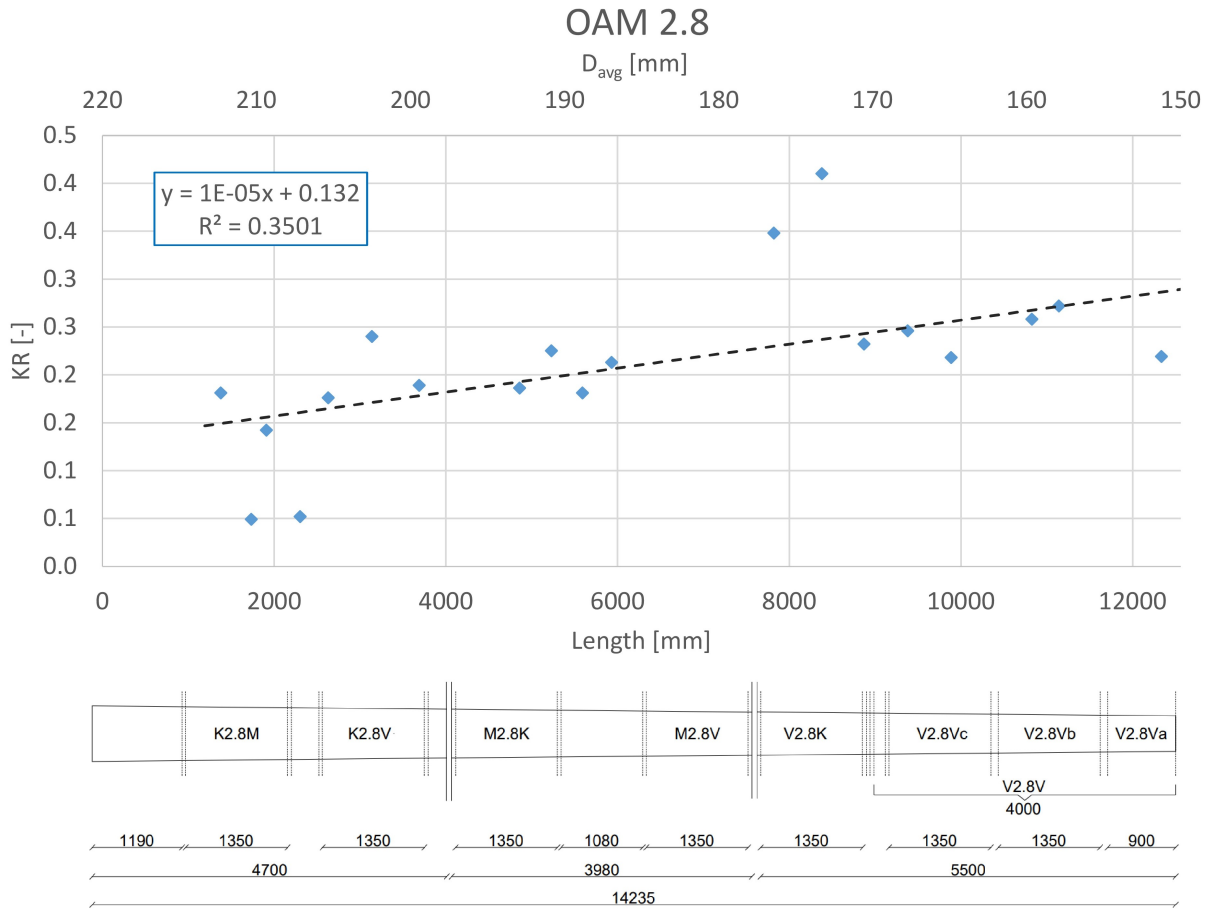

Figure A.0.4: KR trend of pile 2.8;

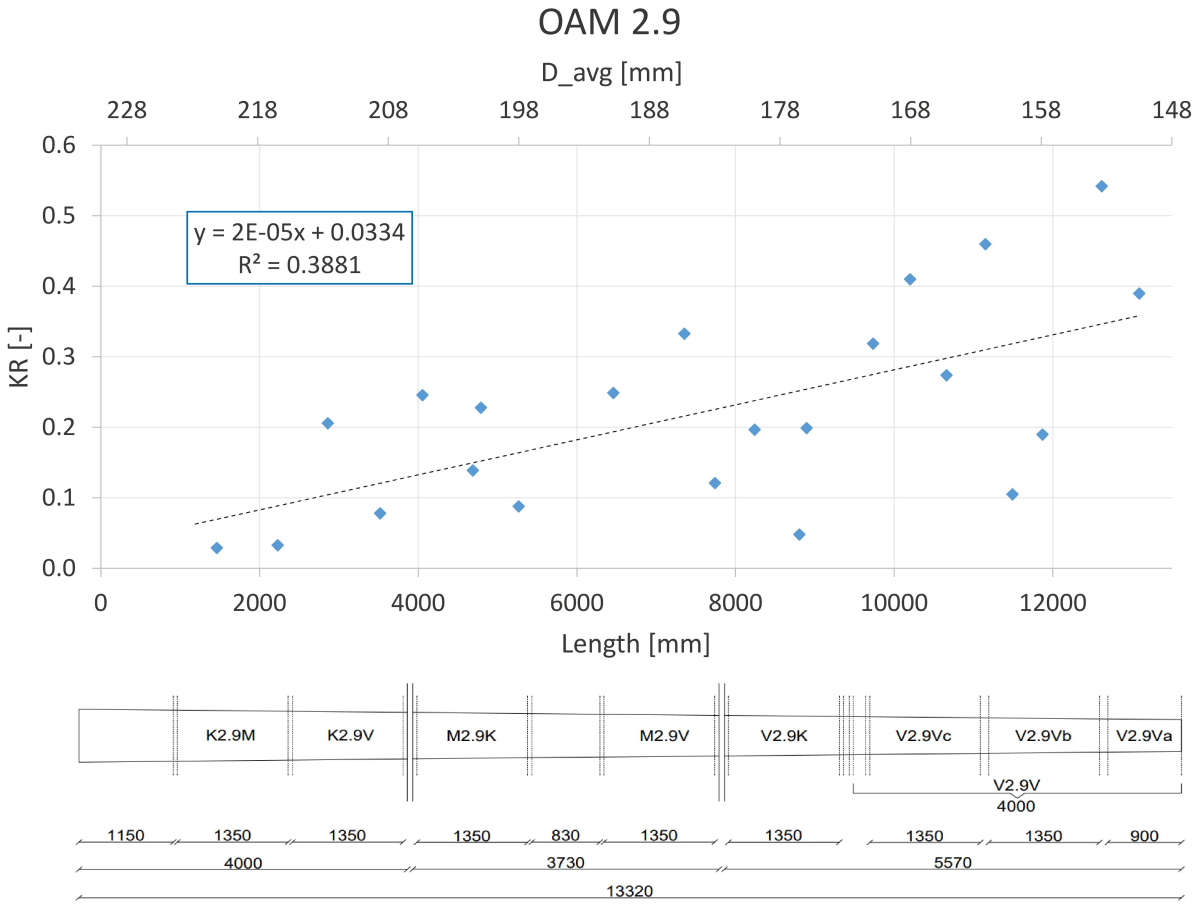

Figure A.0.5: KR trend of pile 2.9;

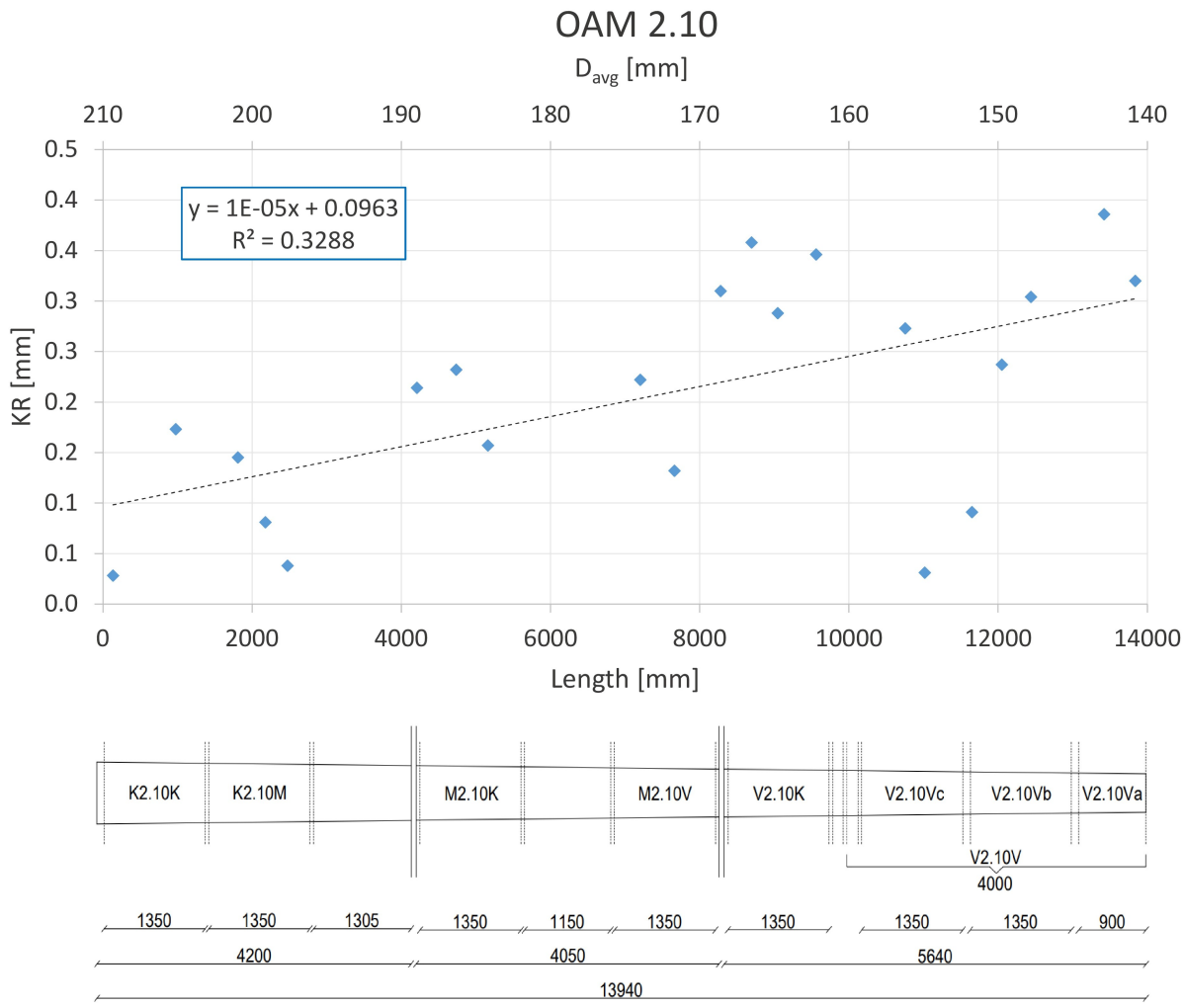

Figure A.0.6: KR trend of pile 2.10;

Appendix B

MOE along full length pile

In the following pages are reported the results of the data anlysis of the variation of the MOE along the length of piles.

Batch	Code	D_{avg} $[mm]$	Length $[mm]$	MOE_{dyn} $[MPa]$	MOE_{static} $[MPa]$
235	K1.1M	247.2	1350	10572	9853
235	K1.1V	232.9	1350	11189	10901
235	M1.1K	224.9	1350	10297	10448
235	M1.1V	209	1350	10568	9330
235	V1.1K	199.5	1350	9800	8647
235	V1.1Vc	183	1350	9480	8894
235	V1.1Vb	165.5	1350	9115	8135
235	V1.1Va	153.8	900	7481	6810
235	K1.4M	281.7	1800	9915	9198
235	M1.4K	259.4	1350	9123	8717
235	M1.4V	236.6	1350	8850	8249
235	V1.4K	221.2	1350	8850	8249
235	V1.4Vc	200.5	1350	8003	6888
235	V1.4Vb	174.5	1350	8069	7231
235	V1.4Va	150.7	900	7699	8009
235	K2.1M	223.3	1350	14066	12853
235	K2.1V	220.7	1350	12988	12210
235	M2.1K	212.7	1350	12123	11609
235	M2.1V	201.6	1350	11275	10968
235	V2.1K	188.9	1350	10576	10352
235	V2.1Vc	183	1350	9589	10484
235	V2.1Vb	165	1350	9421	8514
235	V2.1Va	147	900	8134	7490
235	K2.8M	213.3	1350	10324	9687
235	K2.8V	208.5	1350	9791	9226
235	M2.8K	198.4	1350	9155	9264
235	M2.8V	184.6	1350	9049	8405
235	V2.8K	181.4	1350	7761	7890
235	V2.8Vc	158.1	900	6891	7366
235	V2.8Vb	167.1	1350	7588	7607

Table B.1: mechanical properties of segments of batch 235;

Batch	Code	D_{avg} $[mm]$	Length $[mm]$	MOE_{dyn} $[MPa]$	MOE_{static} $[MPa]$
235	K2.9M	220.2	1350	11816	11489
235	K2.9V	212.2	1330	11291	11527
235	M2.9K	205.8	1350	10339	10243
235	M2.9V	195.8	1350	9288	8963
235	V2.9K	184.1	1350	9271	9113
235	V2.9Vc	177.7	1350	8508	7791
235	V2.9Vb	163.9	1350	8471	8528
235	V2.9Va	148.5	900	9139	8231
235	K2.10K	207.4	1350	15044	11758
235	K2.10M	200	1350	13846	12963
235	M2.10K	178.3	1350	13283	12415
235	M2.10V	168	1350	12230	11140
235	V2.10K	158.1	1350	11900	11634
235	V2.10Vc	154.9	900	10862	9996
235	V2.10Vb	146.6	900	10346	9540
235	V2.10Va	140.1	900	9168	9152
235	K1.10M	265.3	1800	10663	9690
235	M1.10M	224.4	1350	10554	9511
235	V1.10M	184.6	1350	8387	7798
235	K1.11M	236.1	1350	10950	10645
235	M1.11M	229.2	1350	9961	9125
235	V1.11M	198.4	1350	9205	8441
235	K2.2M	266.8	1800	11047	11774
235	M2.2M	223.3	1350	10713	9556
235	V2.2M	170.3	1350	9643	8891
235	K2.3M	271.6	1800	10507	9837
235	M2.3M	224.4	1350	10733	10035
235	V2.3M	191	1350	8768	8168
235	K2.4M	255.2	1800	11682	11286
235	M2.4M	218	1350	10900	10195
235	V2.4M	177.7	1350	9791	9070
235	K2.5M	276.8	1800	9495	8666
235	M2.5M	237.7	1350	9420	8865
235	V2.5M	197.9	1350	8989	8048
235	K2.7M	234	1350	12875	12163
235	M2.7M	211.7	1350	10995	10409
235	V2.7M	182.5	1350	9175	9172
235	K2.12M	200	1350	12546	11888
235	M2.12M	185.2	1350	11970	11365

Table B.2: mechanical properties of segments of batch 235;

Batch	Code	D_{avg} $[mm]$	Length $[mm]$	MOE_{dyn} $[MPa]$	MOE_{static} $[MPa]$
449	K1.2M	263.1	1810	9862	9665
449	M1.2M	226.5	1360	11987	11716
449	V1.2M	183	1360	11841	11687
449	K1.3M	288.6	1810	9433	8727
449	M1.3M	255.7	1810	8801	8435
449	V1.3M	198.9	1360	8585	8497
449	K1.5M	253.6	1810	8834	8315
449	M1.5M	233.4	1360	8545.7	7999
449	V1.5M	178.2	1360	8189	7717
449	K1.6M	281.2	1810	9083.1	9160.5
449	M1.6M	234.5	1360	9292.3	9253
449	V1.6M	197.7	1360	7314	7075.9
449	K1.7M	283.8	1810	8371.5	8563.3
449	M1.7M	242.4	1360	10405	9908
449	V1.7M	188.8	1360	8251	8095
449	K1.8M	243.5	1810	10791.5	10294
449	M1.8M	221.7	1360	11231	10299.7
449	V1.8M	176.6	1360	10295	9133
449	M1.9M	216.9	1360	13245	11845.1
449	V1.9M	175.6	1360	11810.3	
449	K1.12M	276.9	1810	11435	10041
449	M1.12M	231.3	1360	11182.1	10955.4
449	V1.12M	187.8	1360	9095	8691
449	K2.6M	211.1	1360	12211.8	11148.8
449	M2.6M	179.3	1360	11389	11511
449	V2.6M	154.4	900	8445	8197
449	K2.11M	231.3	1360	12756	12415
449	M2.11M	196.3	1360	11895	10171
449	V2.11M	171.4	1360	10358	
449	K3.10M	213.3	1360	10859	10336
449	M3.10M	190.4	1360	8461	8095
449	V3.10M	159.7	900	6320	6389
449	K3.11M	270.03	1810	10944.1	10225.3
449	V3.11M	186.2	1360	9292.3	8385.8
449	K3.12M	214.8	1360	11597.5	11716.2
449	M3.12M	185.1	1360	9122.4	9117.3
449	V3.12M	156.5	900	7215	6854

Table B.3: mechanical properties of segments of batch 449;

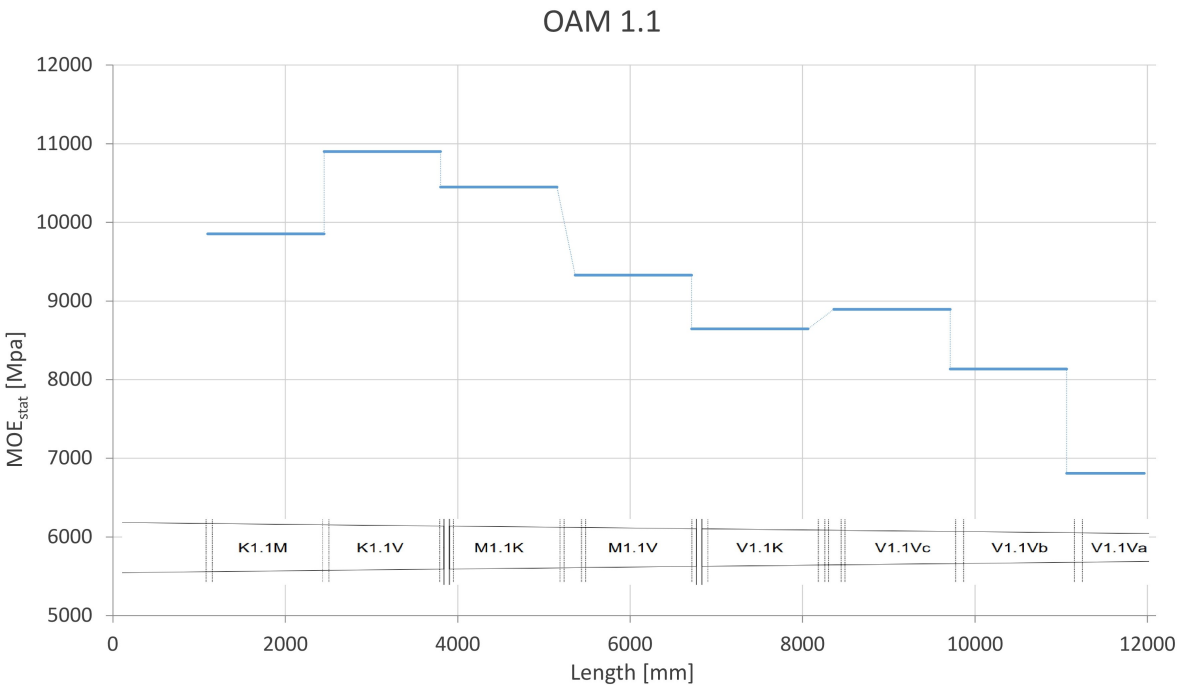

Figure B.0.1: variations of the MOE along the length of the pile OAM1.1.

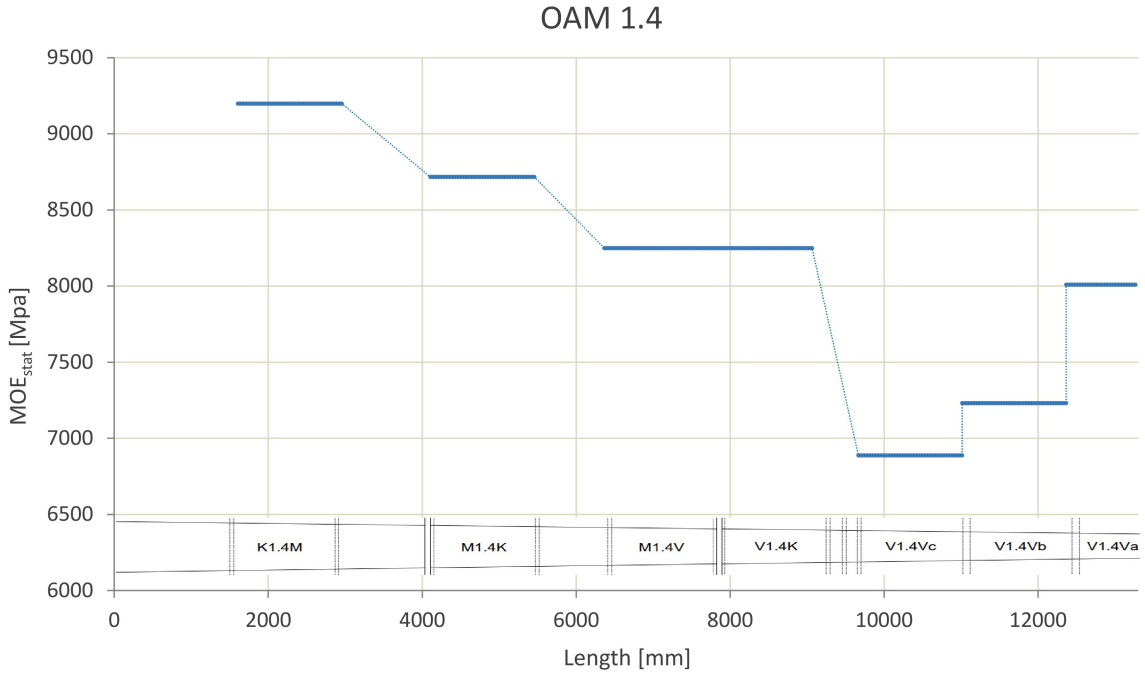

Figure B.0.2: variations of the MOE along the length of the pile OAM1.4.

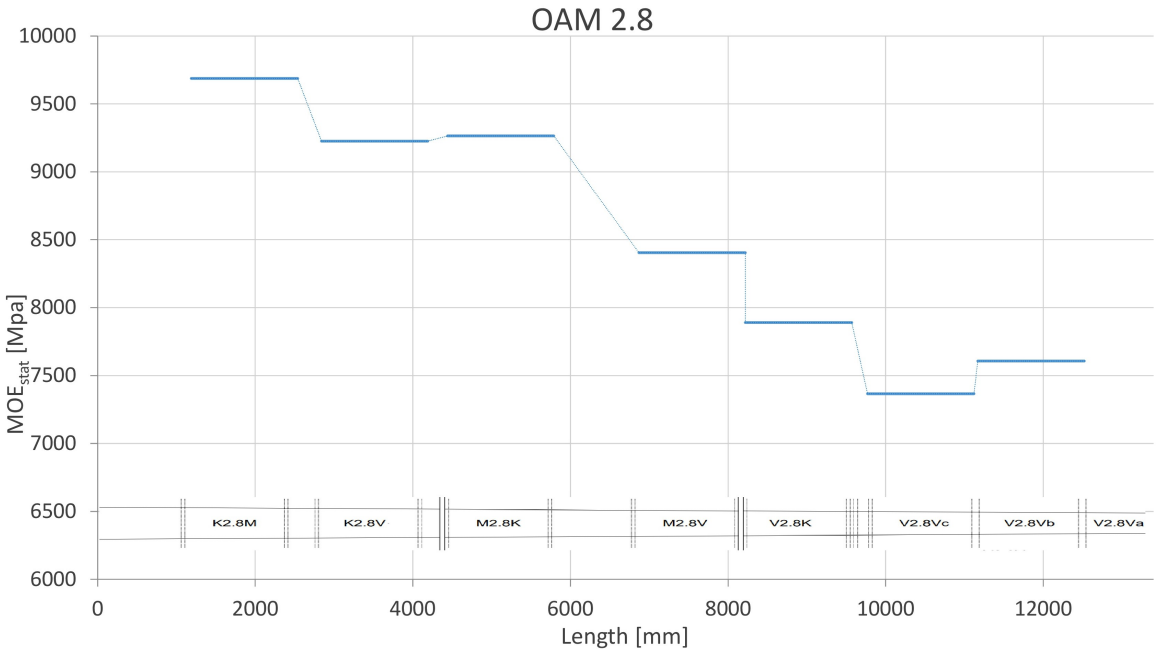

Figure B.0.3: variations of the MOE along the length of the pile OAM2.8.

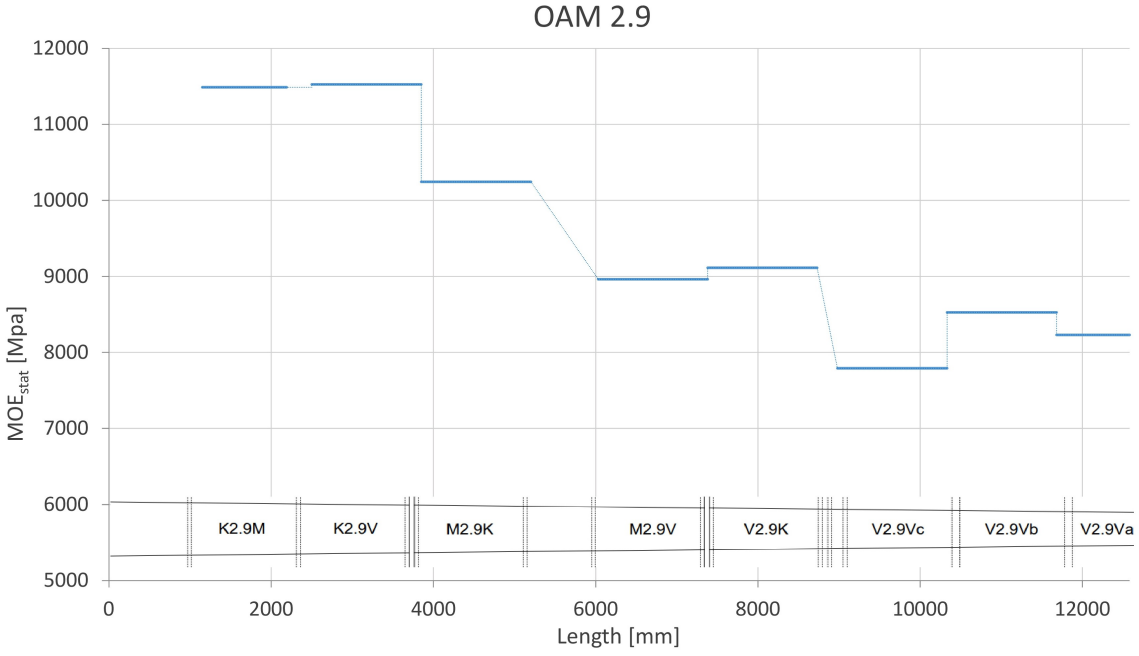

Figure B.0.4: variations of the MOE along the length of the pile OAM2.9.

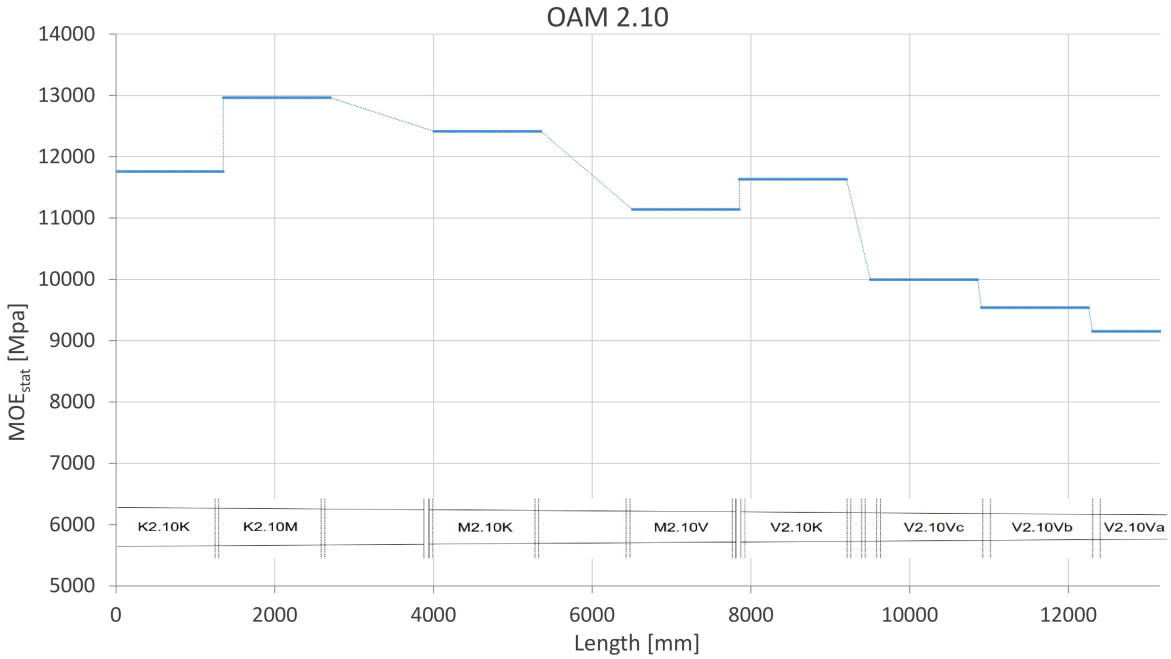

Figure B.0.5: variations of the MOE along the length of the pile OAM2.10.

References

[1] J. W. van de Kuilen and O. Beketova-Humme and G. Pagella and G.J.P. Ravenshorst and W. Gard, (2020). *An integral approach for the assessment of timber pile foundations*, WCTE 2021.

[2] Schreurs, E.C.W. (2017), *Deterioration of timber pile foundations in Rotterdam*, M.Sc. Thesis, TU Delft.

[3] Vieira Rocha, M. F. et al., (2018), *Wood Knots Influence the Modulus of Elasticity and Resistance to Compression*, Floresta e Ambiente.

[4] Ravenshorst, G.J.P. (2015), *Species independent strength grading of structural timber*, Doctoral thesis, TU Delft.

[5] G. Pagella and G.J.P. Ravenshorst (2021). *Lab protocol for the test campaign of wooden foundation piles from ICL PROEFTUIN*, report, TU Delft.

[6] Ravenshorst, G. J. P. and Pagella, G. (2021). *TUD testing report on 6 wooden foundation piles (Container 235) equipped with optic fibers*, report, TU Delft.

[7] Ravenshorst, G. J. P. and Pagella, G. (2021). *Test report on compression test carried out on wooden foundation piles (Container 228) extracted under bridges 30 and 41 in Amsterdam*, Materials testing, TU Delft.

[8] Al-zube, L. and Robertson, D. and Edwards, J. and Sun, W. and Cook, D., (2017). *Measuring the compressive modulus of elasticity of pith-filled plant stems*, Plant Methods.

[9] Honardar, S. , (2020). *Geotechnical Bearing Capacity of Timber Piles in the City of Amsterdam: Derivation of bearing capacity prediction factors based on static load tests conducted on instrumented timber piles*, M.Sc. Thesis.

[10] Van Daatselaar, F. J. (2019), *The geotechnical bearing capacity of old timber piles*, TU Delft.

[11] Morais, J.L and Xavier, J. and Dourado, N. and Louzada, J.L. (2001). *Mechanical behaviour of wood in the orthotropic directions*, Researchgate.

[12] Green, D.W. and Winandy. J.E. and Kret Schanann, D.E. (1999). *Mechanical properties of wood*, Tech. report.

[13] H. Joachim and C. Sandhaas, (2017), *Timber engineering:principle for design*, KIT Scientific Publishing.

[14] W. F. Gard, Biobased Structures and Materials (2019). *Wood as a present-day : Construction Material*, Timber Structures and Wood Technology (CIE4110).

[15] P.S. Savill, J. Evans,(2004), *Plantation silviculture / Thinning*, Encyclopedia of Forest Sciences, Elsevier.

[16] Grosser, D . (1977). *Die Holzer Mitteleuropas*, SpringerVerlag, Berlin and New York.

[17] Arslan, M.B. and Aydemir, D. (2009). *Juvenile wood and its properties*, Journal of Bartin Faculty of Forestry.

[18] Socha, J. and Kulej, M. (2007). *Variation of the tree form factor and taper in European larch of Polish provenances tested under conditions of the Beskid Sądecki mountain range (southern Poland)*, Journal of forest science.

[19] Kaiser S. and Kaiser MS., (2020), *Comparison of wood and knot on wear behaviour of pine timber*, Res. Eng. Struct. Mater.

[20] Nocetti M. and Brunetti M. and Bacher M. (2014). *Effect of moisture content on the flexural properties and dynamic modulus of elasticity of dimension chestnut timber*, European Journal of Wood and Wood Products.

[21] Bengtsson, C. (). *Strength and stiffness grading of structural timber*, Vaxjo University.

[22] Prevaes, M. (2019). *De invloed van kwasten en andere parameters op de druksterkte van houten palen*, Bachelor Thesis, TUDelft.

[23] Kavelaars, J.G.E. (2019). *De resterende druksterkte van houten funderingspalen verklaren*, Bachelor Thesis, TUDelft.

[24] Lukacevic, M. and Fussl, J. (2014). *Numerical simulation tool for wooden boards with a physically based approach to identify structural failure*, Eur. J. Wood Prod.

[25] Oh, JK. et al. , (2009), *Quantification of knots in dimension lumber using a single-pass X-ray radiation*, J Wood Sci .

[26] Wang, X. and Ross, R. and Erickson, J.R. and Forsman, J.W. and McGinnis, G.D. and Groot, (2001), *Nondestructive evaluation of potential quality of creosote-treated piles removed from service*, Forest Products Journal.

[27] Hossein, M.A. and Shahverdi, M. and Roohnia, M., (2011). *The Effect of Wood Knot as a Defect on Modulus of Elasticity (MOE) and Damping Correlation.*, Notulae Scientia Biologicae.

[28] Hu, M. and Johansson, M. and Olsson, A. and Oscarsson, J. and Enquist, B., (2014). *Local variation of modulus of elasticity in timber determined on the basis of non-contact deformation measurement and scanned fibre orientation*, European Journal of Wood and Wood Products.

[29] Abdulqader, A. and Rizos, D., (2020). *Advantages of Using Digital Image Correlation Techniques in Uniaxial Compression Tests*, Results in Engineering.

[30] Acciaioli, A. and Lionello, G. and Baleani M. (2018) *Experimentally Achievable Accuracy Using a Digital Image Correlation Technique in measuring Small-Magnitude (<0.1%) Homogeneous Strain Fields*, Materials (Basel).

[31] Carter, J.L.W. and Uchic, D.M. and Mills M.J. (2014) *Impact of Speckle Pattern Parameters on DIC Strain Resolution Calculated from In-situ SEM Experiments*, researchgate.

[32] Satoru Y. and Go M.(2007). *Digital Image Correlation*, EOLSS.

[33] van der Mark, A. (2019). *Invloed van opstellingsmethoden op gemeten eigenschappen van houten funderingspalen*, Bachelor Thesis, TU Delft.

[34] K. Samiul and K. Mohammad, (2019), *Comparison of wood and knot on wear behaviour of pine timber*, Research on Engineering Structures and Materials.

[35] Spiegel, M. and Schiller, J. and Srinivasan, R. (2000) *Schaum's Outline of Probability and Statistics*, McGraw Hill Professional.

Standards

[1] EN 408 (2010) Timber structures – Test methods – Pull through resistance of timber fasteners, CEN.

[2] EN 14251 (2003) Structural round timber - Test methods, CEN.

[3] EN 13183-1 (2002) Moisture content of a piece of sawn timber – Part 1: Determination by oven dry method, CEN.

[4] EN 384 (2016) Structural timber - Determination of characteristic values of mechanical properties and density, CEN.

[5] EN 5461 (2011) Requirements for timber (KVH 2010) - Sawn timber and round wood - General part, Neder-lands Normalisatie-instituut (NEN).

[6] EN 5491 (2010) Quality requirements for timber - Piles - Coniferous timber, Nederlands Normalisatie-instituut (NEN).

[7] EN 14358 (2016) Timber structures - Calculation and verification of characteristic values, Nederlands Normalisatie-instituut (NEN).

[8] EN 24294 (2021) Wood, sawlogs and sawn timber, ISO/TC 218 Timber.